5-2023

Ecological, evolutionary, and temporal dynamics of animal mortality events

Simon Patrick Tye
University of Arkansas-Fayetteville

Ecological, Evolutionary, and Temporal Dynamics of Animal Mortality Events

A dissertation submitted in partial fulfillment
of the requirements for the degree of
Doctor of Philosophy in Biological Sciences

by

Simon Tye
University of Nebraska at Kearney
Bachelor of Science in Biology, 2018

May 2023
University of Arkansas

This dissertation is approved for recommendation to the Graduate Council.

_____
Adam M. Siepielski, Ph.D.
Dissertation Director

_____
Andrew J. Alverson, Ph.D.
Committee Member

_____
Samuel B. Fey, Ph.D.
Committee Member

_____
J. D. Willson, Ph.D.
Committee Member

Abstract

Global declines of animal abundances are emblematic of the Anthropocene. Recent animal declines have increasingly involved more frequent and intense die-offs within populations, or mass mortality events (MMEs). These extreme demographic events can lead to rapid changes in biological communities, either by imperiling the affected population or influencing populations remaining within communities. To date, there is still limited information about the effects of predator MMEs on immediate ecological dynamics within communities and rapid evolutionary dynamics within remaining populations that may ensue. Moreover, few approaches exist to predict future occurrences of predator MMEs across broad spatial scales. To address these gaps, I conducted two experiments to understand how predator MMEs affected (1) tri-trophic freshwater food web dynamics, and (2) rapid adaptive evolution of consumer life history traits. Lastly, I compiled one of most comprehensive datasets of freshwater fish MMEs (3) to predict their future frequency under a warmer climate. In Chapter 1, I conducted a freshwater mesocosm experiment to understand how community dynamics were affected by two key features of predator MMEs: weakened top-down effects following the death of predators (i.e., removing predators), and a strengthened bottom-up (i.e., resource) effects via the decomposition of predator carrion. Predator MMEs led to trophic biomass responses that were best predicted by the additive effect of removing predators and adding predator carrion, as well as distinct zooplankton and, to a lesser extent, microalgae biomass dynamics compared to similar perturbations. In Chapter 2, I conducted a rapid evolution experiment to understand how two main biotic drivers that could be change in strength following the loss of fish predators affect consumer population dynamics and life history trait evolution. Specifically, some fish predators are known to exert strong selective pressures on consumer body size (size-selective predation) and other key life history traits,

whereas contrasting resource levels can lead to divergent life history changes and generate opposing effects on population dynamics (e.g., increase or population density). Resource level drove population dynamics, predation type had the greatest impact on rapid adaptive evolution of life history traits, but there was only evidence for feedback between rapid trait evolution and concurrent population dynamics under size-selective predation and low resource levels. In Chapter 3, I compiled the most comprehensive databases of freshwater fish mortalities and concurrent temperature estimates across North American north temperate lakes. I then used future water and air temperature projections across lakes to predict the annual frequency of fish MMEs related to warm temperature over the 21st century. Collectively, these studies improve our basic understanding about the immediate effects of rapid predator losses on ecological dynamics within communities and evolutionary dynamics within consumer populations, as well as help establish baseline predictions of their future frequency in an increasingly volatile world.

Acknowledgements

Everyone is a product of their family, friends, and environment. The work and opportunities presented here were possible because of many family members, friends, and colleagues. Special thanks are necessary for my partner, Caitlin, and our cats, Magnolia and Charlie, all of whom give me purpose each day. We've grown together, limb by limb, branch by branch, and built something greater than the whole. I would also like to thank all members of the Tye, Vigil, and Romero families – my loving parents Thomas and Mikki, brother Nate; my aunts and uncles, Gina, Chris, Gene, Juliana, Julie, Mike, Debbie, Bruce, Matt, Chris; and my paternal grandparents Thomas Sr. and Gloria, and many more. It's always been too long, and I hope we see each other soon. I also want to especially thank my maternal grandparents, Gene Vigil and Roseanne Vigil, who lived and are living joyful, humble, and honorable lives that would inspire many. Born in small coal-mining communities of southeastern Colorado, they volunteered, conserved materials, biked, hiked, gardened, composted, and restored a vintage Volkswagen Beetle well before Front Range flowers wilted. Lastly, I would like to thank all my friends and colleagues in Fayetteville and beyond for meaningful memories. In particular, I would like to thank James Boyko, Tyler Chafin, Miguel Gomez-Llaño, Eric Hagen, Adam Hasik, Zachery Zbinden; my doctoral advisor, Adam Siepielski; my committee members, Andrew Alverson, Samuel Fey, and J. D. Willson; my undergraduate mentors, Keith Geluso, Mary Harner, and Letty Reichart, and Dawn Simon; and my recent collaborators Andrew Bray, J. P. Gibert, Andrew Rypel, and Nicholas Phelps. Thank you all for the many valuable teaching moments and sharing your knowledge about nature.

Table of Contents

List of Published Papers

Chapter 1. Tye, SP, SB Fey, JP Gibert, and AM Siepielski. Predator mass mortality events restructure freshwater food webs via trophic recoupling. In Review at *Nature*.

Chapter 2. Tye, SP, and AM Siepielski. Size selective predation generates divergent consumer life history trait evolution under contrasting resource levels. Under preparation for *Ecology Letters*.

Chapter 3. Tye, SP, AM Siepielski, A Rypel, A Bray, N Phelps, and SB Fey. Climate change amplifies the frequency of fish mass mortality events across north temperate lakes. Published in *Limnology and Oceanography Letters*.

Introduction

Most major animal groups have declined in abundance over the past century (Estes et al., 2011; Dirzo et al., 2014; Rosenberg et al., 2019). These animal abundance declines have been increasingly accompanied by sudden die-offs that are often referred to as mass mortality events (MMEs; Fey et al., 2015). These extreme demographic events often decimate populations (Fey et al., 2015) and can either primarily affect one species – such as following disease outbreaks (e.g., Gizzi et al., 2020), the leading cause of documented MMEs (Fey et al., 2015) – or several species such as during a catastrophic wildfire (e.g., Jolly et al., 2021). In particular, many recent MMEs have involved predator populations (Fey et al., 2015). Yet, most knowledge about rapid predator declines involves long-term impacts of their absence, such as trophic downgrading (Estes et al., 2021), sustained defaunation (Dirzo et al., 2014), and erosion of ecosystem functions and services (Schmitz et al., 2010). By comparison, much less is known about the immediate effects of predator MMEs on ecological dynamics within communities and evolutionary dynamics within populations, in part due to the rarity and unpredictability of these events. Additionally, few approaches exist for either predicting future occurrences of MMEs (e.g., Till et al., 2019) or assessing temporal patterns of species mortalities (e.g., Blancher, 2013) across broad spatial scales. Improving our understanding of MMEs in wild communities will both further basic knowledge about the implications of extreme demographic events and bolster applied research focused on reducing future animal abundance declines.

Indeed, many animal populations have declined amidst widespread environmental degradation over recent decades, centuries, and millennia (e.g., Estes et al., 2011; Dirzo et al., 2014; Fricke et al., 2022). In the mid-20th century, two overarching environmental perturbations were widespread predator declines (Leopold, 1949) and sustained nutrient enrichment that

elevates primary productivity (i.e., eutrophication; Schindler, 1974). These perturbations shaped foundational theories in community ecology and led to discussions about the roles of top-down (i.e., predator-controlled) effects and bottom-up (i.e., resource-controlled) effects in influencing community structure and food web dynamics (Hairston et al., 1960; Paine, 1966; Paine, 1980). However, an increasing assemblage of global drivers have since intensified predator declines (Dirzo et al., 2014) and sustained nutrient enrichment (Vitousek, 1994). Yet, it remains unknown whether the existing top-down/bottom-up paradigm remains useful for anticipating community responses to emerging types of perturbations. Recent theory suggests that the effects of predator MMEs have two key features (Fey et al., 2019): a sharp reduction in predation (i.e., weakened top-down control) and a concurrent resource pulse via decomposing carrion (i.e., strengthened bottom-up effect). Understanding whether food web responses to predator MMEs can be anticipated by considering the additive or interactive effects of predator removals and resource pulses, rather than solely their independent effects, would increase the utility of existing knowledge about top-down/bottom-up effects across systems (e.g., Estes et al., 2011; Polis et al., 1997).

In addition to ecological dynamics, rapid predator losses could potentially have profound impacts on evolutionary dynamics, either within the population of affected predators (e.g., bottleneck event; Pirog et al., 2019) or other populations within the community (e.g., Blumstein and Daniel, 2005). While both are worth additional research, the latter leads to interesting questions about whether evolutionary dynamics within consumer populations are directly affected by the death (i.e., change in predation) and/or decomposition (i.e., increase in resources) of predators. For example, many predators exert strong selective pressures on key consumer life history traits, such as by disproportionately eating consumers with large body sizes (i.e., size-

selective predation; Brooks and Dodson, 1965; Galbraith, 1967). Additionally, local enhancement of primary productivity can increase resource availability (Polis et al., 1997), as well as lead to a partially contrasting set of rapid adaptive changes in life history traits (Reznick et al., 2002; Cuenca-Cambronero et al., 2018) than would be expected under size-selective predation (Reznick and Endler, 1982; Lyberger et al., 2021). Better understanding how size-selective predation and high productivity drive rapid adaptive evolution of consumer life history traits will improve predictions about how consumers respond to these common selective pressures. Moreover, this information will further inquiries about how MMEs of freshwater fish, which could alter the effects of size-selective predation (i.e., the death of predators) and increase primary productivity (i.e., the decomposition of predators; Boros et al., 2015) that could thereby influence community recovery.

Importantly, however, better understanding consequences of sudden animal die-offs has critical implications beyond advancing basic knowledge. For example, few approaches exist for predicting future occurrences of MMEs in natural communities (e.g., Till et al., 2019), which hinders accurate portrayals of future ecosystem changes. Over the past century, most documented MMEs have involved lake fish (Fey et al., 2015), and most lakes occur in north temperate regions of the global (Verpoorter et al., 2014). Lake fish MMEs often occur due to environmental conditions associated with higher intensities (Phelps et al., 2019; Till et al., 2019) and rapid shifts (Genin et al., 2020) in local temperature that reduce dissolved oxygen concentration (Barica, 1975). However, while strong links exist between fish MMEs and either concurrent water (Till et al., 2019) or air (Phelps et al., 2019) across temperate lakes of North America, regional air-water temperature dynamics are variable across space (e.g., O'Reilly et al., 2015) and time (e.g., Kraemer et al., 2015). Therefore, it remains unknown whether these key

temperature measurements, which have contrasting levels of availability across broad spatial regions (e.g., Sharma et al., 2015), provide similar predictions of frequencies of lake fish MMEs under future climate projections. Enhancing approaches for predicting frequencies of these events help define baseline expectations for how ecosystems have change under future climate scenarios.

This dissertation addressed these three important topics about the effects of predator MMEs on community dynamics, the effects of predators and resources on rapid eco-evolutionary dynamics in consumer populations, and predicted extents of future predator MMEs. These three questions involved two experiments and one data synthesis, and their answers were prepared as three separate publications for peer-reviewed journals.

1) Do predator MMEs generate distinct ecological dynamics in freshwater food webs?
2) Do the combined effects of selective predation and contrasting resource levels generate predictable eco-evolutionary responses in consumer populations?
3) What are reasonable predictions of the future frequency of freshwater fish MMEs across north temperate lakes based on local water or air temperature projections?

By addressing these questions, I aimed to further both basic and applied research about understanding rapid abundance declines of wild animal populations. More generally, I hoped to inform people about consequential changes that may occur as the natural world rapidly degrades.

References

Barica, J. 1975. Summerkill risk in prairie ponds and the possibilities of its prediction. *Journal of the Fisheries Research Board of Canada*, **32**:1283-1288. doi:10.1139/f75-149

Blumstein, D. T., and J. C. Daniel. 2005. The loss of anti-predator behaviour following isolation on islands. *Proceedings of the Royal Society B*, **272**(1573):1663-1668. doi:10.1098/rspb.2005.3147

Brooks, J. L., and S. I. Dodson. 1965. Predation, body size, and composition of plankton. *Science*, **150**:28-35. doi:10.1126/science.150.3692.

Cuenca-Cambronero, M., H. Marshall, L. De Meester, T. A. Davidson, A. P. Beckerman, and L. Orsini. 2018. Predictability of the impact of multiple stressors on the keystone species *Daphnia*. *Scientific Reports*, **8**(1):17572. doi:10.1038/s41598-018-35861-y.

Dirzo, R., H. S. Young, M. Galetti, G. Ceballos, N. J. B. Issac, and B. Collen. 2014. Defaunation in the Anthropocene. *Science*, **345**:401-406. doi:10.1126/science.1251817

Estes, J. A., J. Terborgh, J. S. Brashares, M. E. Power, J. Berger, W. J. Bond, S. R. Carpenter, T. E. Essington, R. D. Holt, J. B. C. Jackson, R. J. Marquis, L. Oskanen, T. Oksanen, R. T. Payne, E. K. Pikitch, W. J. Ripple, S. A. Sandin, M. Scheffer, T. W. Schoener, J. B. Shurin, A. R. E. Sinclair, M. E. Soulé, R. Virtanen, and D. A. Wardle. 2011. Trophic downgrading of planet Earth. *Science*, **333**:301-306. doi:10.1126/science.120510

Fey, S. B., A. M. Siepielski, S. Nusslé, K. Cervantes-Yoshida, J. L. Hwan, E. R. Huber, M. J. Fey, A. Catenazzi, and S. M. Carlson. 2015. Recent shifts in the occurrence, cause, and magnitude of animal mass mortality events. *Proceedings of the National Academy of Sciences*, **112**:1083-1088. doi:10.1073/pnas.1414894112

Fey, S. B., J. P. Gibert, and A. M. Siepielski. 2019. The consequences of mass mortality events for the structure and dynamics of biological communities. *Oikos*, **128**:1679-1690. doi:10.1111/oik.06515

Fricke, E. C., C. Hsieh, O. Middleton, D. Gorczynski, C. D. Cappello, O. Sanisidro, J. Rowan, J. C. Svenning, and L. Beaudrot. 2022. Collapse of terrestrial mammal food webs since the Late Pleistocene. *Science*, **377**:1008-1011. doi:10.1126/science.abn4012

Galbraith, M. G. 1967. Size-Selective predation on *Daphnia* by rainbow trout and yellow perch. *Transactions of the American Fisheries Society*, **96**(1):1–10. doi:10.1577/1548-8659(1967)96[1:spodbr]2.0.CO;2.

Genin, A., L. Levy, G. Sharon, and A. Diamant. 2020. Rapid onsets of warming events trigger mass mortality of coral reef fish, *Proceedings of the National Academy of Sciences*, **117**:25378-25385. doi:10.1073/pnas.2009748117

Gizzi, F., J. Jiménez, S. Schäfer, N. Castro, S. Costa, S. Lourenço, R José, J. Canning-Clode, and J. Monteiro. 2020. Before and after a disease outbreak: tracking a keystone species recovery from a mass mortality event. *Marine Environmental Research*, **156**:104905.

Hairston, N. G., F. E. Smith, and L. B. Slobodkin. 1960. Community structure, population control, and competition. *The American Naturalist* **94**:421-425. doi:10.1086/282146

Jolly, C. J., C. R. Dickman, T. S. Doherty, L. M. van Eeden, W. L. Geary, S. M. Legge, J. C. Z. Woinarski, and D. G. Nimmo. 2022. Animal mortality during fire. *Global Change Biology*, **28**:2053-2065. doi:10.1111/gcb.16044

Kraemer, B. M., O. Anneville, S. Chandra, M. Dix, E. Kuusisto, D. M. Livingstone, A. Rimmer, S. Geoffrey Schladow, E. Silow, L. M. Sitoki, R. Tamatamah, Y. Vadeboncoeur, and P. B. McIntyre. 2015. Morphometry and average temperature affect lake stratification responses to climate change. *Geophysical Research Letters*, **42**:4981-4988. doi:10.1002/2015GL064097

Lande, R. 1993. Risks of population extinction from demographic and environmental stochasticity and random catastrophes. *The American Naturalist*, **142**:911-927. doi:10.1086/285580

Leopold, A. 1949. "Thinking Like a Mountain" in *A Sand County Almanac*. Oxford University Press, pp. 129-133.

Lyberger, K., T. W. Schoener, and S. J. Schreiber. 2021. Effects of size selection versus density dependence on life histories: a first experimental probe. *Ecology Letters*, **24**(7):1467–73. doi:10.1111/ele.13767.

Lenoch, J. B. 2016. WHISPers, the USGS-NWHC Wildlife Health Information Sharing Partnership Event Reporting System. *Online Journal of Public Health Informatics*, **8**(1). doi:10.5210/ojphi.v8i1.6480

Loss, S. R., T. Will, and P. P. Marra. 2013. The impact of free-ranging domestic cats on wildlife of the United States. *Nature Communications*, **4**:1396. doi:10.1038/ncomms2380

O'Reilly, C. M., S. Sharma, D. K. Gray, S. E. Hampton, J. S. Read, R. J. Rowley, P. Schneider, J. D. Lenters, P. B. McIntyre, B. M. Kraemer, G. A. Weyhenmeyer, D. Straile, B. Dong, R. Adrian, M. G. Allan, O. Anneville, L. Arvola, J. Austin, J. L. Bailey, J. S. Baron, J. D. Brookes, E. de Eyto, M. T. Dokulil, D. P. Hamilton, K. Havens, A. L. Hetherington, S. N. Higgins, S. Hook, L. R. Izmest'eva, K. D. Joehnk, K. Kangur, P. Kasprzak, M. Kumagai, E. Kuusisto, G. Leshkevich, D. M. Livingston, S. MacIntyre, L. May, J. M. Melack, D. C. Mueller-Navarra, M. Naumenko, P. Noges, T. Noges, R. P. North, P. D. Plisnier, A. Rigosi, A. Rimmer, M. Rogora, L. G. Rudstam, J. A. Rusak, N. Salmaso, N. R. Samal, D. E. Schindler, S. Geoffrey Schladow, M. Schmid, S. R. Schmidt, E. Silow, M. Evren Soylu, K. Teuber, P. Verburg, A. Voutilainen, A. Watkinson, C. E. Williamson, and G. Zhang. 2015. Rapid and highly variable warming of lake surface waters around the globe. *Geophysical Research Letters*, **42**:10773-10781. doi:10.1002/2015GL066235

Paine, R. T. 1966. Food web complexity and species diversity. *The American Naturalist*, **100**:65-75. doi:10.1086/282400

Paine, R. T. 1980. Food webs: linkage, interaction strength, and community infrastructure. *Journal of Animal Ecology*, **49**:666-685. doi:10.2307/4220

Pirog, A, S Jaquemet, V Ravigné, G Cliff, E Clua, BJ Holmes, NE Hussey, JEG Nevill, AJ Temple, P Berggren, L Vigliola, H Magalon. Genetic population structure and demography of an apex predator, the tiger shark *Galeocerdo cuvier*. *Ecology and Evolution*, **9**:5551-5571. doi:10.1002/ece3.5111

Polis, G. A., W. B. Anderson, and R. D. Holt. 1997. Toward an integration of landscape and food web ecology: the dynamics of spatially subsidized food webs. *Annual Review of Ecology and Systematics*, **28**:289-316. doi:10.1146/annurev.ecolsys.28.1.289

Phelps, N. B. D., I. Bueno, D. A. Poo-Muñoz, S.J. Knowles, S. Massarani, R. Rettkowski, L. Shen, H. Rantala, P. L. F. Phelps, and L. E. Esobar. 2019. Retrospective and predictive investigation of fish kill events. *Journal of Aquatic Animal Health*, **31**:61-70. doi:10.1002/aah.10054

Reznick, D., and J. A. Endler. 1982. The impact of predation on life history evolution in Trinidadian guppies (*Poecilia reticulata*). *Evolution*, **36**(1):160-177. doi:10.2307/2407978

Reznick, D., M. J. Bryant, and F. Bashey. 2002. r- and K-selection revisited: the role of population regulation and in life-history evolution. *Ecology*, **83**(6):1509-1520. doi:10.1890/0012-9658(2002)083[1509:raksrt]2.0.co;2

Rosenberg, K. V., A. M. Dokster, P. J. Blancher, A. C. Smith, P. A. Smith, J. C. Stanton, A. Panjabi, L. Helft, M. Parr, and P. P. Marra. 2019. Decline of the North American avifauna. *Science*, **366**(5461):120-124. doi.101126/science.aaw1313

Schindler, D. W. 1974. Eutrophication and recovery in experimental lakes: implications for lake management. *Science*, **184**:897-899. doi:10.1126/science.184.4139.897

Schmitz, O. J., D. Hawlena, and G. C. Trussell. 2010. Predator control of ecosystem nutrient dynamics. *Ecology Letters*, **13**:1199-1209. doi:10.1111/j.1461-0248.2010.01511.x

Sharma, S., D. K. Gray, J. S. Read, C. M. O'Reilly, P. Schneider, A. Qudrat, C. Gries, S. Stefanoff, S. E. Hampton, S. Hook, J. D. Lenters, D. M. Livingstone, P. B. McIntyre, R. Adrian, M. G. Allan, O. Anneville, L. Arvola, J. Austin, J. Bailey, J. S. Baron, J. Brookes, Y. Chen, R. Daly, M. Dokulil, B. Dong, K. Ewing, E. de Eyto, D. Hamilton, K. Havens, S. Haydon, H. Hetzenauer, J. Heneberry, A. L. Hetherington, S. N. Higgins, E. Hixson, L. R. Izmesta'eva, B. M. Jones, K. Kangur, P. Kasprzak, O. Köster, B. M. Kraemer, M. Kumagai, E. Kuusisto, G. Leshkevich, L. May, S. MacIntyre, D. Müller-Navarra, M. Naumenko, P. Noges, T. Noges, P. Niederhauser, R. P. North, A. M. Paterson, P. D. Plisnier, A. Rigosi, A. Rimmer, M. Rogora, L. Rudstam, J. A. Rusak, N. Salmaso, N. R. Samal, D. E. Schinder, G. Schladow, S. R. Schmidt, T. Schultz, E. A.

Silow, D. Straile, K. Teubner, P. Verburg, A. Voutilainen, A Watkinson, GA Weyhenmeyer, C. E. Williamson, and K. H. Woo. 2015. A global database of lake surface temperatures collected by in situ and satellite methods from 1985-2009. *Scientific Data*, **2**:150008. doi:10.6073/pasta/379a6cebee50119df2575c469aba19cs

Till, A., A. L. Rypel, A. Bray, and S. B. Fey. 2019. Fish die-offs are concurrent with thermal extremes in north temperate lakes. *Nature Climate Change*, **9**:637-641. doi:10.1038/s41558-019-0520-y

Valerio, F., M. Basile, and R. Balestrieri. 2021. The identification of wildlife-vehicle collision hotspots: citizen science reveals spatial and temporal patterns. *Ecological Processes*, **10**:6. doi:10.1186/s13717-020-00271-4

Verpoorter, C., T. Kutser, A. Seekell, and L. J. Tranvik. 2014. A global inventory of lakes based on high-resolution satellite imagery. *Geophysical Research Letters*, **41**:6396-6402. doi:10.1002/2014GL060641

Vitousek, P.M. 1994. Beyond global warming: ecology and global change. *Ecology*, **75**:1861-1876. doi:10.2307/1941591

Chapter 1

Predator mass mortality events restructure freshwater food webs via trophic recoupling

Simon P. Tye, Samuel B. Fey, Jean P. Gibert, and Adam M. Siepielski

Abstract

Predators play a key role in structuring ecosystems (Hairston et al., 1960; Paine, 1966; Paine, 1980; Estes et al., 2011). Yet predator loss is accelerating globally (Estes et al., 2011; Myers and Worm, 2003; Dirzo et al., 2014), and predator mass mortality events (MMEs; Fey et al., 2015) – rapid, large-scale die-offs – are now emblematic of the Anthropocene (Dirzo et al., 2014). Due to their rare and unpredictable nature (Fey et al., 2015), we lack an understanding of how MMEs immediately impact ecosystems. Past predator removal studies (Paine, 1966; Paine, 1980) may be insufficient to understand ecological consequences of MMEs because, in nature, dead predators decompose *in situ* and generate a resource pulse (Fey et al., 2019), which may substantially alter ensuing ecosystem dynamics by temporarily enhancing productivity (MacArthur, 1955). Here we experimentally induce MMEs in freshwater food webs and report ecological dynamics that are distinct from predator losses (Paine, 1966; 1980) or resource pulses (Polis et al., 1997) alone, but can be predicted from theory (Fey et al., 2019). MMEs led to proliferation of diverse consumer and producer communities resulting from weakened top-down predator control (Hairston et al., 1960; Paine, 1966; Paine, 1980) and stronger bottom-up effects via predator decomposition (Fey et al., 2019). MMEs also led to stable functional trait and food web dynamics, indicating they may be cryptic disturbances in nature. Collectively, these dynamics led to trophic reshuffling following MMEs, whereby indirect effects of predators on primary producers were initially lost, then materialized as direct bottom-up effects that stabilized ecosystems even though intensified herbivory. These results elucidate the ecological signatures of MMEs and demonstrate the feasibility of forecasting novel ecological dynamics arising amidst intensifying global change.

Introduction

Mass mortality events (MMEs) are rapid, large-scale die-offs in wild populations (Fey et al., 2015). Unlike other episodic die-offs (e.g., anadromous fish spawns or cicada emergence), MMEs simultaneously affect all life-stages (Fey et al., 2015) and often decimate populations (Hamilton et al., 2021). Over the last century, MMEs have increased in frequency and magnitude across most animal groups, including many predator populations (Fey et al., 2015). The magnitudes of MMEs are staggering – eradicating more than a billion fish, eliminating hundreds of thousands of mammals and birds, and producing hundreds of millions of tons of dead biomass almost instantly (Fey et al., 2015). Over long timescales, these events can contribute to trophic downgrading (Estes et al., 2011) and sustained defaunation (Dirzo et al., 2014). Despite progress in detecting (Fey et al., 2015) and predicting (Fey et al., 2019; Tye et al., 2022) their occurrence, our empirical understanding of their ensuing ecological repercussions is far less established. This lack of understanding precludes accurate forecasts of food web responses to these increasingly frequent catastrophes.

Ecological theory on the immediate food web consequences of predator MMEs (Fey et al., 2019) proposes that ensuing dynamics may be explained either by the additive effects of predator losses and resource pulses (Hairston et al., 1960; Paine, 1966; Paine, 1980), or through emergent non-additive effects of these perturbations (Threlkeld, 1988; Vanni and Findla,y 1990). These predictions remain untested and hinge on two key features of MMEs (Fey et al., 2019): 1) rapidly weakened top-down (i.e., predator-controlled) effects, which release intermediate trophic levels from predation but increase consumption at lower trophic levels (Leopold, 1949; Hairston et al., 1960; Paine, 1966; Paine, 1980), and 2) concurrent strengthening of bottom-up (i.e., resource-controlled) effects as predators decompose and release nutrients (Fey et al., 2019).

These features are reminiscent of predator removals (Leopold, 1949) and intensified resource inputs (e.g., eutrophication; Schindler, 1974) – overarching environmental perturbations of the Anthropocene that shaped foundational ecological theory on community structure and food web dynamics (Leopold, 1949; Hairston et al., 1960; Paine, 1966; Paine, 1980). While a consensus exists regarding the independent effects of predator removals and resource inputs on community dynamics (Hairston et al., 1960; Paine, 1966; Paine, 1980), an expanding list of global drivers have intensified predator declines (Dirzo et al., 2014) and excessive nutrient additions that enhance productivity (Vitousek, 1994) since the mid-20th century when these ideas were formulated. Such widespread degradation raises questions about whether food web responses to predator MMEs can be adequately predicted by paradigms established in a less volatile world.

Here, we use freshwater mesocosms to experimentally resolve the ecological aftermath of predator MMEs and determine whether foundational ecological theory can readily anticipate the structure and dynamics of post-perturbation communities. We used a freshwater system because it has extremely well-understood trophic links (Porter, 1973; Threlkeld, 1988; Vanni and Findlay, 1990; Bergquist and Carpenter, 1986; Hansen et al., 1997; Su et al. 2021) and exhibits rapid nutrient cycling and remineralization (Threlkeld, 1988; Vanni and Findlay, 1990; Boros et al., 2015). Also, most documented MMEs have affected freshwater lake fish (Fey et al., 2015), and these events are predicted to occur more frequently in the future (Tye et al., 2022). Within mesocosms, we established food webs containing phytoplankton, zooplankton, and planktivorous fish that resemble natural freshwater pond food webs. We then implemented a 2×2 factorial experiment with treatments that included the presence/absence of live predators and/or predator carrion (Fig. 1). This created an experimental control (fish present, carrion absent) and three perturbations: predator removal (fish and carrion absent), resource pulse (fish and carrion

present), and MME (fish absent, carrion present). To compare perturbations, we extensively sampled zooplankton, microalgae (primary producers frequently consumed by zooplankton (Porter, 1973; Bergquist and Carpenter 1986; Hansen et al., 1997), and total productivity for 120 days. We then determined whether trophic biomass responses to predator MMEs can be predicted from classic theory – by exhibiting additive effects of predator removals (i.e., fish removed) and resource pulses (i.e., carrion added). In the presence of non-additive (interactive) effects, classic theory would fail to correctly forecast trophic biomass following a predator MME. Lastly, we compared three key aspects of food webs – community structure, traits that influence consumer-resource interactions (i.e., body size), and transient community dynamics.

Trophic biomass responses

Our results demonstrate that predator MMEs, predator removals, and resource pulses generate predictable trophic biomass responses over time, while also exhibiting distinct food web structure and dynamics (Fig. 1). Relative to control treatments, MMEs increased zooplankton biomass (general additive mixed model, +106%, $t_{9.53} = 10.78$, $p < 0.01$; Fig. 1A, 1D), increased productivity (+137%, chlorophyll-*a*, $t_{33.21} = 16.73$, $p < 0.01$; Fig. 1B, 1E), and decreased biomass of microalgae (-82%, $t_{13.59} = -7.80$, $p < 0.01$; Fig. 1C, 1F). Comparatively, predator removals strongly increased zooplankton biomass (+95%, $t_{9.53} = 8.64$, $p < 0.01$; Fig. 1A, 1D), but decreased productivity (-22%, $t_{33.21} = -7.57$, $p < 0.01$; Fig. 1B, 1E) and decreased microalgae biomass (-75%, $t_{13.59} = -5.26$, $p < 0.01$; Fig. 1C, 1F), whereas resource pulses primarily increased productivity (+195%, $t_{33.21} = 22.54$, $p < 0.01$; Fig. 1B, 1E). Distinct trophic biomass responses to MMEs, predator removals, and resource pulses were particularly evident when comparing coupled time-series (Fig. 1G-1H). Only MMEs led to concurrent proliferation of consumers and

across producers (Fig. 1G), yet overall declines in microalgae (Fig. 1H), which highlighted the capacity for zooplankton to rapidly regulate these resources (Porter, 1973; Bergquist and Carpenter, 1986; Hansen et al., 1997).

While previous work has indicated excessive resource inputs can strengthen trophic cascades following predator losses(Su et al. 2021), there were no interactive effects of MMEs on zooplankton biomass (2-way ANOVA, predator removal × resource pulse; $F_{1,14} = 0.06$, $p = 0.82$; Fig. 1 D), total productivity ($F_{1,14} = 0.49$, $p = 0.50$; Fig. 1E), or microalgae biomass ($F_{1,14} = 0.01$, $p = 0.93$; Fig. 1F) over time. Instead, food web responses to MMEs were predicted by additive effects of predator removals and resource pulses on zooplankton biomass ($F_{1,14} = 5.59$, $p = 0.03$; $F_{1,14} = 0.62$, $p = 0.44$), total productivity ($F_{1,14} = 7.89$, $p = 0.01$; $F_{1,14} = 230.37$, $p < 0.01$), and microalgae biomass ($F_{1,14} = 3.97$, $p = 0.07$; $F_{1,14} = 0.70$, $p = 0.42$). This suggests that the effects of predator MMEs on trophic biomass over short timescales can be readily predicted by combining knowledge about how predator removals (Estes et al., 2011) and resource pulses (Polis et al., 1997) propagate through food webs in other systems. Below, we subsequently explore the mechanisms underlying zooplankton and microalgae dynamics following perturbations.

Community structural responses

Broad similarities in zooplankton and microalgae community structure following predator MMEs and predator removals indicated that structural changes were predominately driven by predator and zooplankton consumer-mediated effects (Fig. 2, S1-S2). Relative to controls, both treatments without predators had higher biomass of key consumer competitors (Fig. S3; Table S1), including Cyclopoida (MMEs: +64%; predator removals: +88%), Daphniidae (MMEs:

+231; predator removals: +199%), and Bosminidae (MMEs: +53%; predator removals: +31%). Treatments with resource additions had higher biomass of other competitors with varied functional roles (Fig. S3; Table S1), including Cyprididae (MMEs: +29%; resource pulses +28%) and Brachionidae (MMEs: +53%). These shifts in zooplankton composition and functional roles were likely attributable to altered competitive interactions (DeMott and Kerfoot, 1982; Gibert et al., 2022), and changes in productivity, as diverse competitor communities often proliferate following resource inputs (DeMott and Kerfoot, 1982; Threlkeld, 1988; Vanni and Findlay, 1990).

Overall, biomass differences across trophic levels (Fig. 1-2, S3-S4) largely resulted from substantial density differences (Fig. S1, S5-S6) combined with modest zooplankton body size differences (Fig. 2A, S2, S7) and microalgae biovolume (Fig. 2B, S2, S8). Planktivorous fish are well-known to structure lake food webs by regulating zooplankton densities(Threlkeld 1988), and mean zooplankton density increased in both treatments without predators (MMEs: +34%; predator removals: +33%; Fig. S5). Planktivorous fish also exert selection on consumer body size (Brooks and Dodson, 1965), and both treatments without predators had larger mean zooplankton body size (MMEs: +14%; predator removals: +11%; Fig. S2), particularly among key consumer competitors following MMEs (Fig. S7). Comparatively, predator removals had larger mean body size of fewer key consumer competitors (Fig. S7) and smaller mean body size of Brachionidae (-5%). Thus, removing predators likely indirectly increased resource competition (Threlkeld, 1988; Vanni and Findlay, 1990) following increased consumer densities (e.g., Fig. 1H, 2B). Moreover, these findings indicate that zooplankton biomass simultaneously responded to relaxation of size-selective predation (Brooks and Dodson, 1965) and temporary productivity enhancement (Polis et al., 1997) following the death and decomposition of

predators, respectively. Therefore, accounting for changes in body size dynamics (Fig. 2), which drive rapid ecological changes (Gibert et al., 2022), could enhance forecasting community responses to MMEs.

Microalgae community responses to MMEs were also affected more by fish predator- and zooplankton consumer-mediated effects rather than resource pulses (Fig. 2B, S2-S4), which corroborates observations of fish MMEs in nature (Vanni et al., 1990; Nagdali and Gupta, 2002). These effects were particularly evident several weeks after perturbations, when MMEs experienced sustained declines in productivity and microalgae biomass that were indicative of intensified herbivory (Fig. 1G-1H; Vanni and Findlay, 1990; Hansen et al., 1997), but also consistent with reductions in predator-mediated nutrient cycling (e.g., excretion; Vanni, 2002), and/or their combined effect (e.g., "dead fish paradox"; Threlkeld, 1988; Vanni and Findlay, 1990). Three lines of evidence, though, suggest that intensified herbivory played the dominant role in this system.

First, MMEs and predator removals increased mean biomass of key zooplankton competitors (Cyclopoida, Daphniidae; Fig. 2A, S3) that have high consumption rates on phytoplankton (Hansen et al., 1997). Second, mean biomass of green algae (Chlorophyta; Fig. S4), which are frequently consumed by zooplankton (Porter, 1973; Bergquist and Carpenter, 1986; Hansen et al., 1997) was relatively low following predator removals (-42%, $t_{10.01} = -1.75$, $p = 0.08$) and high following resource pulses (+11%, $t_{10.01} = 3.19$, $p < 0.01$). Additionally, both treatments without predators had higher mean biovolume of green algae (MMEs +17%; predator removals +23%; Fig. 2B, Fig. S8), which often attain larger size through grazer-induced plasticity (Van Donk et al., 2011). Third, resource pulses had relatively high mean cyanobacteria biomass (+69%, $t_{22.1} = 2.05$, $p = 0.04$; Fig. 2B, S4) and density (+63%; $t_{21.86} = 1.93$, $p = 0.06$;

Fig. S6), whereas MMEs had relatively low mean cyanobacteria biomass (-48%, $t_{22.1}$ = -1.85, p = 0.07) and density (-47%, $t_{21.86}$ = -1.68, p = 0.10). This possible suppression of cyanobacteria differentiates microalgae responses of MMEs from resource pulses and is consistent with observations that zooplankton herbivory can facilitate recovery from cyanobacteria blooms (Conley et al., 2009).

Community biomass dynamics

Ecological trajectory analysis (de Cáceres et al., 2019) indicated that MMEs generated unique and more stable community dynamics through time compared to other perturbations (Fig. 3). Among zooplankton (Fig. 3A; Table S1), MMEs dynamics were largely contained in community space occupied by smaller competitors; predator removal dynamics occurred in space occupied by key competitors; and resource pulse dynamics occurred in space occupied by smaller consumers with varied functional roles (Table S1). Mean directed segment path dissimilarities (DSPD; Fig. 3B, 3D) – the relative distance in community ordination space between treatments (Fig. 3B, 3D) – also differed. Zooplankton community dynamics following MMEs were, surprisingly, most like controls (lowest DSPD in Fig. 3B). Zooplankton dynamics in MMEs and controls exhibited greater directionality stability than predator removals and resource pulses (higher directionality in Fig. S9B) – which also helps explain why MME dynamics were closest to controls over time (Fig. 3B). Additionally, zooplankton dynamics following MMEs and resource pulses, but not predator removals, ultimately converged with controls (Table S2). Thus, enhanced productivity following MMEs temporarily stabilized zooplankton communities, even after fish predation was removed and diverse consumers proliferated (Fig. S7; Threlkeld, 1988; Vanni and Findlay, 1990). These stabilizing features may have resulted from novel ecological

opportunities that arose in the aftermath of MMEs – namely enhanced productivity providing resources, lowering competition, and helping maintain diverse consumer communities[20].

Compared to zooplankton, microalgae community dynamics were similar across perturbations (Fig. 3C-3D, S2, S6) and ultimately converged with the control (Table S3). Two differences in microalgae dynamics suggested the independent, but not additive, effects of predator removals and resource pulses destabilized communities. First, directional stability of microalgae dynamics was less variable following MMEs and controls (Fig. S9C), which indicated they exhibited more consistent compositional shifts through time compared to predator removals and resource pulses. Second, microalgae dynamics following predator removals and resource pulses consistently had long mean segment lengths that indicated fast structural change (Fig. S9C), whereas MMEs and controls often had lower mean segment lengths indicative of slower structural change. These differences suggest MMEs temporarily stabilize biomass dynamics of primary producers (Threlkeld ,1988; Vanni and Findlay, 1990), though to a lesser extent than consumer biomass dynamics. While nutrients released from decomposing predators helped stabilize this freshwater system, MMEs can destabilize systems if nutrients are not readily recycled into producer biomass (Fey et al., 2019).

Considerable work has focused on how predator losses destabilize ecosystems over long timescales (Estes et al. 2011; Dirzo et al., 2014; Fricke et al., 2022). Yet, understanding how communities transition following predator losses may be critical for resolving their short- and long-term effects (Pimm, 1984; Ives and Cardinale, 2004). Only predator removals, which had high consumer densities and low resource inputs, destabilized food webs. Comparatively, MMEs generated diverse consumer communities, which led biomass dynamics of consumers and producers to stabilize and converge with undisturbed systems (Table S2-S3). This indicated

greater productivity and diversity enhanced system stability, as expected from the productivity-stability (MacArthur, 1955) and diversity-stability hypotheses (McCann, 2000). Paradoxically, these properties also indicate that the ecological aftermath of predator MMEs may be cryptic in nature (Ives and Cardinale, 2004), potentially leading to underestimations of their occurrence and effects over short timescales.

The roles of top-down and bottom-up effects in shaping communities have influenced ecology for over 50 years (Leopold, 1949; Hairston et al., 1960; Paine, 1966; Schindler, 1974; Paine, 1980). Our study shows that predator MMEs generate trophic biomass responses that can be predicted by integrating classic theory on top-down and bottom-up regulation (Fey et al., 2019) – yet also exhibit distinct food web dynamics and community structure that cannot be readily predicted by integrating these ideas. That the effects of MMEs are not predicted simply from predator removals is notable. Indeed, our results indicate that the effects of trophic downgrading that ensue in the immediate aftermath of an MME might be thought of as "a trophic reshuffling". During this reshuffling, the effects of predators are initially decoupled from lower trophic levels, but their biomass is later assimilated by producers and subsequently promulgated upwards. Predator mortalities can thus generate direct bottom-up effects in ecosystems that may facilitate their eventual recovery. Future studies may be able to anticipate ecological outcomes of these and other types of increasingly common ecological catastrophes in natural communities (Fey et al., 2015; Tye et al., 2022) by similarly synthesizing foundational concepts formulated in a once less volatile world.

Acknowledgements

We thank Arkansas Game and Fish Commission for providing fish; Dr. J. D. Willson and the University of Arkansas Facilities for study site access; University of Arkansas Agricultural Facilities for equipment use; Kayleigh Smith and Adrienne Ingram for administering the electroshocker; Wade Boys for helping monitor mesocosms and loaning his kayak to collect zooplankton; James Boyko for helping cover and protect mesocosms from heavy precipitation; and Mathilde Cordellier, Matt Crook, Maxime Dahirel, Harold N Eyster, Collin Gross, Mali'o Kodis, and Sergio A. Muñoz-Gómez for contributing taxonomic silhouettes to PhyloPic.

Data and Code Availability

All data and code for analyses are available on a public GitHub repository (https:://github.com/simontye/2019_MME) and a permanent Zenodo repository (https://doi.org/10.5281/zenodo.7534673).

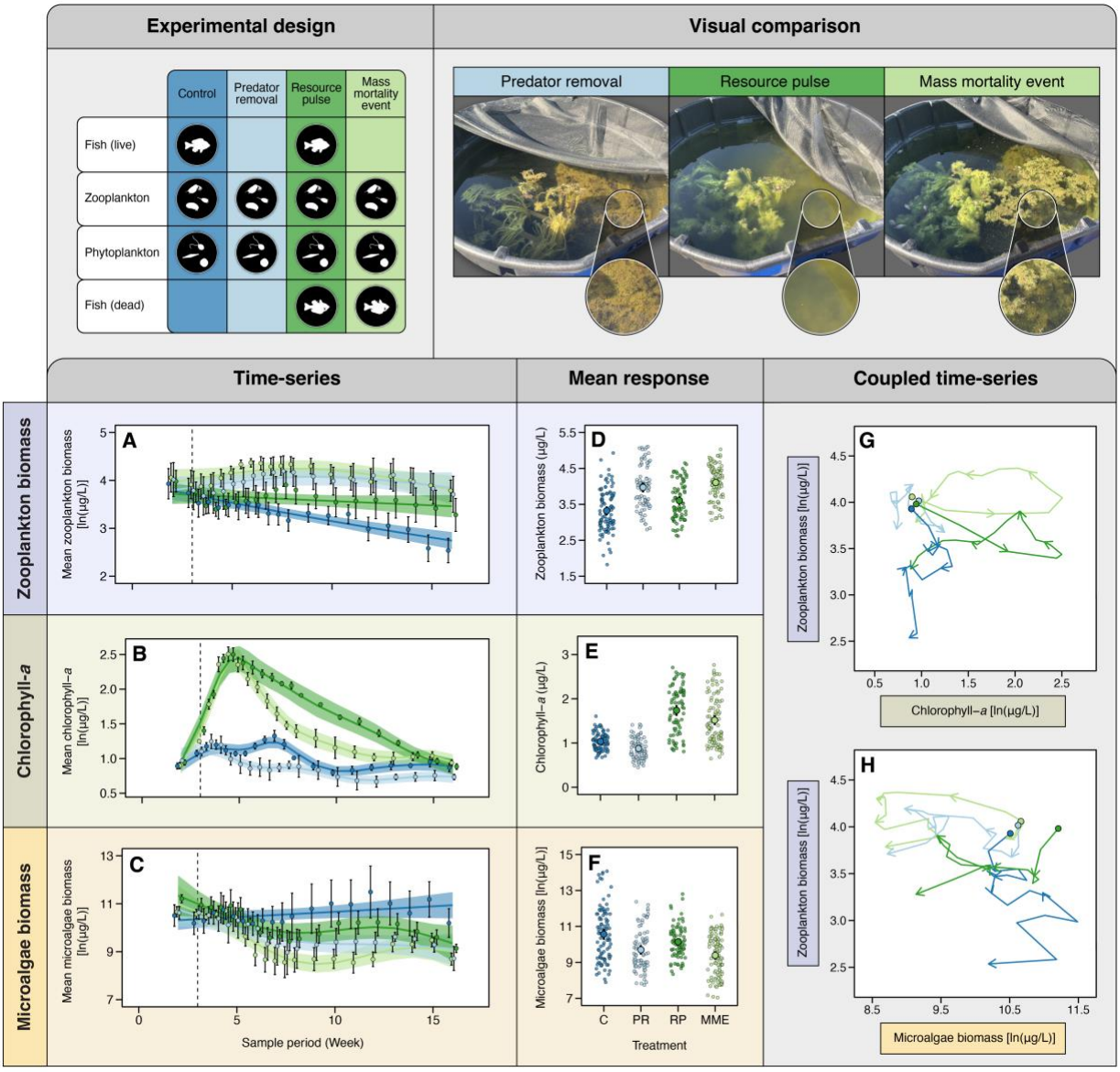

Figure 1. Food web biomass responses to predator removals, resource pulses, and mass mortality events. Factorial design to create four ecological scenarios in tri-trophic freshwater food webs: a control (live fish; dark blue; *n* = 5 replicates), predator removal (no fish; light blue; *n* = 4 replicates), resource pulse (live fish with additional dead fish added; dark green; *n* = 4 replicates), and MME (dead fish; light green; *n* = 5 replicates). Visual comparison shows illustrative photographs of each disturbed treatment. Times-series show mean consumer biomass (A, zooplankton) and producer (B, chlorophyll-*a*) or microalgae biomass (C) after inducing

treatments (dashed lines) over 120 days. Solid lines and shaded regions indicate model predictions and 95% CIs, respectively, based on smooth-moving averages (see Supplemental Materials); and points and lines indicate means +/- 1 SE by sampling period and treatment, with points jittered. Mean responses show mean consumer (D), producer (E), and microalgae biomass (F) across mesocosms and samples, with large points, lines, and small points indicating means, 95% CIs, and raw data, respectively. Coupled-time series plot mean consumer biomass alongside mean producer (G) or microalgae biomass (H), with circles and arrows indicating starting locations and direction through time, respectively.

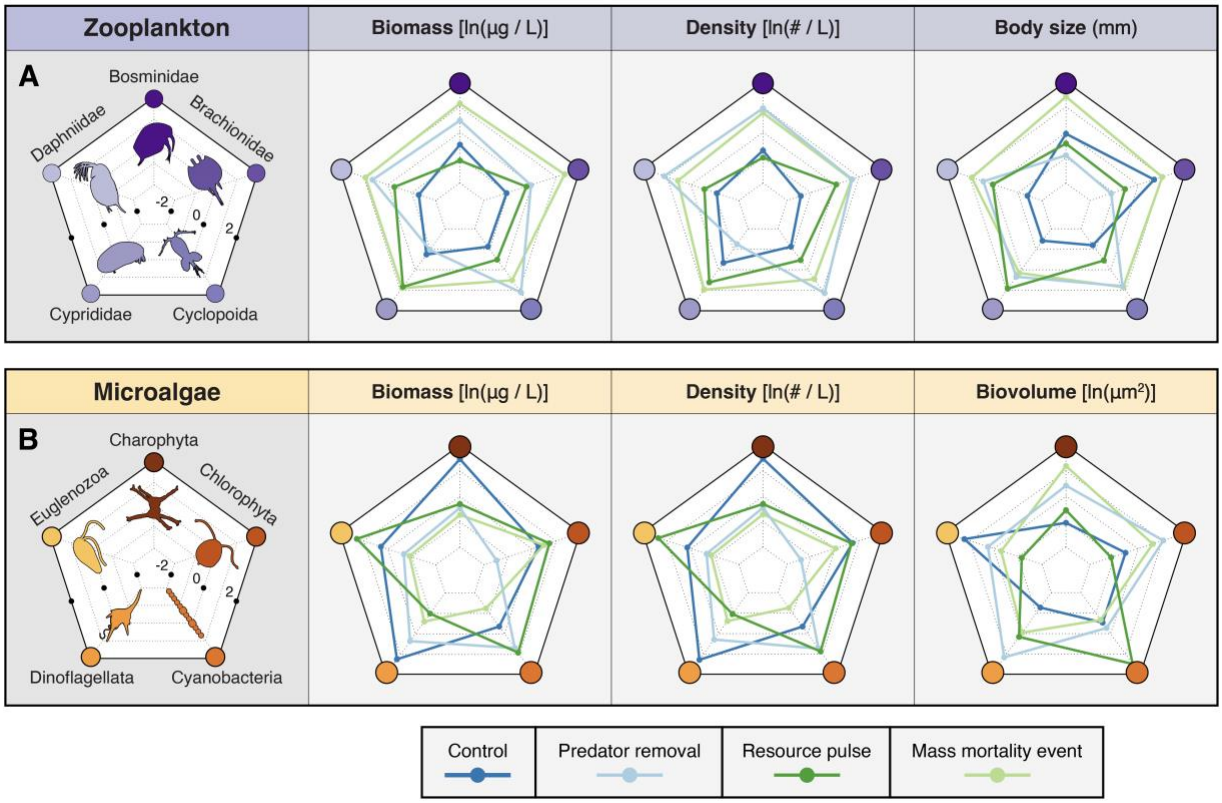

Figure 2. Community-wide biomass, density, and functional trait responses to predator removals, resource pulses, and mass mortality events. Community structure of consumers (A, zooplankton) and key producers (B, microalgae) following predator removals, resource pulses, MMEs, or controls. Radar plots zooplankton (A) and microalgae (B) biomass (ln[µg/L]), density (ln[#/L]), and body size (mm) or volume (ln[μm^2]) by treatment. Colored points that are connected by lines within radar plots represent scaled and centered mean values by treatment for dominant zooplankton and microalgae. Colored circles bordering radar plots indicate specific zooplankton and microalgae. Full time-series are shown in Fig. S1-S8.

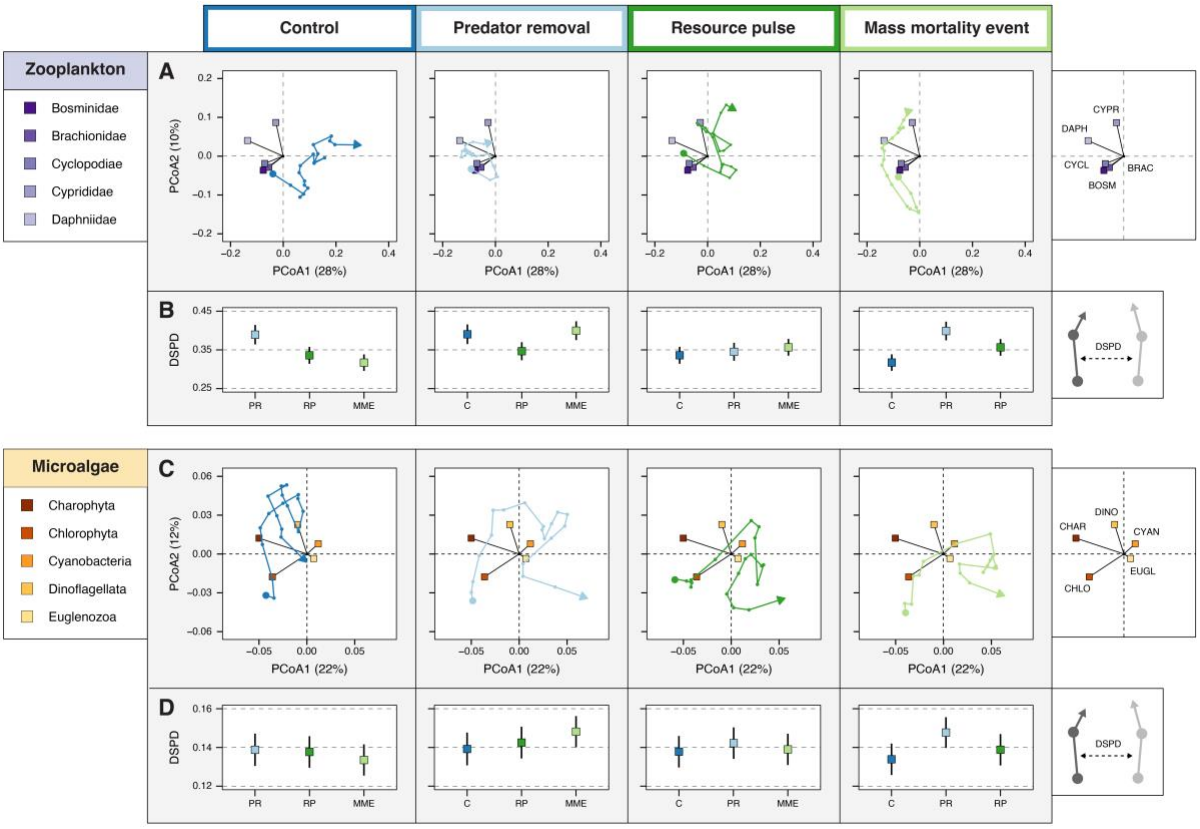

Figure 3. Distinct zooplankton and microalgae community biomass trajectories following predator removals, resource pulses, and mass mortality events. Large plots (A, C) show principal coordinate analyses (PCoA) from ecological trajectory analyses of zooplankton (A) and microalgae (C) biomass dynamics following predator removals (light blue, PR), resource pulses (dark green, RP), mass mortality events (light green, MME), and the control (dark blue, C). Trajectories show smooth-moving averages across sample periods, with trajectory starts, junctions, and ends indicated by large circles, small circles, and arrows, respectively. PCoA loadings of zooplankton and phytoplankton are shown by purple and orange squares. Smaller plots (B, D) below focal disturbances show mean directed segment path dissimilarities (DSPD) and 95% CIs via squares and lines, respectively. This metric indicates the average distance

between the focal trajectory and a comparison trajectory during the same sample periods through time (as illustrated by small inset panel, right) for zooplankton (B) and microalgae (D).

References

Bergquist, A. M., and S. R. Carpenter. 1986. Limnetic herbivory: effects on phytoplankton populations and primary production. *Ecology*, **67**:1351-1360. doi:10.2307/1938691

Brooks, J. L., and S. I. Dodson. 1965. Predation, body size, and composition of plankton. *Science,* **150**:28-35. doi:10.1126/science.150.3692.

de Cáceres M., L. Coll, P. Legendre, R. B. Allen, S. K. Wiser, M. J. Fortin, R. Condit, and S. Hubbell. 2018. Trajectory analysis in community ecology, *Ecological Monographs*, **89**:e01350. doi:10.1002/ecm.1350

Conley, D. J., H. W. Paerl, R. W. Howarth, D. F. Boesch, S. P. Seitzinger, K. E. Havens, C. Lancelot, and G. E. Likens. 2009. Controlling eutrophication: nitrogen and phosphorus. *Science,* **323**:1014-1015. doi:10.1126/science.1167755

DeMott, W. R., and W. C. Kerfoot. 1982. Competition among cladocerans: nature of the interaction between *Bosmina* and *Daphnia*. *Ecology,* **63**:1949-1966. doi:10.2307/1940132

Dirzo, R., H. S. Young, M. Galetti, G. Ceballos, N. J. B. Issac, and B. Collen. 2014. Defaunation in the Anthropocene. *Science,* **345**:401-406. doi:10.1126/science.1251817

Estes, J. A., J. Terborgh, J. S. Brashares, M. E. Power, J. Berger, W. J. Bond, S. R. Carpenter, T. E. Essington, R. D. Holt, J. B. C. Jackson, R. J. Marquis, L. Oskanen, T. Oksanen, R. T. Payne, E. K. Pikitch, W. J. Ripple, S. A. Sandin, M. Scheffer, T. W. Schoener, J. B. Shurin, A. R. E. Sinclair, M. E. Soulé, R. Virtanen, and D. A. Wardle. 2011. Trophic downgrading of planet Earth. *Science*, **333**:301-306. doi:10.1126/science.120510

Fey, S. B., A. M. Siepielski, S. Nusslé, K. Cervantes-Yoshida, J. L. Hwan, E. R. Huber, M. J. Fey, A. Catenazzi, and S. M. Carlson. 2015. Recent shifts in the occurrence, cause, and magnitude of animal mass mortality events. *Proceedings of the National Academy of Sciences*, **112**:1083-1088. doi:10.1073/pnas.1414894112

Fey, S. B., J. P. Gibert, and A. M. Siepielski. 2019. The consequences of mass mortality events for the structure and dynamics of biological communities. *Oikos*, **128**:1679-1690. doi:10.1111/oik.06515

Fricke, E. C., C. Hsieh, O. Middleton, D. Gorczynski, C. D. Cappello, O. Sanisidro, J. Rowan, J. C. Svenning, and L. Beaudrot. 2022. Collapse of terrestrial mammal food webs since the Late Pleistocene. *Science,* **377**:1008-1011. doi:10.1126/science.abn4012

Gibert, J. P., Z. Y. Han, D. J. Wieczynski, S. Votzke, and A. Tammine. 2022. Feedbacks between size and density determine rapid eco-phenotypic dynamics. *Functional Ecology*, **36**(7):1668-1680.

Hairston, N. G., F. E. Smith, and L. B. Slobodkin. 1960. Community structure, population control, and competition. *The American Naturalist* **94**:421-425. doi:10.1086/282146

Hamilton, S. L., V. R. Saccomanno, W. N. Heady, A. L. Gehman, S. I. Lonhart, R. Beas-Luna, F. T. Francis, L. Lee, L. Rogers-Bennet, A. K. Salomon, and S. A. Gravem. 2021. Disease-driven mass mortality events leads to widespread extirpation and variable recovery potential of a marine predator across the eastern Pacific. *Proceedings of the Royal Society: B*, **288**:20211195. doi:10.1098/rspb.2021.1195

Hansen, P. J., P. K. Bjørnsen, and B. W. Hansen. 1997. Zooplankton graving and growth: scaling within the 2-2000-um body size range, *Limnology and Oceanography,* **42**:687-704. doi:10.4319/lo.1997.42.4.0687

Leopold, A. 1949. "Thinking Like a Mountain" in *A Sand County Almanac*. Oxford University Press, pp. 129-133.

MacArthur, R. 1955. Fluctuations of animal populations and a measure of community stability. *Ecology*, **36**:533-536. doi:10.2307/1929601

McCann, K. S. 2000. The diversity-stability debate. *Nature*, **405**:228-233. doi:10.1038/35012234

Myers, R. A., and B. Worm. 2003. Rapid worldwide depletion of predatory fish communities. *Nature*, **423**:280-283. Doi.10.1038/nature01610

Paine, R. T. 1966. Food web complexity and species diversity. *The American Naturalist*, **100**:65-75. doi:10.1086/282400

Paine, R. T. 1980. Food webs: linkage, interaction strength, and community infrastructure. *Journal of Animal Ecology*, **49**:666-685. doi:10.2307/4220

Pimm, S. L. 1984. The complexity and stability of ecosystems. *Nature*, **307**:321-326. doi:10.1038/307321a0

Polis, G. A., W. B. Anderson, and R. D. Holt. 1997. Toward an integration of landscape and food web ecology: the dynamics of spatially subsidized food webs. *Annual Review of Ecology and Systematics*, **28**:289-316. doi:10.1146/annurev.ecolsys.28.1.289

Porter, K. G. 1973. Selective grazing and differential digestion of algae by zooplankton. *Nature*, **244**:179-180. doi:10.1038/244179a0

Schindler, W. 1974. Eutrophication and recovery in experimental lakes: implications for lake management. *Science*, **184**: 897-899. doi:10.1126/science.184.4139.897

Su, H., Y. Feng, J. Chen, J. Chen, S. Ma, J. Fang, and P. Xie. 2021. Determinants of trophic cascade strength in freshwater ecosystems: a global analysis. *Ecology*, **102**:e03370. doi:10.1002/ecy.3370

Threlkeld, T. S. 1988. Planktivory and planktivore biomass effects on zooplankton, phytoplankton, and trophic cascade. *Limnology and Oceanography*, **33**:1362-1375. doi:10.4319/lo.1988.33.6.1362

Tye, S. P., A. M. Siepielski, A. Bray, A. L. Rypel, N. B. D. Phelps, and S. B. Fey. 2022. Climate warning amplifies frequency of fish mass mortality events across north temperature lakes. *Limnology and Oceanography Letters*, **7**:510-519. doi:10.1002/lol2.10274

Van Donk, E., A. Ianora, and M. Vos. 2011. Induced defences in marine and freshwater phytoplankton: a review. *Hydrobiologia*, **668**:3-19. doi:10.1007/s10750-010-0395-4

Vanni, M. J. 2002. Nutrient cycling by animals in freshwater ecosystems. *Annual Review of Ecology and Systematics*, **33**:341-3070. doi:10.1146/annurev.ecolsys.33.010802.15051

Vanni, M. J., and D. L. Findlay. 1990. Trophic cascades and phytoplankton community structure, *Ecology*, **71**:921-937. doi:10.2307/1937363.

Vanni, M. J., C. Luecke, J. F. Kitchell, Y. Allen, J. Temte, and J. J. Magnuson. 1990. Effects on lower trophic levels of massive fish mortality. *Nature*, **344**:333-335. doi:10.1038/344333a0

Vitousek, P. M. 1994. Beyond global warming: ecology and global change. *Ecology*, **75**:1861-1876. doi:10.2307/1941591

Supplemental Materials

Experiment overview

We aimed to experimentally compare ecological dynamics in tri-trophic food webs (producers, consumers, and predators) following three different ecological perturbations: predator removals (i.e., top-down effects only), resource pulses (i.e., bottom-up effects only), and predator mass mortality events (i.e., both top-down and bottom-up effects manipulated, henceforth "MMEs"). We specifically aimed to compare these perturbations to an undisturbed experimental control (i.e., no top-down or bottom-up effects) and make comparisons amongst different perturbations. The predator MME that was experimentally induced for this study exemplifies a single trophic-level event, such as might occur during a disease outbreak – the leading cause of MMEs in freshwater fish (Fey et al., 2015; Tye et al., 2022).

We focused these inquiries on lentic tri-trophic food web responses for four reasons. First, freshwater systems have well-understood trophic links, such as between planktivorous fish and herbivorous zooplankton (Brooks and Dodson, 1965; Porter, 1973; DeMott and Kerfoot, 1982; Bergquist and Carpenter, 1986; Threlkeld, 1988; Vanni and Findlay, 1990; Hansen et al., 1997). Second, freshwater lake systems frequently experience fish MMEs (Fey et al., 2015; Tye et al., 2022), and fish carrion rapidly decomposes and remineralizes within lentic systems (Threlkeld, 1988; Vanni and Findlay, 1990; Vanni et al., 1990; Nagdali and Gupta, 2002; Boros et al., 2015). Moreover, fish MMEs in nature rapidly generate temporary increases in total productivity (Vanni et al., 1990) limiting nutrient concentrations (Nagdali and Gupta, 2002). Third, the addition and/or removal of fish predators and resources rapidly alters zooplankton and phytoplankton community structure (Threlkeld, 1988; Vanni and Findlay, 1990). Lastly, freshwater lake community ecology dynamics can be coarsely approximated using smaller-scale

experimental mesocosms (Spivak et al., 2011; Dzialowski et al., 2014). This approach is also important because mesocosm experiments, unlike whole lake manipulations and natural observations, can be replicated and controlled (Spivak et al., 2011; Dzialowski et al., 2014) and are amendable toward studying extreme events that are relatively rare in nature, such as MMEs in wild populations (Vanni et al., 1990; Nagdali and Gupta, 2002).

Recent theory predicts that predator MMEs simultaneously generate top-down and bottom-up forces, and thereby exhibit distinct temporal ecological dynamics that cannot be explained solely by the independent effects of predator removals or resource pulses (Fey et al., 2019). We therefore conducted a mesocosm experiment with a 2×2 factorial design (Fig. 1: Experimental design; 5 replicates each) by manipulating the presence/absence of live fish predators and the presence/absence of dead fish predators (i.e., fish carrion) to create three different ecological perturbations and an experimental control. These perturbations included predator removals (10 live fish absent, dead fish absent), resource pulses (10 live fish present, 10 dead fish added), and predator MMEs (live fish absent, 10 dead fish added), in addition to an undisturbed control treatment (10 live fish present, dead fish absent).

Freshwater mesocosms

We prepared twenty mesocosms by sequentially adding trophic levels over five weeks, waiting three weeks, removing all fish predators across mesocosms to induce similar disturbances and perform fish euthanasia via approved procedures (IACUC #191060), and inducing treatments with live and euthanized fish (Fig. 1: Visual comparison). We then extensively monitored (Fig. S1B) zooplankton communities, microalgae communities (i.e., phytoplankton within the size range of 2-100 μm that are readily consumed by common zooplankton (Porter, 1973; Bergquist

and Carpenter, 1986; Hansen et al., 1997), and total productivity (chlorophyll-*a*) for 120 days. This experimental duration encompassed the timespan that limiting nutrient concentrations (i.e., N, P) are typically elevated and diminish after experimentally induced bluegill mortalities in similar sized mesocosms (Boros et al., 2015). We checked mesocosms roughly daily for inadvertently dead bluegill and, when necessary, replaced each with a similarly sized live bluegill. We later excluded one replicate each from the predator removal and resource pulse treatments because frogs deposited eggs and a *Euglena* algal bloom occurred, respectively. Thus, there were 5 mesocosm replicates for the MME and control treatments, and 4 mesocosm replicates for the predator removal and resource pulse treatments.

We arranged twenty 1000-L mesocosms (1.61 m × 1.75 m × 0.64 m) in a 2 × 10 matrix at an outdoor facility at the University of Arkansas, Fayetteville, USA. Each mesocosm was filled with 750-L of low-nutrient tap water that was allowed to dechlorinate for one week. We added 10 partially unraveled strands of 0.91 m × 0.95 cm polyester rope weighted down by a cinderblock to the same quadrant of each mesocosm to serve as underwater refugia for fish and zooplankton. Each mesocosm was covered with 1-mm plastic mesh to hinder introduction of non-target taxa, as well equipped with a plastic tarp that was used to cover mesocosms when heavy precipitation occurred to help mitigate substantial water level changes. We obtained leaf litter from deciduous forests surrounding Lake Wilson, Arkansas, USA (35.999387º, -94.136369º, WGS84) and dried it for 1-week, after which we added 500-g of dried leaf litter to each mesocosm for an initial nutrient source and microbial detritivore community.

After one week, we inoculated each mesocosm with local phytoplankton communities via ~189 L of filtered lake water (125-µm sieve) obtained from the littoral zone of Lake Wilson, AR. We then allowed phytoplankton communities to proliferate for two weeks before adding

zooplankton. We collected zooplankton from the littoral zone of Lake Wilson, AR, USA at day (~0.5 m depth) and night (<1 m depth) via a 50-µm mesh net. Lake Wilson is a low-productivity lake with low chlorophyll-*a* (~3.7 µg/L) and zooplankton densities (~59 individuals/L) over recent surveys. We removed insect taxa from each zooplankton sample to the best of our ability and then consolidated zooplankton samples in a separate 1000-L mesocosm that was assembled as described above. This sample consolidation process was necessary to acquire adequate zooplankton abundances for stocking mesocosms at target densities. After collecting zooplankton for two weeks, we passed the consolidated zooplankton samples through a 50-µm sieve and aliquoted filtered samples into 20 subsamples that contained ~200 individuals of each locally dominant zooplankton family: Brachionidae, Bosminidae, Cyclopoida, Cyprididae, and Daphniidae.

We allowed zooplankton communities to proliferate for 10 days before adding 10 live bluegill (*Lepomis macrochirus*) of similar length (mean = 5.15 cm; *SD* = 0.33 cm), which were obtained from the Arkansas Department of Game and Fish, to each mesocosm. Bluegill are common planktivorous fish that act as keystone predators in littoral communities (Hall et al., 1970). To ensure all mesocosms initially experienced similar ecological dynamics, we maintained tri-trophic food webs across mesocosms for three weeks before inducing treatments. Next, we used an electroshocker to remove all fish from all mesocosms and perform euthanasia by rapid chilling for at least 1 hr (~2-4ºC) and then freezing fish (for those assigned to predator mortalities) for at least 24 hrs (IACUC #191060; Appendix I). We administered the electroshocker to all mesocosms to ensure that there were no potential effects of electroshocking specific treatments and so all community members within mesocosms (i.e., producers, consumers) were equally affected. Additionally, this approach helped avoid potential

confounding factors from chemical-based euthanasia approaches (Neiffer and Stamper, 2009). The following day, we used additional live bluegill, that were housed in non-experimental mesocosms, and euthanized bluegill, obtained from the above procedure, to induce treatments. To haphazardly assign treatments to mesocosms (n = 5 per treatment), we used a random number generator.

Sample collection

We were specifically interested in whether predator removals, resource pulses and predator MMEs generated disparate responses via trophic biomass, community structure, functional trait composition, and transient ecological dynamics. Therefore, we extensively monitored zooplankton communities, microalgae communities, and chlorophyll-*a* over the entire experimental duration to make comparisons between these four key aspects of food web dynamics. Because recent theory suggests predator MMEs generate transient dynamics that are distinguishable from dynamics expected from independent effects of predator removals or resource pulses[6], we used a high-intensity sampling regime to capture transient dynamics that may differentiate these perturbations. This sampling regime involved two different sampling intensities over the experimental duration: once per week for the first three weeks (i.e., before treatments were induced), then twice per week for five weeks, then once per week for ten additional weeks. For each sampling effort, we collected zooplankton and phytoplankton samples over three consecutive days. This sampling effort was necessary due to logistical constraints and involved acquiring phytoplankton samples over two consecutive days and zooplankton samples over one separate day for each respective sampling period. We used these samples to estimate total productivity (chlorophyll-*a*) and enumerate characteristics of

zooplankton and microalgae communities, which were identified to taxonomic levels (family and phyla, respectively) that are often considered different functional groups (Barnett et al., 2007; Cupertino et al., 2019).

To estimate total water column productivity and quantify microplankton community structure, we collected 250 mL of surface water from the center of each mesocosm to measure chlorophyll-*a* and perform flow cytometry, respectively. For chlorophyll-*a* estimates, two 50-mL subsamples were passed through 47-mm wide nylon filters with 0.22-um perforations (AllPure Biotechnology, New Oxford, PA), placed in separate scintillation tubes with 4 mL of 95% ethanol, and refrigerated for 24 hrs. We used a fluorometer (Trilogy, Turner Designs Inc., San Jose, CA) to quantify chlorophyll-*a* from both samples: the mean value was used in all analyses.

To quantify microalgae community structure, we examined the remaining water sample via flow cytometry (FlowCAM VS-Series, Fluid Imaging Inc., Scarborough, MN). To perform flow cytometry, we first passed each water sample through a 125-µm sieve and homogenized them, after which a 2-mL subsample was placed through a 100-µm x 1-mm FlowCell (Fluid Imaging Inc., Scarborough, MN). FlowCam settings across image collection included an *AutoImage rate* of 20 frames / sec and *flow rate* of 0.170 mL / min, which resulted in an approximate run time of ~18 mins and a 23.4% efficiency rate per sample. These settings were similar to previous studies that used flow cytometry (Hrycik et al., 2019). To classify microalgae taxa, we post-hoc examined all images from every fifth sample from each mesocosm to create image libraries of dominant genera. We then manually assigned images to microalgae genera and categorized genera by phylum: Charophyta (*Cosmarium*, *Mougeotia*, *Staurastrum*), Chlorophyta (*Ankistrodesmus, Closteriopsis, Closterium, Coelastrum, Crucigenia, Franceia, Oocystis,*

Scenedesmus), Cyanobacteria (*Anabaena*), Dinoflagellata (*Gymnodinium*), Euglenozoa (*Euglena*). In total, we identified 28,161 microalgae to phylum for analyses.

Because we were interested in understanding how perturbations affected microalgae community dynamics through time, we used flow cytometry data to enumerate microalgae biomass, density, and biovolume (area-based volume) through time. For microalgae density estimates, we converted abundance estimates of each microalgae phylum and across phyla from each flow cytometry sample (2-mL) to natural log-transformed density per L. For microalgae biovolume estimates, we used the area-based volume of each microalgae individual and the FlowCam VS-Series image scaling factor (0.56) to estimate mean biovolume of each phylum and across phyla for each sample. Specifically, we used mean area-based volume in volume-biomass equations of congener microalgae (Verity et al., 1992; Menden-Deuer and Lessard, 2000) to estimate biomass of each microalgae individual. We used these data to calculate natural log-transformed biomass per L of each phylum and across phyla. Microalgae density and biomass estimates were similar to estimates in previous studies with similar flow cytometry equipment (Hrycik et al., 2019). We used chlorophyll-*a* as a proxy for total productivity and microplankton biomass as a proxy for the availability of key resources to consumers.

We also quantified zooplankton biomass, density, and body size through time. To acquire zooplankton samples, we lightly mixed each mesocosm with a perforated Secchi disk (~20 cm diameter), allowed disturbed leaf litter to settle, and placed an integrated tube sampler (~5 cm diameter, ~91 cm length) through the water column. We used standardized measurements on the side of the integrated tube sampler to measure the water level of each mesocosm to improve estimates of mesocosm water volume when samples were acquired, and thus zooplankton density estimates, through time. All zooplankton samples were collected from the same quadrant across

mesocosms. We passed zooplankton samples through a 125-µm sieve and placed samples in Lugol's iodine solution for preservation and to aid visual identification. In total, we identified 10,642 zooplankton to taxonomic family for analyses.

We used light microscopy (20x; Leica Camera Model EC4, Wetzlar, Germany) to identify and measure body sizes of dominant zooplankton families: Bosminidae (*Bosmina*), Brachionidae (*Brachionus*), Cyclopidae (*Cyclops*), Cypridídae (*Cypridopsis*), and Daphniidae (*Daphnia*). We measured body sizes of 10 haphazardly selected individuals (or all individuals if there were < 10) for each zooplankton family from each sample. We used mean body size of each zooplankton family and sample period to estimate mean zooplankton biomass via length-weight regressions for Bosminidae (Bottrell et al., 1976), Brachionidae (Bottrell et al., 1976), Cyclopidae (Bottrell et al., 1976), Cypridídae (Bottrell et al., 1976), and Daphniidae (Davis and Wiebe, 1985). We used these data to calculate natural log-transformed biomass per L of each zooplankton family and across families. Lastly, we converted abundances of each zooplankton family and across families to natural log-transformed density per L.

Prior to statistical analyses, we calculated smooth-moving averages, as in similar studies (Vanni and Findlay, 1990), to reduce the propagation of sampling error into temporal variation of chlorophyll-*a*, zooplankton community characteristics (biomass, density, body size), microalgae community characteristics (biomass, density, biovolume). These smoothed averages were over three adjacent sample periods (i.e., a focal, previous, and subsequent sample period) and, therefore, the earliest and latest sample period were excluded from this summarized dataset. We used smoothed data at the replicate-level for all statistics except for one set of analyses, noted below, in which when we used smoothed averages at the treatment-level (i.e., averaged by treatment).

Statistical analyses

We used three statistical approaches to compare ecological dynamics following disturbances. First, we used two-sided, two-way ANOVAs to understand whether MMEs exhibited additive or non-additive (i.e., synergistic or antagonistic) effects of predator removals and resource pulses on trophic biomass. This was possible because treatments included all combinations of these two factors: 1) predator removals (both fish and carrion absent), 2) resource pulses (both fish and carrion present), 3) MMEs (fish absent, carrion present), and 4) a control treatment (fish present, carrion absent). These models had the form: response ~ predator removal × resource pulse with a nested random effect of sampling period and mesocosm. We used trophic biomass (chlorophyll-*a*, zooplankton biomass, or microalgae biomass) as the response variable and considered the control treatment as the reference group. If present, we considered a significant interaction to be indicative of non-additive (i.e., interactive) effects MMEs on trophic biomass over the entire experimental duration that would not be readily predicted by the simple additive effects (i.e., only independent effects) of predator removals and resource pulses.

Second, we used general additive mixed models (GAMMs; Wood, 2004) to understand whether disturbances generated disparate responses in zooplankton and microalgae communities through time. These models had biomass, density, and body size or biovolume of trophic levels (i.e., chlorophyll-*a*, zooplankton, or microalgae) or functional groups (i.e., zooplankton family or microalgae phyla) as separate response variables. All GAMMs had a Gamma error distribution with a log link, except for models with zooplankton body size because they did not require log transformations. For each response variable, we used AIC to compare five GAMM forms (Table S3) that allowed for different or similar shapes, different or similar intercepts, and the presence/absence of a smoothing penalization on the time effect. These models included fixed

effects of treatment, sample, or both treatment and sample, as well as the presence/absence of a smoothing penalization on the time effect. For these models, we used treatment as the predictor variable with the control treatment as the reference group, rather than predictor variables of predator removal × resource pulse as in the first approach, so that there were treatment-specific temporal smoothing penalizations.

For models that were better explained with temporal smoothing penalization (i.e., Models 4-5 in Table S3), we performed additional model selection to obtain the best penalization parameter and account for correlation of autoregressive moving averages via ARMA via the *nlme* package (Pinherio et al., 2022). We used AIC to compare six dimensions (k; 3, 5, 8, 10, 12, and 15), which encompassed the full range of possible dimensions, for the smooth term for each model via penalized spline regressions in the *mgcv* package (Wood, 2004). The final form of each GAMM is listed in Table S4. For all GAMMs, we considered differences in intercepts (i.e., parametric coefficients of treatments and corresponding *t*-values) to indicate differences in mean responses, and differences in model shape (i.e., treatment-specific time effect) to indicate whether treatments had different trajectories, compared to the control. For brevity, we only discuss differences in intercepts for GAMMs in the Main Text. We used this GAMM-based approach for all biomass, density, and body size or biovolume responses except for biovolume of three microalgae phyla (Cyanobacteria, Dinoflagellata, and Euglenozoa), which were too variable within and across mesocosms for meaningful inferences and, therefore, only summarized for descriptive purposes (Fig. 2B).

Third, we used communities trajectory analyses (de Cáceres et al., 2019; Sturbois et al., 2021) to compare the ordination of zooplankton and microalgae community biomass dynamics following perturbations. This recently developed approach can be used to examine and compare

dynamics of biological systems (e.g., communities) via principal coordinate analyses (PCoA). In this approach, experimental units are tracked through time and differences in temporal dynamics are quantified by their position along axes (i.e., PCoA loadings of different taxonomic groups). Importantly, this approach requires data continuity and there were several microalgae samples in which Cyanobacteria and/or Euglenozoa were not observed even though they were usually present in previous and subsequent samples. Therefore, to account for this lack of information and ensure data continuity without distorting trends, we added the minimum observed biomass and density (across all mesocosms and samples) to each microalgae phyla biomass and density estimate prior to performing these analyses.

To obtain and compare metrics about temporal dynamics following perturbations, we performed ecological trajectory analyses at two different experimental resolutions (discussed below). For these analyses, we first determined the most appropriate ordination approach by comparing Euclidean distances to several dissimilarity indices, including Bray-Curtis, local transformation, square root, metric multidimensional scaling (MDS), and non-metric multidimensional scaling (NMDS). We used local transformations because they provided the lowest stress levels (>0.2; Dexter et al., 2018), passed the triangle inequality, and are recommended to limit distortion and aid interpretability of ecological trajectories (de Cáceres et al., 2019).

We conducted these analyses with experimental units at the replicate-level, which provided mean and standard deviation measurements, to compare two characteristics about community biomass dynamics between perturbations (Fig. S9): mean directionality and mean segment length. Mean directionality (Fig. S9A, top) indicates the directional stability of a trajectory through time, such that a greater mean directionality would indicate a straighter and

more directionally stable trajectory through time. Mean segment length (Fig. S9A, bottom) indicates the average distance in ordination space between adjacent sample periods along trajectories. This metric can be interpreted as the rate of community structure change, such that a greater mean segment length would indicate a greater distance spanned over comparable sample periods.

We conducted ecological trajectory analyses with experimental units at the treatment-level (smoothed data averaged by treatment, as shown in Fig. 3) to make two comparisons about generalized temporal dynamics between perturbations. We used coarser experimental units for these comparisons because they involved numerous pairwise comparisons and, therefore, treatment-level analyses provided a single test statistic for each pairwise comparison between perturbations (Fig. 3). For these analyses, we calculated mean directed segment path dissimilarity (DSPD), which represents the average distance between segment midpoints of different trajectories in community ordination space at comparable sample periods. More generally, this metric represents how far or close different trajectories are from each other through time, such that a greater DSPD would indicate trajectories were further apart through time. Second, we used Mann-Whitney tests via the *ecotraj* package (de Cáceres et al., 2019) to examine whether treatment-level trajectories (Fig. 3) converged or diverged over time (Table S1-S2).

We checked models for meeting assumptions of homogeneity of variance and normality. For ANOVAs and GAMMs, we considered treatment effects statistically significant based on a $\alpha = 0.05$. For ecological trajectory analyses, we considered instances where treatments exhibited nonoverlapping 95% confidence intervals to be statistically significantly different from one another. All statistical tests were performed in R (version 4.2.1).

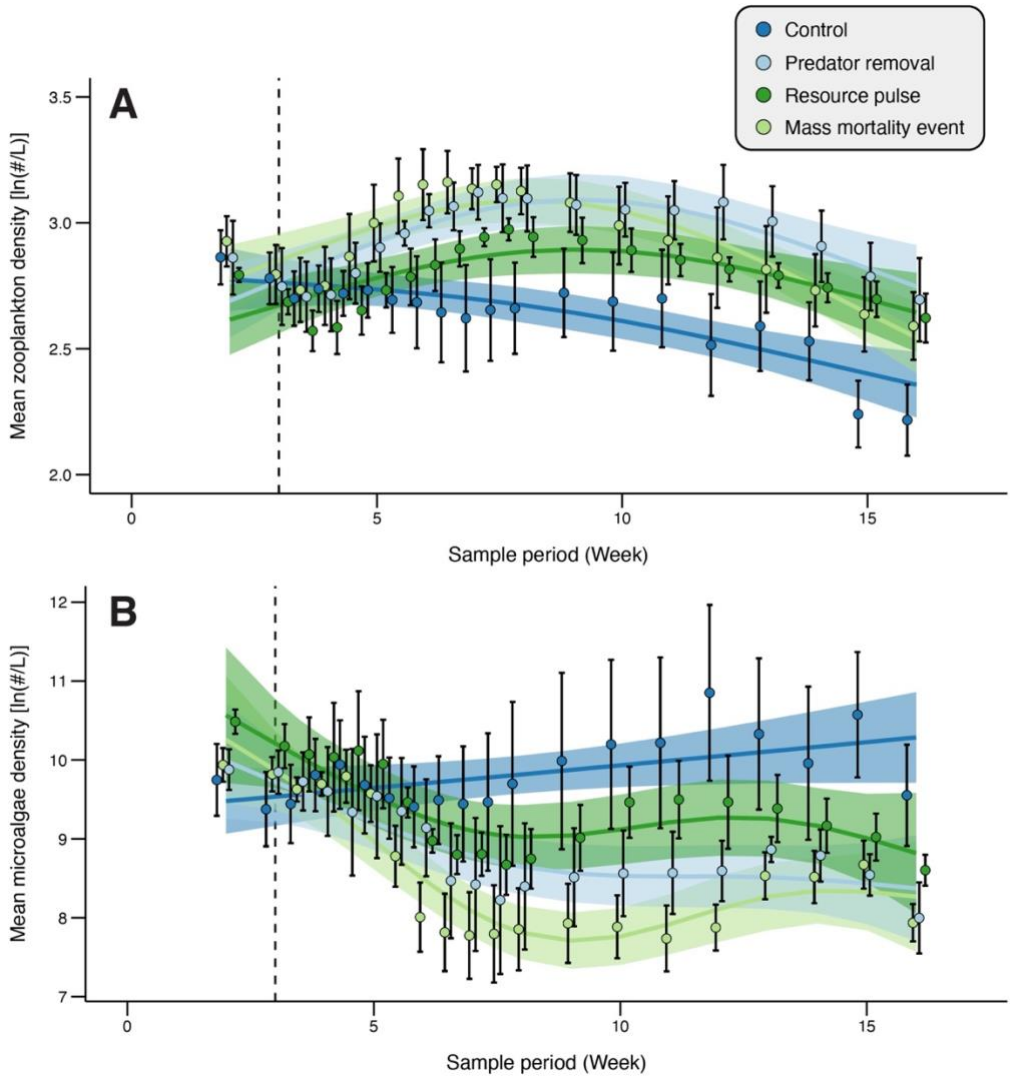

Figure S1. Time-series of mean zooplankton and microalgae density following ecological perturbations. Mean density of zooplankton (A, [ln(individuals/L]) and microalgae (B, [ln(individuals/L]) following predator mass mortality events (MMEs, light green), predator removals (light blue), and resource pulses (dark green), as well as the undisturbed system (control, dark blue). Points and lines indicate means +/- 1 SE for each sampling period and treatment, with points jittered to reduce overlap within sample periods. Solid lines and shaded regions indicate model predictions and 95% confidence intervals, respectively. Relative to the

control, MMEs ($t_{11.42} = 7.51$, $p < 0.01$), predator removals ($t_{11.42} = 7.35$, $p < 0.01$), and, to a lesser extent, resource pulses ($t_{11.42} = 3.73$, $p < 0.01$) increased mean zooplankton density. MMEs ($t_{13.36} = -7.95$, $p < 0.01$), predator removals ($t_{13.36} = -5.28$, $p < 0.01$), and, to a lesser extent, resource pulses ($t_{13.36} = -2.43$, $p = 0.02$) decreased mean microalgae density. Dashed lines indicate when perturbations were induced (i.e., live fish and/or fish carrion added and/or removed).

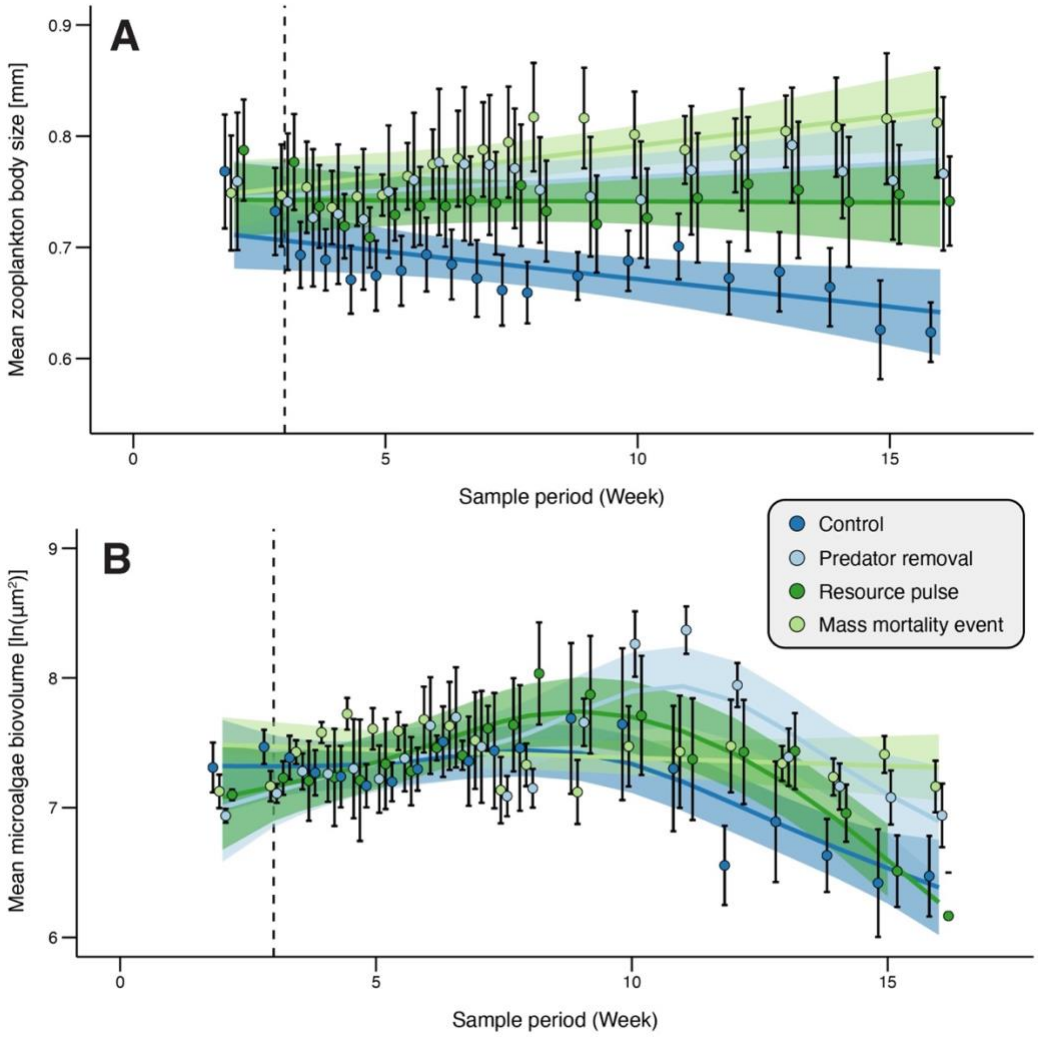

Figure S2. Time-series of mean zooplankton body size and microalgae biovolume following ecological perturbations. Mean zooplankton body size (A, [mm]) and microalgae biovolume (B, [ln(µm^2]) following predator mass mortality events (MMEs, light green), predator removals (light blue), and resource pulses (dark green), as well as the undisturbed system (control, dark blue). Points and lines indicate means +/- 1 SE for each sampling period and treatment, with points jittered to reduce overlap within sample periods. Solid lines and shaded regions indicate model predictions and 95% confidence intervals, respectively. Relative to the control, MMEs (t_8 = 8.42, $p < 0.01$), predator removals (t_8 = 6.29, $p < 0.01$), and resource pulses (t_8 = 4.99, $p <$

0.01) increased mean zooplankton body size. MMEs ($t_{15.06} = 2.58$, $p = 0.02$) and predator removals ($t_{15.06} = 2.48$, $p = 0.02$), but not resource pulses ($t_{15.06} = 1.32$, $p = 0.19$), increased mean microalgae biovolume. Dashed lines indicate when perturbations were induced (i.e., live fish and/or fish carrion added and/or removed).

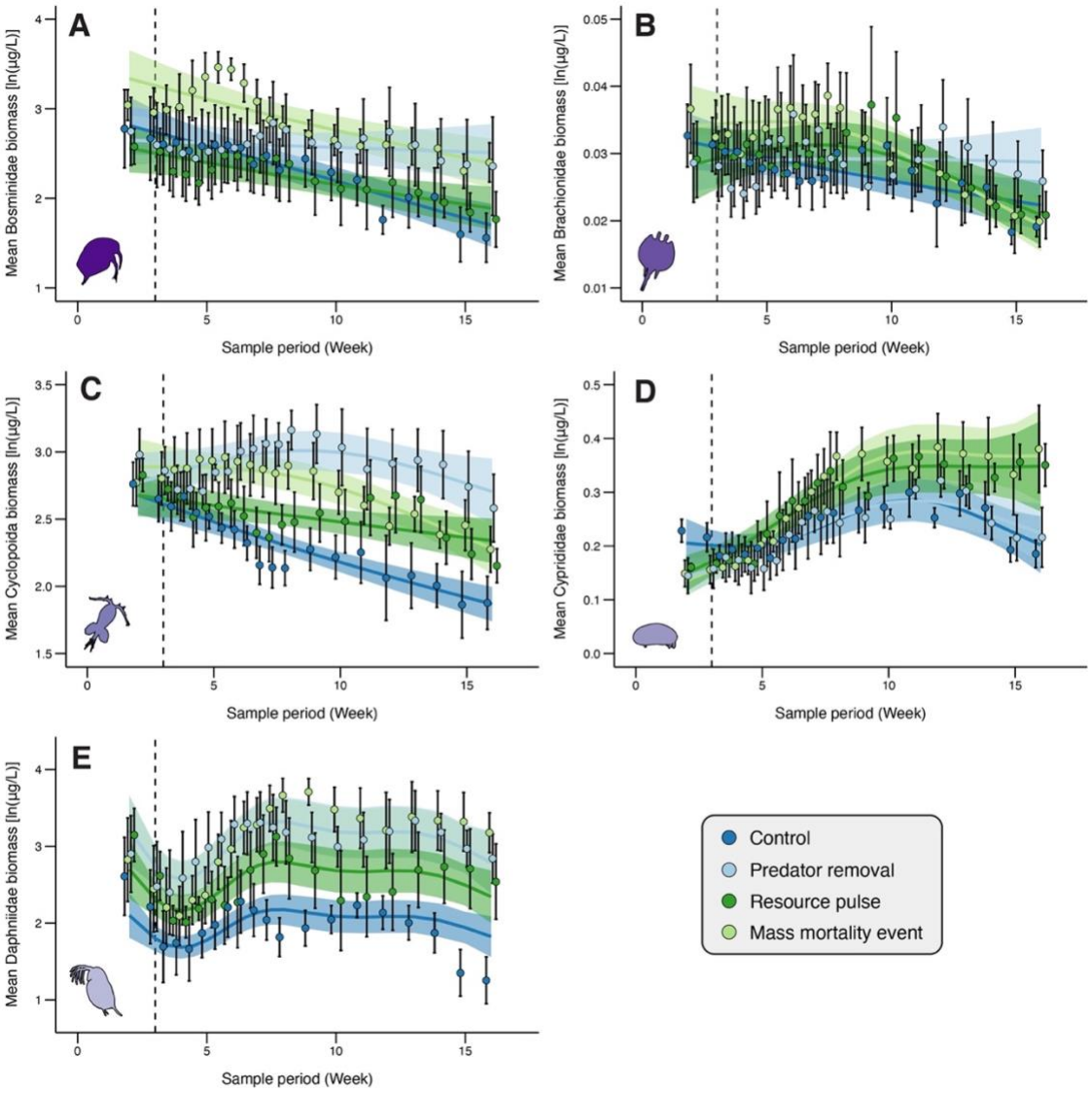

Figure S3. Time-series of mean biomass across five major zooplankton families following ecological perturbations. Zooplankton biomass [ln(µg/L)] of Bosminidae (A), Brachionidae (B), Cyclopoida (C), Cyprididae (D), and Daphniidae (E) following predator mass mortality events (MMEs, light green), predator removals (light blue), and resource pulses (dark green), as well the undisturbed system (control, dark blue). Points and lines indicate means +/- 1 SE for each sampling period and treatment, with points jittered to reduce overlap within sample periods. Solid lines and shaded regions indicate model predictions and 95% confidence intervals,

respectively. Relative to the control, MMEs increased mean biomass of Bosminidae ($t_{8.36} = 5.74$, $p < 0.01$; A), Brachionidae ($t_{9.78} = 2.31$, $p = 0.02$; B), Cyclopoida ($t_{9.59} = 8.33$, $p < 0.01$; C), Cypridiidae ($t_{15} = 2.98$, $p < 0.01$; D), and Daphniidae ($t_{9.34} = 9.31$, $p < 0.01$; E). Predator removals increased mean biomass of Bosminidae ($t_{8.36} = 2.70$, $p = 0.008$; A), Cyclopoida ($t_{9.59} = 10.49$, $p < 0.01$; C) and Daphniidae ($t_{9.34} = 8.84$, $p < 0.01$; E). Resource pulses increased mean biomass of Cyclopoida ($t_{9.59} = 8.42$, $p < 0.01$; C), Cypridiidae ($t_{15} = 2.30$, $p = 0.01$; D), and Daphniidae ($t_{9.34} = 5.23$, $p < 0.01$; E). Dashed lines indicate when perturbations were induced (i.e., live fish and/or fish carrion added and/or removed). Taxa silhouettes and their colors correspond with major zooplankton families as in main figures.

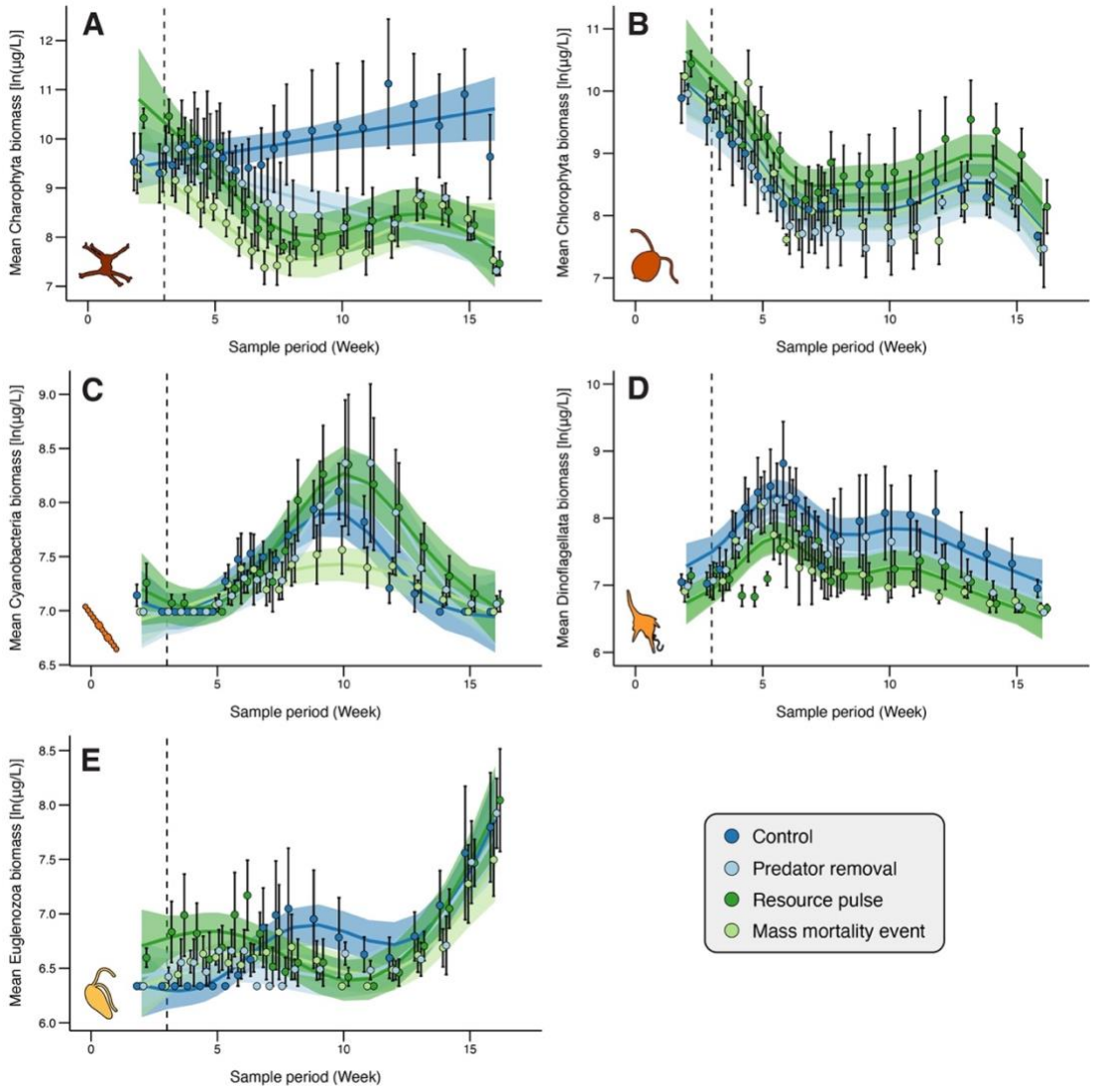

Figure S4. Time-series of mean biomass across five major microalgae phyla following ecological perturbations. Microalgae biomass [ln(µg/L)] of Charophyta (A), Chlorophyta (B), Dinoflagellata (C), Cyanobacteria (D), and Euglenozoa (E) following predator mass mortality events (MMEs, light green), predator removals (light blue), and resource pulses (dark green), as well the undisturbed system (control, dark blue). Points and lines indicate means +/- 1 SE for each sampling period and treatment, with points jittered to reduce overlap within sample periods. Solid lines and shaded regions indicate model predictions and 95% confidence intervals, respectively. Relative to the control, MMEs decreased mean biomass of Charophyta ($t_{12.81}$ = -

9.93, $p < 0.01$; B) and Dinoflagellata ($t_{22.1} = -5.04$, $p < 0.01$; D), and had relatively low mean Cyanobacteria biomass ($t_{22.1} = -1.85$, $p = 0.07$; C). Predator removals decreased mean biomass of Charophyta ($t_{12.81} = -5.69$, $p < 0.01$; B) and Dinoflagellata ($t_{22.1} = -2.47$, $p = 0.01$; D). Resource pulses increased mean biomass of Chlorophyta ($t_{10.01} = 3.19$, $p = 0.01$; B) and Cyanobacteria ($t_{22.1} = 2.05$, $p = 0.04$; C), and decreased mean biomass of Charophyta ($t_{12.81} = -6.07$, $p < 0.01$; A) and Dinoflagellata ($t_{22.1} = -4.89$, $p < 0.01$; D). Dashed lines indicate when perturbations were induced (i.e., live fish and/or fish carrion added and/or removed). Taxa silhouettes and their colors correspond with major microalgae phyla as in main figures.

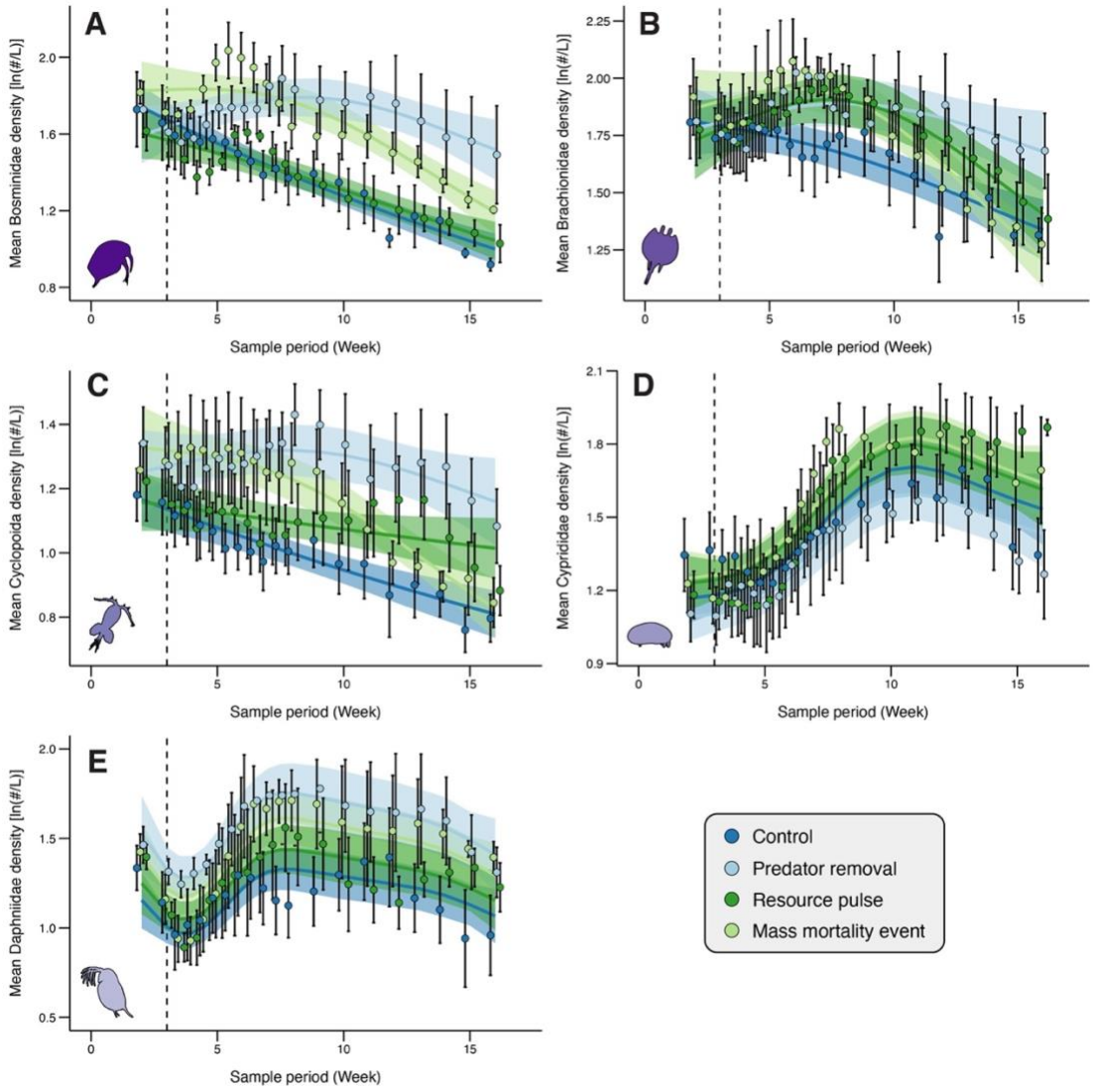

Figure S5. Time-series of mean density across five major zooplankton families following ecological perturbations. Zooplankton density [ln(individuals /L)] of Bosminidae (A), Brachionidae (B), Cyclopoida (C), Cyprididae (D), and Daphniidae (E) following predator mass mortality events (MMEs, light green), predator removals (light blue), and resource pulses (dark green), as well as the undisturbed system (control, dark blue). Points and lines indicate means +/- 1 SE for each sampling period and treatment, with points jittered to reduce overlap within sample periods. Solid lines and shaded regions indicate model predictions and 95% confidence intervals, respectively. Relative to the control, MMEs increased mean density of all major zooplankton

families including Bosminidae ($t_{10.4} = 8.05$, $p < 0.01$; C), Brachionidae ($t_{11.13} = 3.00$, $p < 0.01$; C), Cyclopoida ($t_{9.53} = 5.70$, $p < 0.01$; C), Cyprididae ($t_{7.44} = 2.09$, $p = 0.04$; C), and Daphniidae ($t_{9.4} = 4.38$, $p < 0.01$; C). Predator removals increased mean density of Bosminidae ($t_{10.4} = 8.36$, $p < 0.01$; C), Brachionidae ($t_{11.13} = 4.12$, $p < 0.01$), Cyclopoida ($t_{9.53} = 8.34$, $p < 0.01$; C), and Daphniidae ($t_{9.4} = 5.95$, $p < 0.01$; C) as well as reduced mean Cyprididae density ($t_{7.44} = -1.98$, $p = 0.05$; C). Resource pulses increased mean density of Brachionidae ($t_{11.13} = 2.99$, $p < 0.01$; C) and Cyclopoida ($t_{9.53} = 3.13$, $p < 0.01$; C). Dashed lines indicate when perturbations were induced (i.e., live fish and/or fish carrion added and/or removed). Taxa silhouettes and their colors correspond with major zooplankton families as in main figures.

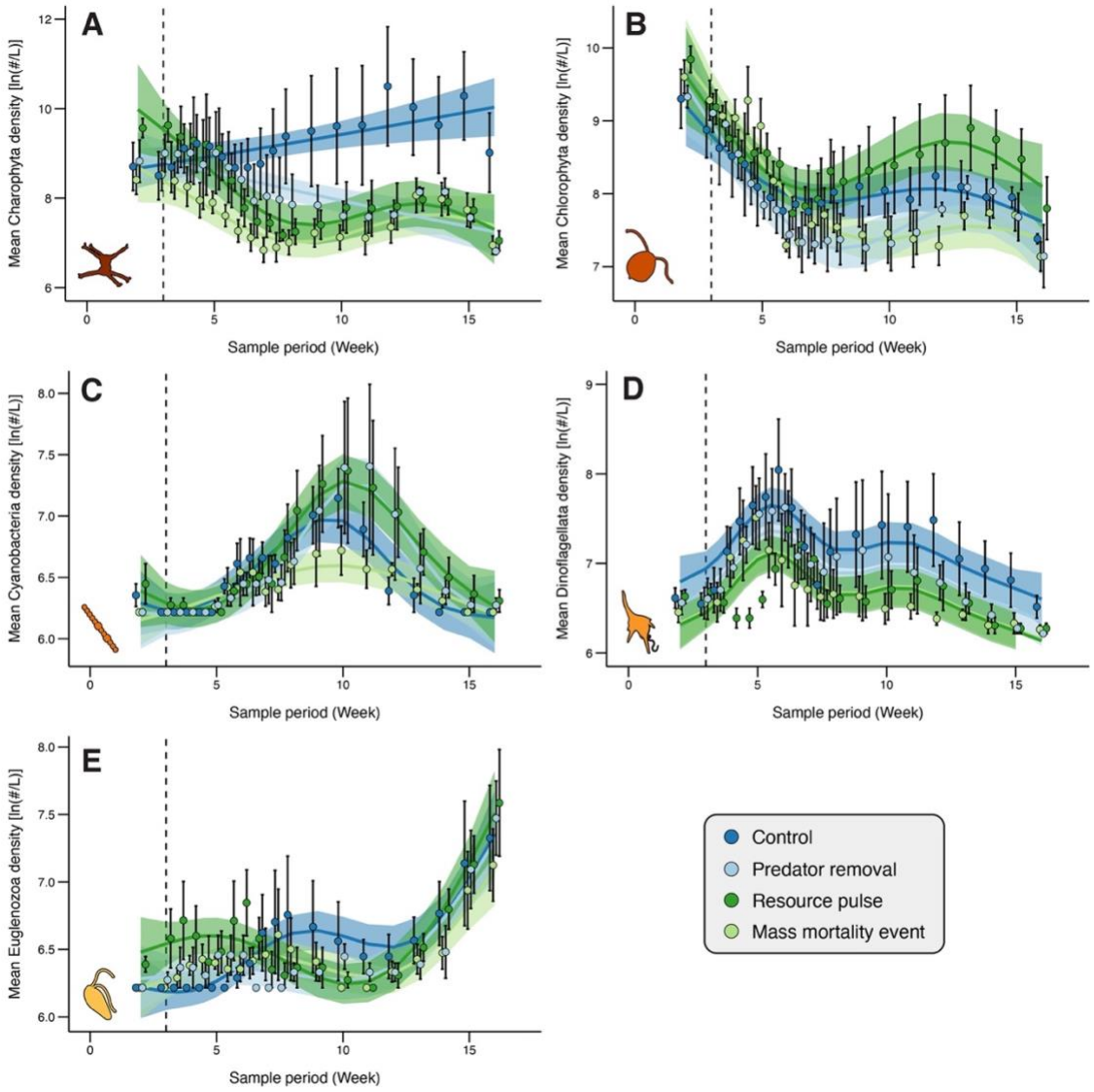

Figure S6. Time-series of mean density across five major microalgae phyla following ecological perturbations. Microalgae density [ln(individuals/L)] of Charophyta (A), Chlorophyta (B), Dinoflagellata (C), Cyanobacteria (D), and Euglenozoa (E) following predator mass mortality events (MMEs, light green), predator removals (light blue), and resource pulses (dark green), as well as the undisturbed system (control, dark blue). Points and lines indicate means +/- 1 SE for each sampling period and treatment, with points jittered to reduce overlap within sample periods. Solid lines and shaded regions indicate model predictions and 95%

confidence intervals, respectively. Relative to the control, MMEs decreased mean density of Charophyta ($t_{12.42}$ = -9.83, p < 0.01) and Dinoflagellata ($t_{9.87}$ = -5.18, p < 0.01), as well as had relatively low mean density of Cyanobacteria ($t_{21.86}$ = -1.67, p = 0.10). Predator removals decreased density of Charophyta ($t_{12.42}$ = -5.63, p < 0.01), Chlorophyta ($t_{17.14}$ = -2.47, p = 0.02), and Dinoflagellata ($t_{9.87}$ = -5.18, p < 0.01). Resource pulses increased mean density of Chlorophyta ($t_{17.14}$ = 2.86, p = 0.01) and reduced mean density of Charophyta ($t_{12.42}$ = -5.98, p < 0.01) and Dinoflagellata ($t_{9.87}$ = -5.11, p < 0.01), as well as had relatively high mean density of Cyanobacteria ($t_{21.86}$ = 1.93, p = 0.06). Dashed lines indicate when perturbations were induced (i.e., live fish and/or fish carrion added and/or removed). Taxa silhouettes and their colors correspond with major microalgae phyla as in main figures.

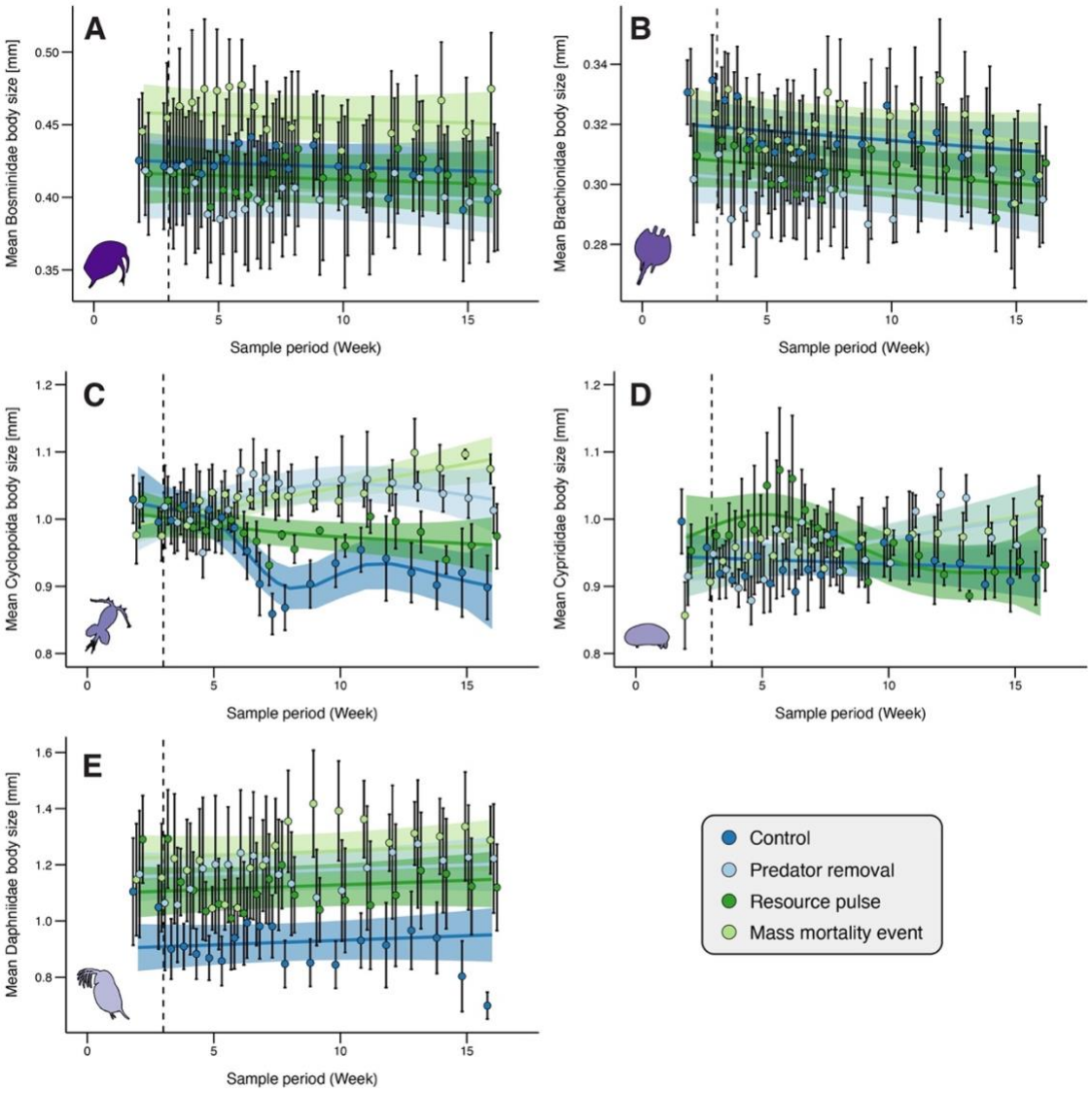

Figure S7. Time-series of mean body size across five major zooplankton families following ecological perturbations. Zooplankton body size (mm) of Bosminidae (A), Brachionidae (B), Cyclopoida (C), Cyprididae (D), and Daphniidae (E) following predator mass mortality events (MMEs, light green), predator removals (light blue), and resource pulses (dark green), as well as the undisturbed system (control, dark blue). Points and lines indicate means +/- 1 SE for each sampling period and treatment, with points jittered to reduce overlap within sample periods. Solid lines and shaded regions indicate model predictions and 95% confidence intervals,

respectively. Relative to the control, MMEs increased mean body size of Bosminidae ($t_5 = 2.98$, $p < 0.01$), Cyclopoida ($t_{12.93} = 7.57$, $p < 0.01$), and Daphniidae ($t_5 = 6.71$, $p < 0.01$). Predator removals increased mean body size of Cyclopoida ($t_{12.93} = 6.98$, $p < 0.01$) and Daphniidae ($t_5 = 5.09$, $p < 0.001$), as well as decreased mean body size of Brachionidae ($t_5 = -3.17$, $p < 0.01$). Resource pulses increased mean body size of Cyclopoida ($t_{12.93} = 2.68$, $p = 0.01$), Cypridiidae ($t_{9.74} = 2.16$, $p = 0.03$), and Daphniidae ($t_5 = 3.88$, $p < 0.01$), as well as decreased mean body size of Brachionidae ($t_5 = -2.14$, $p = 0.03$). Dashed lines indicate when perturbations were induced (i.e., live fish and/or fish carrion added and/or removed). Taxa silhouettes and their colors correspond with major zooplankton families as in main figures.

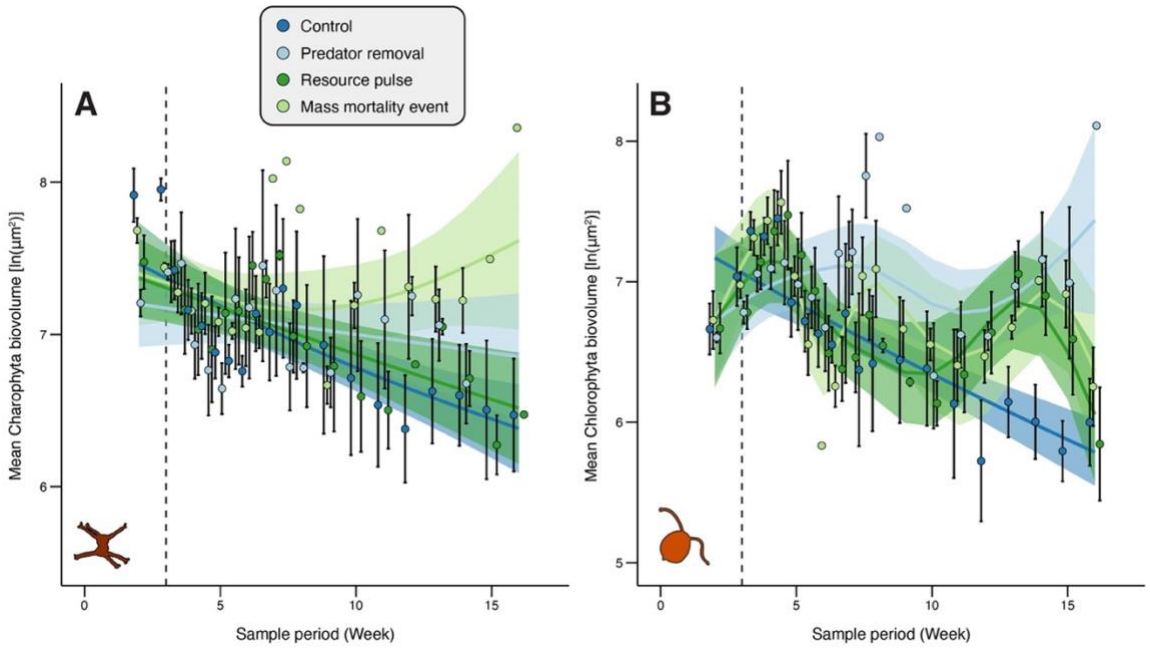

Figure S8. Time-series of mean biovolume across two major microalgae phyla following ecological perturbations. Mean microalgae biovolume [ln(µg^2)] of Charophyta (A) and Chlorophyta (B) following predator mass mortality events (MMEs, light green), predator removals (light blue), and resource pulses (dark green), as well as the undisturbed system (control, dark blue). Points and lines indicate means +/- 1 SE for each sampling period and treatment, with points jittered to reduce overlap within sample periods. Solid lines and shaded regions indicate model predictions and 95% confidence intervals, respectively. Relative to the control, MMEs increased mean biovolume of Charophyta ($t_{8.83} = 2.47$, $p = 0.01$) and Chlorophyta ($t_{20.96} = 2.93$, $p < 0.01$). Predator removals increased mean biovolume of Chlorophyta ($t_{20.96} = 4.32$, $p < 0.01$). Dashed lines indicate when perturbations were induced (i.e., live fish and/or fish carrion added and/or removed). Taxa silhouettes and their colors correspond with major microalgae phyla as in main figures.

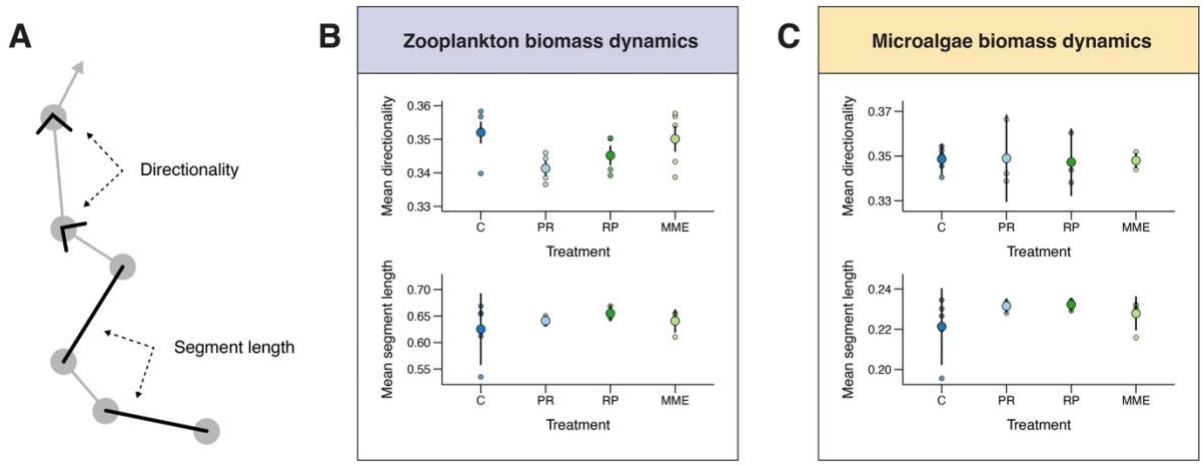

Figure S9. Ecological trajectory analysis metrics of zooplankton and microalgae biomass dynamics following ecological perturbations. Visual representation of ecological trajectory analysis metrics (A) and major characteristics of zooplankton (B) and microalgae (C) biomass dynamics following mass mortality events (MME, light green), predator removals (PR, light blue), resource pulses (RP, dark green) and the control (C, dark blue). Mean directionality represents how much the direction of a trajectory changed through time, such that higher or lower directionality indicate relatively more or less directional stability (e.g., top of A). Mean segment length indicates the average distance along a trajectory between sampling points through time (e.g., bottom of A). Large points and black lines show means of treatments and 95% confidence intervals, and small points show mean values of mesocosms. Ecological trajectories were based on smooth-moving averages of zooplankton and microalgae biomass across three sample periods.

Table S1. Mann-Whitney test results for convergence/divergence of zooplankton biomass trajectories at the treatment-level (i.e., smoothed data averaged by treatment and sample period as shown in Fig. 3A and Fig. 3C) following mass mortality events (MMEs), predator removals, resource pulses, and experimental controls over 120 days. For test results, tau (τ) is bounded by 1 and -1, with greater positive and negative values representing greater trajectory convergence and divergence, respectively. Asterisks indicate significant comparisons ($p < 0.05$).

Focal disturbance	**Comparison disturbance**	***Tau***	***p*-value**
MME	Predator removal	0.18	0.29
MME	Resource pulse	-0.42	0.01*
MME	Control	0.63	< 0.01*
Predator removal	MME	0.06	0.72
Predator removal	Resource pulse	0.12	0.50
Predator removal	Control	0.10	0.46
Resource pulse	MME	-0.11	0.54
Resource pulse	Predator removal	0.10	0.52
Resource pulse	Control	0.57	< 0.01*
Control	MME	0.74	< 0.01*
Control	Predator removal	0.83	< 0.01*
Control	Resource pulse	0.44	0.01*

Table S2. Mann-Whitney test results for convergence/divergence of microalgae biomass trajectories at the treatment-level (i.e., smoothed data averaged by treatment and sample period as shown in Fig. 3A and Fig. 3C) following mass mortality events (MMEs), predator removals, resource pulses, and experimental controls over 120 days. For test results, tau (τ) is bounded by 1 and -1, with greater positive and negative values representing greater trajectory convergence and divergence, respectively. Asterisks indicate significant comparisons ($p < 0.05$).

Focal disturbance	**Comparison disturbance**	***Tau***	***p*-value**
MME	Predator removal	-0.01	0.98
MME	Resource pulse	0.51	0.01*
MME	Control	0.63	< 0.01*
Predator removal	MME	-0.18	0.29
Predator removal	Resource pulse	0.56	< 0.01*
Predator removal	Control	0.79	< 0.01*
Resource pulse	MME	-0.27	0.10
Resource pulse	Predator removal	-0.02	0.92
Resource pulse	Control	0.36	0.03*
Control	MME	0.74	< 0.01*
Control	Predator removal	0.44	0.01*
Control	Resource pulse	0.43	0.01*

Table S3. Descriptions and interpretations of general additive mixed models (GAMMs). For GAMMs, we compared five different model forms that involved: 1) same shape and same intercept without smoothing, 2) different shape and different intercept without smoothing, 3) same shape and same intercept with smoothing, 4) different shape and same intercept with smoothing, and 5) different shape and different intercept with smoothing. Similarities or differences in shape terms would indicate treatment responses exhibited similar or different trends through time, respectively. Similarities or differences in intercept terms would indicate treatment responses had similar or different average values over time, respectively. Lastly, the absence of temporal smoothing penalization (i.e., Models 1-3) would indicate a relatively linear treatment response through time, whereas the presence of a temporal smoothing penalization would indicate a relatively non-linear treatment response through time (i.e., Models 4-5). If either these models provided the best fit (i.e., presence of temporal smoothing penalization), we then compared six different dimensions (k; 3, 5, 8, 10, 12, and 15) for the smooth term to determine the best penalization for the time effect. Predictor variables of these model forms are shown below, in which s(time) indicates the presence of a temporal smooth penalization on the time effect. All best fit models are listed in Table S4, and additional details are in the Methods.

Model	**Form**	**Shape**	**Intercept**	**Penalization**
1	~ time	`Same	Same	Absent
2	~ treatment + time	Different	Different	Absent
3	~ s(time)	Same	Same	Present
4	~ treatment + s(time)	Different	Same	Present
5	~ treatment + s(time, by = treatment)	Different	Different	Present

Table S4. Best fit general additive mixed models (GAMMs) for total productivity (i.e., chlorophyll-*a*), microalgae community characteristics (biomass, density, biovolume), and zooplankton community characteristics (biomass, density, body size). For GAMMs, we first used AIC to compare five different model forms (i.e., Models 1-5) that are fully described in Table S3. For best fit models that had temporal smoothing (i.e., Models 3-5), we then compared six different dimensions (k; 3, 5, 8, 10, 12, or 15) for the smooth term on the time effect for each model.

Trophic level	**Taxonomic group**	**Response variable**	**Model**	**k**
Producer	NA	Chlorophyll-*a*	5	12
Producer	All groups	Biomass	5	5
Producer	All groups	Density	5	5
Producer	All groups	Biovolume	5	8
Producer	Chlorophyta	Biomass	4	10
Producer	Chlorophyta	Density	5	5
Producer	Chlorophyta	Biovolume	5	15
Producer	Charophyta	Biomass	5	5
Producer	Charophyta	Density	5	5
Producer	Charophyta	Biovolume	5	3
Producer	Cyanobacteria	Biomass	5	8
Producer	Cyanobacteria	Density	5	8
Producer	Dinoflagellata	Biomass	4	8
Producer	Dinoflagellata	Density	4	8
Producer	Euglenozoa	Biomass	5	5
Producer	Euglenozoa	Density	5	5
Consumer	All groups	Biomass	5	3
Consumer	All groups	Density	5	3
Consumer	All groups	Body size	5	5
Consumer	Bosminidae	Biomass	5	3

Consumer	Bosminidae	Density	5	3
Consumer	Bosminidae	Body size	2	NA
Consumer	Brachionidae	Biomass	5	3
Consumer	Brachionidae	Density	5	3
Consumer	Brachionidae	Body size	2	NA
Consumer	Cyclopoida	Biomass	5	3
Consumer	Cyclopoida	Density	5	3
Consumer	Cyclopoida	Body size	5	8
Consumer	Cypretidae	Biomass	5	5
Consumer	Cypretidae	Density	4	5
Consumer	Cypretidae	Body size	5	5
Consumer	Daphniidae	Biomass	4	8
Consumer	Daphniidae	Density	4	8
Consumer	Daphniidae	Body size	2	NA

References

Barnett, A. J., K. Finlay, and B. E. Beisner. 2007. Functional diversity of crustacean zooplankton communities: towards a trait-based classification. *Freshwater Biology*, **52**:796-813. doi:10.1111/j.1365-2427.2007.01733.x

Bergquist, A. M., and S. R. Carpenter. 1986. Limnetic herbivory: effects on phytoplankton populations and primary production. *Ecology*, **67**:1351-1360. doi:10.2307/1938691

Boros, G., P. Takács, and M. J. Vanni. 2014. The fate of phosphorus in decomposing fish carcasses: a mesocosm experiment. *Freshwater Biology*, **60**:479-489. doi:10.1111/fwb.12483

Bottrell, H. H., A. Duncan, Z. M. Gliwicz, E. Grygierek, A. Herzig, A. Hillbricht-Ilkowska, H. Kurasawa, P. Larsson, and T. Weglenska. 1976. A review of some problems in zooplankton production studies *Norwegian Journal of Zoology*, **24**:419-456.

Brooks, J. L., and S. I. Dodson. 1965. Predation, body size, and composition of plankton. *Science*, **150**:28-35. doi:10.1126/science.150.3692.

de Cáceres M., L. Coll, P. Legendre, R. B. Allen, S. K. Wiser, M. J. Fortin, R. Condit, and S. Hubbell. 2018. Trajectory analysis in community ecology, *Ecological Monographs*, **89**:e01350. doi:10.1002/ecm.1350

Cupertino, A., B. Gücker, G. Von Rückert, and C. C. Figueredo. 2019. Phytoplankton assemblage composition as an environmental indicator in routine lentic monitoring: taxonomic versus functional groups. *Ecological Indicators*, **101**:522-532. doi:10.1016/j.ecolind.2019.01.054

Davis, S., and P. H. Wiebe. 1985. Macrozooplankton biomass in a warm-core Gulf stream ring: time series changes in size-structure, taxonomic composition, and vertical distribution, *Journal of Geophysical Research: Oceans*, **90**:8871-8884. doi:10.1029/JC090iC05p08871

DeMott, W. R., and W. C. Kerfoot. 1982. Competition among cladocerans: nature of the interaction between *Bosmina* and *Daphnia*. *Ecology*, **63**:1949-1966. doi:10.2307/1940132

Dzialowski, A. R., M. Rzepecki, I. Kostrezewska-Szlakowska, K. Kalinowska, A. Palash, and J. T. Lennon. 2014. Are the abiotic and biotic characteristics of aquatic mesocosms representative of *in situ* conditions?, *Journal of Limnology*, **73**:603-612. doi:10.4081/jlimnol.2014.721

Fey, S. B., A. M. Siepielski, S. Nusslé, K. Cervantes-Yoshida, J. L. Hwan, E. R. Huber, M. J. Fey, A. Catenazzi, and S.M. Carlson. 2015. Recent shifts in the occurrence, cause, and magnitude of animal mass mortality events. *Proceedings of the National Academy of Sciences*, **112**:1083-1088. doi:10.1073/pnas.1414894112

Fey, S. B., J. P. Gibert, and A. M. Siepielski. 2019. The consequences of mass mortality events for the structure and dynamics of biological communities. *Oikos*, **128**:1679-1690. doi:10.1111/oik.06515

Hall, D. J., W. E. Cooper, and E. E. Werner. 1970. An experimental approach to the production dynamics and structure of freshwater animal communities, *Limnology and Oceanograph*y, **15**:839-928. doi:10.4319/lo.1970.15.6.0839

Hansen, P. J., P. K. Bjørnsen, and B. W. Hansen. 1997. Zooplankton graving and growth: scaling within the 2-2000-um body size range, *Limnology and Oceanography*, **42**:687-704. doi:10.4319/lo.1997.42.4.0687

Hrycik, R., A. Shambaugh, and J. D. Stockwell. 2019. Comparison of FlowCAM and microscope biovolume measurements for a diverse freshwater phytoplankton community, *Journal of Plankton Research*, **41**:849-864. doi:10.1093/plankt/fbz056

Menden-Deuer, S., and E. J. Lessard. 2000. Carbon to volume relationships for dinoflagellates, diatoms, and other protist plankton, *Limnology and Oceanography*, **45**:569-579. doi:10.4319/lo.2000.45.3.0569

Nagdali, S. S., and P. K. Gupta. 2002. Impact of mass mortality of a mosquito fish, *Gambusia affinison*, on the ecology of a fresh water eutrophic lake (Lake Naini Tal, India). *Hydrobiologia*, **368:**45-51. doi:10.1023/a:1015270206187

Neiffer, D. L., and M. A. Stamper. 2009. Fish sedation, anesthesia, analgesia, and euthanasia: considerations, methods, and types of drugs. *ILAR Journal*, **50**:343-360. doi:10.1093/ilar.50.4.343

Pinheiro, J., D. Bates, and R Core Team. nlme: linear and nonlinear mixed effects models. R Package, version 3.1-157

Porter, K. G. 1973. Selective grazing and differential digestion of algae by zooplankton. *Nature*, **244**:179-180. doi:10.1038/244179a0

Schindler, W. 1974. Eutrophication and recovery in experimental lakes: implications for lake management. *Science*, **184**: 897-899. doi:10.1126/science.184.4139.897

Spivak, A. C., M. J. Vanni, and E. M. Mette. 2010. Moving on up: can results from simple aquatic mesocosm experiments be applied across broad spatial scales, *Freshwater Biology*, **56**:279-291. doi:10.1111/j.1365-2427.2010.02495.x

Sturbois, A., M. de Cáceres, M. Sánchez-Pinillos, G. Schall, O. Gauthier, P. Le Mao, A. Ponsero, and N. Desroy. 2021. Extending community trajectory analysis: new metrics and representation. *Ecological Modelling*, **440**:109400. doi:10.1016/j.ecolmodel.2020.109400

Threlkeld, T. S. 1988. Planktivory and planktivore biomass effects on zooplankton, phytoplankton, and trophic cascade. *Limnology and Oceanography*, **33**:1362-1375. doi:10.4319/lo.1988.33.6.1362

Tye, S. P., A. M. Siepielski, A. Bray, A. L. Rypel, N. B. D. Phelps, and S. B. Fey. 2022. Climate warning amplifies frequency of fish mass mortality events across north temperature lakes. *Limnology and Oceanography Letters*, **7**:510-519. doi:10.1002/lol2.10274

Vanni, M. J., and D. L. Findlay. 1990. Trophic cascades and phytoplankton community structure, *Ecology*, **71**:921-937. doi:10.2307/1937363.

Vanni, M. J., C. Luecke, J. F. Kitchell, Y. Allen, J. Temte, and J. J. Magnuson. 1990. Effects on lower trophic levels of massive fish mortality. *Nature*, **344**:333-335. doi:10.1038/344333a0

Verity, P. G., C. Y. Robertson, C. R. Tronzo, M. G. Andrews, J. R. Newlson, and M. E. Sieracki. 1992. Relationships between cell volume and the carbon and nitrogen content of marine photosynthetic nanoplankton. *Limnology and Oceanography*, **37**:1434-1446. doi:10.4319/lo.1992.37.7.1434

Wood, S. N. 2004. Stable and efficient multiple smoothing parameter estimation for generalized addition models. *Journal of the American Statistical Association*, **99**:673-686. doi:10.1198/016214504000000980

Chapter 2

Size-selective predation generates divergent consumer life history trait evolution under contrasting resource levels

Simon P. Tye and Adam M. Siepielski

Abstract

A lingering question of ecology and evolutionary biology is whether similar or different factors drive similar or different ecological and evolutionary changes. Two main drivers of ecological and evolutionary change are selective predation and food resource levels, yet selective predation and resource levels can generate opposing effects on consumer population dynamics and life history trait evolution. In turn, their combined effects may generate counterintuitive life history changes that could dampen expected eco-evolutionary responses be weakening effects of trait changes on population dynamics. To partition the roles of selective predation and resource availability on consumer eco-evolutionary dynamics, we conducted an artificial selection experiment that exposed *Daphnia pulicaria* populations to the independent or combined effects of nonselective or large body size-selective predation and contrasting low or high resource levels. We then compared how these selective pressures affected population density, per capita population growth rate, and rapid adaptive changes in life history traits related to body size, growth, maturation, and fecundity. Size-selective predation slightly increased population density, reduced body size, and extended juvenile growth period. High resource levels increased population density and mediated changes in maturation size and fecundity. The only evidence that rapid trait evolution shaped population dynamics was a positive relationship between maximum body size and per capita growth rate under size-selective predation and low resource levels. Therefore, size-selective predation can generate partially divergent life history trait responses under contrasting resource levels, and ensuing eco-evolutionary dynamics are context dependent.

Introduction

Predators and food resources are two major biotic drivers of ecological (Hairston et al., 1960; Paine, 1966; Paine, 1980; Estes et al., 2011) and evolutionary dynamics (Reznick and Endler, 1982; Gibbs and Grant, 1987; Siepielski et al., 2020) within consumer populations. Consumer densities are frequently reduced by predator consumptive effects (Vanni, 1987), which also generate selective pressures that can lead to rapid adaptive changes in consumer life history traits (Siepielski et al., 2020; Lyberger et al., 2021). For example, many predators disproportionately eat larger-bodied consumers (henceforth size-selective predation; Brooks and Dodson, 1965), which can lead to adaptive declines in consumer maximum body size and lengthening of the juvenile growth period (Lyberger et al., 2021). Smaller maximum body size is predicted to reduce exposure to size-selective predators (Brooks and Dodson, 1965; Hall et al., 1976), whereas an extended juvenile growth period requires less forgaging time that also reduces predation risk (Lima and Dill, 1990; Werner and Anholt, 1993). However, size-selective predation can lead to either high (Lyberger et al., 2021) or low age at maturity (Reznick and Endler, 1982; Reznick et al., 1990), and such adaptive changes may be potentially confounded by an underappreciated role of resource level (Graether, et al., 2001; Reznick et al., 2002). Moreover, both empirical (Vanni, 1987) and theoretical work (Day et al., 2002) suggest that the coupled effect of size-selective predation and high resource levels can lead to counterintuitive ecological and evolutionary outcomes (Fig. 1)

First, both predators and high resource levels are predicted to reduce consumer foraging rates and thereby can cause consumers to be less active and susceptible to predation (Lima and Dill, 1990). Yet high resource levels can increase consumer density despite the consumptive effects predators (Vanni, 1987), as well as faciliate adaptive increases in consumer fecundity

(Tessier et al., 1992). Thus, high resources may still result in many consumers being exposed to predators, which could be exacerbated if excessive resources are allocated toward fecundity rather than large body size or fast development (Fig. 1, fecundity). Second, life history theory suggests that the combined effect of high resource levels and size-selective predation can increase per capita population growth rates (Fig. 1, per capita growth rate; Day et al., 2002), which could counterintuitively increase predation risk for species that experience a tradeoff between activity rates and growth rates (e.g., Lima and Dill, 1990; Werner and Anholt, 1993). Third, size-selective predation and high resource levels can generate opposing changes in age at maturity (Fig. 1; Cuenca-Cambronero et al., 2018; Lyberger et al., 2021), and theory suggests size-selective predation should have a greater effect than resource level on age at maturity because early life stages would experience low predation risk (Day et al., 2002). Therefore, the combined effects of high resources and size-selective predation may generate dense consumer populations that experience surprisingly strong selective pressures on key life history traits. In turn, such a scenario could generate life history trait responses that partially diverge from expectations based on the independent effects of either size-selective predation or high resource levels (Fig. 1), and thereby lead to a convoluted eco-evolutionary response that reflects aspects of both selective pressures.

Here we examine the independent and combined effects of selective predation and food resource levels on *Daphnia pulicaria* population dynamics (i.e., density and per capita growth rate) and rapid adaptive evolution of life history traits related to body size, growth rate, maturation, and fecundity. *Daphnia* have well-described interactions with fish predators (Brooks and Dodson, 1965; Cerny and Bytel, 1991) and algal resources (Burns, 1995; McCauley et al., 1999), making them an ideal focal organism to test our hypotheses. We hypothesized that the

net-effects of size-selective predation and high resource levels would reduce maximum body size and increase fecundity, but also shorten juvenile growth period and lower age at maturity. We therefore predicted resource level would have a greater effect than predation type on population dynamics, predation type would largely drive adaptive changes in offspring life history traits, and their combined effect would lead to a weak eco-evolutionary response due to contrasting effects of size-selective predation and high resource levels on both population dynamics (e.g., Vanni, 1987) and consumer life history trait evolution (e.g., Cuenca-Cambronero et al., 2018; Lyberger et al., 2021).

Materials and Methods

Experiment overview

Our primary goal was to understand how size-selective predation and contrasting food resources levels affected consumer population dynamics and life history traits. We therefore conducted an artificial selection experiment with a 2 × 2 factorial design that exposed *Daphnia pulicaria* populations to 1) one of two different types of predation (nonselective, uniform across body size classes or size-selective of larger-bodied individuals), and 2) either low or high amounts of common algal resource (*Scenedesmus* sp.). We induced these selective pressures and monitored population dynamics over 28 days (Fig. S1, population dynamics), or ~3-4 generations (Alekseev and Lampert, 2004). We then haphazardly selected individuals within populations and reared F3 individuals in a controlled environment to measure five life history traits over an additional 28 days (Fig. S1, life history traits).

Artificial selection experiment

We obtained 10 unique *D. pulicaria* genotypes, that were originally acquired from natural populations at Lake Mendota, WI. These genotypes were determined to be genetically distinct (Gillis and Walsh, 2017). To rear individuals before experimentation, we placed each *Daphnia* genotype in multiple, separate 3-L containers with modified COMBO growth medium (Kilham et al. 1998) in an environmental chamber (20ºC, 12L:12D). To provide *Daphnia* with algal food resources, we reared cultures of *Scenedesmus*, obtained from the Culture Collection of Algae at the University of Texas (UTEX), in the same environmental chamber and in several 1-L containers that contained COMBO growth medium. We fed *Scenedesmus* to *Daphnia* every other day, replaced COMBO medium every two weeks. We reared *Daphnia* in these containers until their densities were ~100-150 individuals / L because these densities allowed for enough neonates of each genotype to enact our experimental design.

To maintain the densities of *Daphnia* genotypes (i.e., in separate containers described above), we had to employ a haphazard culling procedure that provided enough time for genotypes that appeared to exhibit slow population growth rates (i.e., few individuals of one genotype compared to other genotypes) while also accounting for the opposing pattern (i.e., many individuals of one genotype compared to other genotypes). Therefore, we used a 90-µm sieve to haphazardly remove ~20% of individuals across body size classes weekly across all containers. This culling approach also helped haphazardly reduce population densities and thus dissuade sexual reproduction, which generally occurs for *Daphnia* under higher density (Burns, 1995). No resting eggs were observed during this time, which indicated no sexual reproduction occurred. We maintained these conditions for approximately ~65 days or ~7-8 generations (Alekseev and Lampert, 2004) before experimentation.

To begin the experiment, we created 40 1-L microcosms (10 replicates per treatment) that were filled with 900-mL of COMBO growth medium and connected to an aeration system. We inoculated each replicate with 2 neonates of each of the 10 *Daphnia* genotypes. All neonates had body sizes < 500 µm and were 1-2 days old when placed in microcosms. This starting density (~22 individuals / L) is within the intermediate range of natural *D. pulicaria* populations (Cerny and Bytel, 1991). One week after inoculating microcosms, we implemented the 2 × 2 factorial design with different predation types and resource levels.

To simulate the effects of size-selective and nonselective predation, we used a gradient of stainless-steel sieves (90 µm, 500 µm, 1 mm, 1.4 mm, 2 mm) to sequentially sort individuals within each replicate into five different categorical body size classes: extra small (90 to 500 µm), small (500 µm to 1 mm), medium (1 to 1.4 mm) large (1.4 to 2 mm) and extra-large (> 2 mm) once per week for four weeks. We recorded the density of each body size class (individuals / L) by counting all individuals within each of the five body size classes, then haphazardly removed 20% of each population (based on the total abundance across these five body size classes) and according to the ascribed type of predation. Specifically, we either removed larger-bodied individuals that were usually larger than 1.4 mm across sample periods (i.e., large or extra large body size classes), to mimic size-selective predation (e.g., Brooks and Dodson, 1965) or uniformly individuals across body size classes to generate nonselective predation (i.e., no selective pressure on body size; Abrams and Rowe, 1996). To generate different resource levels, we provided replicates with either 5-mL (low) or 10-mL (high) amounts of *Scendemus* sp. every other day. This method slightly changed water volume between treatments with contrasting resource levels (i.e., 905 mL for low resource levels vs. 910 mL for high resource levels), though this small volume difference likely had a negligible effect on observed patterns. We repeated

population cullings (weekly) and feedings (every other day) over 28 consecutive days (14 total feedings and 4 total cullings for each replicate).

Importantly, the population culling procedure described above necessitated sorting individuals within each microcosm into discrete body size classes. We therefore used this information to also calculate total population density (i.e., across all body size classes) and the density of each body size class separately each week for four weeks. We used total population density estimates to calculate per capita growth rate through time. To assess shifts in population size structure while helping account for resampling of some individuals each week given the focal species' generation time (Alekseev and Lampert, 2004), we then calculated the average density of different body size classes for each microcosm (replicate average). We removed one microcosm with size-selective predation and low resource levels from analyses because many individuals unexpectedly died during the first week of the experiment.

Life history traits

After imposing selective pressures and monitoring population dynamics, we then haphazardly selected 5 individuals from each replicate (i.e., 50 per all treatment except 45 for the treatment with one fewer replicate noted above). We then reared these individuals in a controlled environment and obtain F3 individuals to measure five life history traits (Fig. S1): maximum body size (mm), a proxy for juvenile growth rate (days until half maximum body size), age at maturity (days), body size at maturity, and total fecundity (over 28 days). We chose these traits because they strongly influence population dynamics (Lynch, 1989) and can experience rapid evolution (Cuenca-Cambronero et al., 2018; Lyberger et al., 2021).

To obtain F3 individuals, the haphazardly selected individuals (F1 individuals) were placed in separate 90-mL containers with COMBO growth medium. We fed each individual 3-mL of *Scenedesmus* and replaced growth medium every other day. We checked each container daily for neonates and, if present, we removed all individuals except a single neonate and replaced the growth medium. We repeated this process across all containers until at least two generations occurred for each individual (i.e., F3 individuals were present) to reduce potential maternal and grand-maternal effects (Alekseev and Lampert 2004). In total, we measured all five life history traits for 14 to 17 individuals for each treatment. Specifically, we measured 17 individuals from the treatment with nonselective predation and low resources, 16 individuals from the treatment with nonselective predation and high resources, 17 from the treatment with size-selective predation and low resources, and 14 from the treatment with size-selective predation and high resources.

We then used established methods (Lynch, 1989; Lyberger et al., 2021) to measure the five life history traits related to growth, body size, maturation, and fecundity. To measure body size through time, we used a DSLR camera (Nikon, D5600, Tokyo, Japan) and micro lens (Nikon, AF-S 40mn) to take multiple photographs of each individual. Photographs were taken every other day (before replacing growth medium) for at least 28 days for each individual unless individuals died earlier. To estimate body size, we used ImageJ (version 1.5.1, Schneider et al., 2012) to measure the length between the anterior eye and base of the tail of each individual. To estimate fecundity, we checked each container daily to see if neonates were present. If present, we recorded the date of first brood for each individual to determine both age (days) and body size (mm) at maturity, then preserved neonates in 70% ethanol. We used light microscopy (20x;

Leica Camera Model EC4, Wetzlar, Germany) to count the number of neonates produced by each individual, which we considered total fecundity.

We used body size measurements of individuals through time to estimate juvenile growth rate and maximum body size by fitting an asymptotic regression model via the *nlme* package (Pinherio et al., 2022). This model has the form: $body\ size = Asym * 1 - e^{-e^{lrc} * day}$, with *lrc* being the natural log of the growth rate constant and *Asymp* being the asymptotic (maximum) individual body size. This model generated a natural log growth rate constant (*lrc*) based on each individual's body size measurements through time. We converted this growth rate constant to days until half maximum body size, as in a similar experiment, using the following equation: $\log(2) / e^{lrc}$ (Lyberger et al., 2021). This is more biologically meaningful metric because it can be considered a proxy for juvenile growth period, since most body size change occurs in early life stages rather than late life stages (Lynch, 1989).

Statistical analyses

We performed three main sets of analyses to examine how different types of predation, contrasting resource levels, and their interaction affected population dynamics and rapid adaptive evolution of life history traits. First, we assessed effects of predation type and resource level on three aspects of population dynamics: average population density, replicate average density of body size classes, and average per capita growth rate. We also assessed the strength and sensitivity of density dependence within each treatment, described below, to understand which combination(s) of predation and resource level may contribute to particularly rapid changes in population density over ecological timescales. Second, we compared average life history trait values of F3 individuals between treatments and calculated correlation coefficients between life

history traits for separately each treatment. Third, we examined whether rapid adaptive changes in life history traits shaped characteristics of concurrent population dynamics in each treatment.

For the first set of analyses, we used general linear mixed effects models (GLMM) via the *afex* package (Signmann et al., 2023) that included average population density or per capita growth rate as the response variable; predation type (i.e., nonselective or size-selective), resource level (i.e., low or high), and their interaction as predictor variables; and a random effect of replicate (the original microcosm of the sampled individual). For these and all subsequent analyses, we considered nonselective predation and low resource levels to be the reference group, which allowed for inferences about the independent and combined effects of size-selective predation and higher resources on response variables (Fig. 1).

Next, to coarsely assess population size structure, we compared the replicate average density of body size classes (i.e., the original microcosms) over time by treatments. To do so, we used a linear mixed effect model via the *nlme* package (Pinheiro et al., 2023) that included the replicate average density of body size classes as the response variable; predation type, resource level, and their interaction as predictor variables; and a random effect of replicate. We used this approach to compare densities of discrete body size classes because we counted the number of individuals within each class prior to performing weekly cullings (i.e., when imposing predation types). Thus, we do not have exact body measurements of all individuals within populations through time, but rather the number of individuals in each size class at each sample period (i.e., week).

Lastly, we assessed the strength, directionality, and sensitivity of density dependence within each treatment. To assess the strength of density dependence, we performed separate linear models for each treatment with replicate average per capita growth rate as the response

variable and replicate average population density as the predictor variable. The slopes from these models were our measure of the strength of density dependence. To assess the directionality and sensitivity of density dependence, we calculated correlation coefficients Pearson's *r*) between average population density and per capita growth rate of microcosms separately for each treatment via the *Hmisc* package (Harrell, 2002). For this analysis, we considered a significant positive correlation between average population density and per capita growth rate to be indicative of positive density dependence (e.g., Allee effect; Allee and Bowen, 1932) and a significant negative correlation to be indicative of negative density dependence. We considered the strength of correlation to indicate the sensitivity of density dependence, such that stronger correlations indicated a stronger relationship between average population density and per capita growth rate.

For the second set of analyses, we examined how predation type and resource level affected recorded life history traits and calculated correlations between life history traits separately for each treatment. Specifically, we used linear models with either the average values of all traits as response variables (i.e., MANOVA) or the average values of each trait as separate response variables (i.e., ANOVA); predation type, resource level, and their interaction as fixed effects; and replicate as a random effect. We used this approach to assess whether there was an overall effect of predation type, resource level, and/or their interaction on this assortment of life history traits, as well as whether there were independent effects of these factors on each trait separately. We then calculated correlation coefficients (Pearson's *r*) between average life history trait values separately for each treatment (Table S1-S4) to understand whether combinations of selective pressures generated life history tradeoffs. We calculated these correlation coefficients via the *RcmdrMisc* package (Fox, 2022) to account for multiple comparisons via the Holm

method. We considered significant negative correlations between average life history trait values within specific treatments to indicate life history tradeoffs were present. We were unable to track individual genotypes in this experimental design, and thus cannot make inferences about genetic correlations between traits. Lastly, we used the *cocor* package (Diedenhofen and Musch, 2015) to make pairwise comparisons of life history trait correlation coefficients between different treatments (e.g., whether the correlation changed between maximum body size and fecundity under two different combinations of predation type and resource level). This analysis did not account for multiple comparisons, which is noted when discussed in the Results. Raw differences between life history trait correlation coefficients of treatments are shown in Fig S2.

For the third set of analyses, we evaluated relationships between life history trait values of individuals and population density and per capita growth rate in their original microcosm separately for each treatment. To make these comparisons, we used separate multivariate multiple linear regressions for each treatment that included average population density and average per capita growth rate as the responses variables; and average maximum body size (mm), size at maturity (mm), age at maturity (days), and total fecundity (over 28 days) as predictor variables. We excluded juvenile growth period as a predictor variable from these models because it was strongly correlated with maximum body size across all treatments (Table S1-S4), and maximum body size was more directly affected by our culling procedure. Thus, these models provided information about whether life history trait values in treatments affected two key characteristics of population dynamics and, in conjunction with the preceding analyses about trait changes, yielded knowledge about whether rapid adaptive trait evolution affected population dynamics. We used an α value of 0.05 for significance tests and performed all analyses in R (version 4.2.1, R Core Team, 2021).

Results

Population dynamics

Daphnia population dynamics were affected more by resource levels than predation types (Fig. 2). Relative to the experimental control (nonselective predation and low resource levels), size-selective predation decreased average population density (Fig. 2A-2B; -13%, ANOVA; $F_{1,35}$ = 15.16, $p < 0.001$), high resource levels increased average population density (+56%, $F_{1,35}$ = 59.73, $p < 0.001$), and there was no interaction between predation type and resource level on average population density ($F_{1,35} = 2.82$, $p = 0.10$). In addition, high resource levels increased the replicate average density of body size classes (Fig. 2C; ANOVA, +55%, $F_{1,35} = 13.72$, p = 0.001), but there was no effect of size-selective predation (-13%, $F_{1,35} = 0.55$, $p = 0.46$) or the interaction between predation type and resource level ($F_{1,35} = 0.55$, $p = 0.47$) on replicate average density of body size classes. Average per capita growth rate generally declined over time across treatments (Fig. 2D). However, there was no effect of predation type (ANOVA, $F_{1,35}$ = 2.42 $p = 0.13$), resource level ($F_{1,35} = 1.57$, $p = 0.22$), or their interaction ($F_{1,35} = 3.59$ $p = 0.07$) on average per capita growth rate (Fig. 2D).

There were significant negative relationships between average population density and per capita growth rate under nonselective predation and high resource levels (Fig. S3B; β = -0.02, SE = 0.003, t = -5.76, $p < 0.001$; *adjusted* $R^2 = 0.53$) or size-selective predation and high resource levels (Fig. S3D; β = -0.008, SE = 0.003, t = -2.31, $p = 0.02$; *adjusted* $R^2 = 0.13$). By comparison, there were no relationships between average population density and per capita growth rate under size-selective predation and low resource levels (Fig. S3C; β = -0.007, SE = 0.009, t = -0.77, p = 0.45; *adjusted* $R^2 = 0.02$) or nonselective predation and low resources levels (Fig. S3A; β = -0.01, SE = 0.008, t = -1.76, $p = 0.09$; *adjusted* $R^2 = 0.08$). Therefore, the directionality density

dependence was consistent, and its sensitivity was especially strong under treatments in high resource levels.

Trait evolution

Exposing populations to different predation types and resource levels led to rapid changes in most of the five recorded offspring life history traits (Fig. 3). There were significant effects of predation type (MANOVA, $F_{5,31} = 4.15$, $p = 0.005$; $\eta^2 = 0.40$, 95% CI = 0.11 to 1.00) and its interaction with resource level ($F_{5,31} = 2.79$, $p = 0.03$; $\eta^2 = 0.31$, 95% CI = 0.02 to 1.00) on the set of five life history traits, but there was no independent effect of resource level ($F_{5,31} = 0.43$, $p = 0.82$; $\eta^2 = 0.06$, 95% CI = 0.00 to 1.00). We thus examined the effect of predation type separately for each resource level, which showed that predation type had a strong effect on average life history trait values at low resource levels (MANOVA, $F_{1,18} = 4.31$, $p = 0.01$; $\eta^2 = 0.61$, 95% CI = 0.15 to 1.00) and high resource levels ($F_{1,17} = 4.24$, $p = 0.02$; $\eta^2 = 0.62$, 95% CI = 0.14 to 1.00).

Separate linear models for each life history trait response indicated there were several appreciable differences in average trait values between treatments. First, relative to the control (nonselective predation and low resource levels), size-selective predation reduced average maximum body size (Fig. 3A; ANOVA, -13%, $F_{1,35} = 14.32$, $p = 0.001$). Second, size-selective predation slightly increased the average number of days until half maximum body size (i.e., extended juvenile growth period; Fig. 3B; ANOVA, +3%, $F_{1,35} = 11.06$, $p = 0.002$). Third, there was weak evidence that size-selective predation increased age at maturity (Fig. 3C; ANOVA, +12%, $F_{1,35} = 3.27$ $p = 0.08$). Fourth, there were no effects of predation type (ANOVA, $F_{1,35} = 0.01$, $p = 0.92$) or resource level ($F_{1,35} = 0.63$ $p = 0.43$) on size at maturity (Fig. 3D). However,

there was a significant interaction between predation type and resource level on size at maturity ($F_{1,35}$ = 8.27, p = 0.007). Separate models for each factor combination indicated predation type affected size at maturity under high resource levels ($F_{1,18}$ = 4.68, p = 0.05) but not low resources levels ($F_{1,17}$ = 4.68, p = 0.06), and resource level affected size at maturity under nonselective predation ($F_{1,18}$ = 5.98, p = 0.02) but not size-selective predation ($F_{1,17}$ = 8.27, p = 0.09). Thus, there was crossover effect, such that the combination of low resource levels and size-selective predation or high resource levels and nonselective predation led to relatively large size at maturity (Fig. 3D), whereas the combination of low resource levels and nonselective predation or high resource levels and size-selective predation led to small size at maturity. Lastly, there was no effect of size-selective predation (ANOVA, -2%, $F_{1,35}$ = 2.54, p = 0.12), high resource levels (+26%, $F_{1,35}$ = 0.65, p = 0.43), or an interaction between predation type and resource level ($F_{1,35}$ = 2.05, p = 0.16) on total fecundity (Fig. 3E).

There were few significant correlations between average life history trait values of individuals in treatments (Fig. 4; Table S1-S4). Most notably, there was a strong negative correlation between average maximum body size and juvenile growth period (i.e., days until half maximum body size) in all treatments (Fig. 4; Table S1-S4; r = -0.83 to -0.68). Additionally, there was a negative correlation between size at maturity and juvenile growth period (r = -0.64, p = 0.05) under nonselective predation and low resource levels (Fig. 4A, Table S1). There were no additional significant correlations between average life history trait values under nonselective predation and high resource levels (Fig. 4, Fig. S2, Table S2), size-selective predation and low resource levels (Table S3), or size-selective predation and high resource levels (Table S4).

Lastly, there was only one significant pairwise comparison between correlation coefficients of life history traits in different treatments. Specifically, there was a significant

difference in the correlation between maximum body size and total fecundity (z = 2.10, p = 0.04, *95% CI* = 0.04 to 1.26) in treatments with nonselective predation and low resource levels (Fig. 4A, Fig. S2A; r = 0.50, p = 0.04) or high resource levels (Fig. 4B, Fig. S2B; r = -0.26, p = 0.34). Accounting for multiple pairwise comparisons would swiftly negates the statistical significance of this difference, although it is still noteworthy that the most appreciable difference in trait correlations between treatments was mediated by resource level and involved maximum body size and total fecundity.

Eco-evolutionary dynamics

Life history trait values had minor effects on average population density and per capita growth rate, but only under low resource levels (Fig. S4-S7). Under nonselective predation and low resource levels, there was an effect of total fecundity (MANOVA, $F_{2,9}$ = 16.16, p = 0.001; η^2 = 0.78, 95% CI = 0.35 to 0.90), but not maximum body size ($F_{2,3}$ = 1.60, p = 0.24; η^2 = 0.27, 95% CI = 0.00 to 0.61), size at maturity ($F_{2,3}$ = 0.10, p = 0.79; η^2 = 0.05, 95% CI = 0.00 to 0.35), or age at maturity ($F_{2,3}$ = 0.05, p = 0.72; η^2 = 0.07, 95% CI = 0.00 to 0.40), on average population density and per capita growth rate. However, separate linear regressions for each response variable indicated there was no relationship between total fecundity and average population density (Fig. S3A; β = 0.22, *SE* = 0.18, t = 1.25, p = 0.23; *adjusted* R^2 = 0.04), nor between total fecundity and per capita growth rate under nonselective predation and low resource levels (Fig. S5A; β < 0.001, *SE* < 0.001, t < 0.001, p = 0.10; *adjusted* R^2 = 0.13). There was no effect of maximum body size (MANOVA, $F_{2,4}$ = 0.51, p = 0.64; η^2 = 0.20, 95% CI = 0.00 to 0.65), size at maturity ($F_{2,4}$ = 0.98, p = 0.45; η^2 = 0.33, 95% CI = 0.00 to 0.73), age at maturity ($F_{2,4}$ = 0.46, p = 0.66; η^2 = 0.19, 95% CI = 0.00 to 0.64), or total fecundity ($F_{2,4}$ = 0.06, p = 0.94; η^2 = 0.03,

95% CI = 0.00 to 0.30) on average population density and per capita growth rate under nonselective predation and high resource levels.

Under size-selective predation and low resource levels, there was an effect of maximum body size (MANOVA, $F_{2,4} = 8.45$, $p = 0.04$; $\eta^2 = 0.81$, 95% CI = 0.00 to 0.93), but not size at maturity ($F_{2,4} = 0.02$, $p = 0.98$; $\eta^2 = 0.01$, 95% CI = 0.00 to 0.00), age at maturity ($F_{2,4} = 1.64$, $p = 0.30$; $\eta^2 = 0.45$, 95% CI = 0.00 to 0.79) or total fecundity ($F_{2,4} = 4.95$, $p = 0.08$; $\eta^2 = 0.71$, 95% CI = 0.00 to 0.90) on average population density and per capita growth rate. Separate linear regressions for each response variable indicated that there was a positive relationship between maximum body size and average per capita growth rate (Fig. S6C; $\beta = 0.008$, $SE = 0.003$, $t = 2.82$, $p = 0.01$; $F_{1,15} = 7.60$, $p = 0.01$, *adjusted* $R^2 = 0.30$), and no relationship between maximum body size and population density (Fig. S6; $\beta = 9.38$, $SE == 22.27$, $t = 0.42$, $p = 0.68$; $F_{1,15} = 0.18$, $p = 0.68$, *adjusted* $R^2 = 0.05$), under size-selective predation and low resource levels. There was no effect of maximum body size (MANOVA, $F_{2,4} = 0.51$, $p = 0.64$; $\eta^2 = 0.51$, 95% CI = 0.00 to 0.83), size at maturity ($F_{2,4} = 0.98$, $p = 0.45$; $\eta^2 = 0.17$, 95% CI = 0.00 to 0.65), age at maturity ($F_{2,4} = 0.46$, $p = 0.66$; $\eta^2 = 0.22$, 95% CI = 0.00 to 0.69), or total fecundity ($F_{2,4} = 0.06$, $p = 0.94$; $\eta^2 = 0.21$, 95% CI = 0.00 to 0.69) on average population density and per capita growth rate under size-selective predation and high resource levels.

Discussion

Food resource levels and predator consumptive effects are major biotic drivers of consumer population dynamics (Hairston et al., 1960; Paine, 1966; Polis et al., 1997; Paine, 1980) and life history trait evolution (Stearn, 1992). Consumer population dynamics were affected more by resource levels than selective predation (Fig. 2), consistent with previous studies (e.g., Vanni,

1987). By comparison, life history trait evolution was primarily driven by predation type, especially for traits related to growth and development (Fig. 3), whereas resource level mediated marked changes in traits related to maturation and fecundity. These trait changes largely corroborate predictions based on life history theories (Levins, 1968; Lima and Dill, 1990; Werner and Anholt, 1993; Abrams and Rowe, 1996; Day et al., 2002), observations (Brooks and Dodson, 1965; Reznick and Endler, 1982; Reznick et al., 2002), and experiments (Cuenca-Cambronero et al., 2018; Lyberger et al., 2021). Yet, the combined effects of size-selective predation and high resource levels led to several counterintuitive trait changes – low maturation size and total fecundity – that were not predicted by the independent effects revealed in these studies (Fig. 1) and generally showed that predation had a larger role than resource level in driving such responses. Additionally, only the combined effects of size-selective predation and low resource levels yielded evidence that trait evolution affected concurrent population dynamics. Therefore, size-selective predation can lead to partially divergent sets of consumer life history traits under contrasting resource levels (Fig. 3), and eco-evolutionary dynamics only arose in certain situations (i.e., context-dependent).

The greatest differences in life history traits between treatments involved maximum body size (Fig. 3A) and juvenile growth period (Fig. 3B), and changes in both traits are predicted to be common adaptive responses to either size-selective (Lyberger et al., 2021), or age-selective predation (Reznick and Endler, 1982). Size-selective predation is predicted to reduce consumer body size (Brooks and Dodson, 1965; Hall et al., 1976), and predation is predicted to reduce consumer foraging time and thereby decrease individual growth rates (i.e., growth-predation risk tradeoff; Lima and Dill, 1990; Anholt and Werner, 1993). In turn, low consumer growth rates are often associated with longer juvenile growth periods (e.g., Reznick and Endler, 1982), as

individuals with low growth rates require more time to acquire the resources necessary for growth, development, and maturation. Notably, however, low resource levels can lead to similar changes in maximum body size and juvenile growth period (Grether et al., 2001), as resource level often positively correlates and covaries with extents of predation. For example, predation can reduce consumer density which can indirectly increase resource levels (Reznick et al., 2001). Indeed, a recent re-evaluation of foundational studies about the effects of selective predation has highlighted an overlooked role of resource level (Reznick et al., 2002), although the effects of selective predation and resource level were intentionally isolated in this study.

In addition to exhibiting the largest change, maximum body size and juvenile growth period also experienced the strongest tradeoff in life history traits (Fig. 4). This tradeoff was present in every treatment (Fig. 4; Table S1-S4) and indicated large-bodied individuals consistently had short juvenile growth periods and, by extension, fast individual growth rates (e.g., larger body sizes were attained over shorter timespans), or vice-versa, under different predation types and resource levels. This strongly affirmed the growth-predation risk tradeoff (Lima and Dill, 1990; Anholt and Werner, 1993), as individuals with fast growth rates were removed from populations via selective predation which led to lower individual growth rates (Fig. 3A-3B). There was only appreciable evidence that one additional tradeoff was present across treatments – between juvenile growth period and size at maturity (Fig. 4; Table S1-S4). Notably, these two negative correlations were linked by a positive relationship between maximum body size and size at maturity, which was weaker and more variable in strength but also present across treatments (Fig. 4; Table S1-S4). Collectively, this set of rapid trait changes and trait correlations largely corroborates experimental results about congener zooplankton under similar selective pressures (Lyberger et al., 2021) and observations of omnivorous fish traits that

have been attributed to age-selective predation (Reznick and Endler, 1982) or high resource levels (Reznick et al., 2002). In this study, rapid changes in maximum body size and juvenile growth period appeared to be strongly driven by selective predation, and additional findings indicated that resource level may have had a minor role in mediating size at maturity.

Specifically, both size-selective predation (Lyberger et al., 2021) and high resource levels (Cuenca-Cambronero et al., 2018) can lead to rapid adaptive increases in size at maturity, yet, predation type and resource level generated a crossover effect in this study. Only size-selective predation and low resource levels or nonselective predation and high resource levels led to large average size at maturity (Fig. 3C), and thus there was a notable lack of increase under size-selective predation and high resources. On one hand, maximum body size and size at maturity were strongly positively correlated under size-selective predation and high resources (Table S2) and weakly correlated in both treatments with large size at maturity (Table S1, Table S4). Therefore, this lack of an effect may simply indicate predation strongly reduced maximum body size. Even so, however, the lack of apparent resource allocation toward maturation under high resource levels remains intriguing because other potential contributing factors, such as conspecific density (Lyberger et al., 2021), have limited effects on size at maturity in closely related species.

By comparison, theory suggests that the effects of predation should supersede the effects of resource level on consumer age at maturity (Day et al., 2002). Moreover, selective predation of adults, which often generates similar selective pressures as the predation of larger individuals (e.g., reduced body size; Reznick et al., 1990; Lyberger et al., 2021) is expected to generally reduce age at maturity (Charlesworth, 1980). These patterns are predicted to occur because maintaining an age of maturity that is under low predation risk can help propagate population

abundance through time (Charlesworth, 1980; Day et al., 2002). In partial corroboration, predation type had a stronger effect than resource level on age at maturity (Day et al., 2002), but size-selective predation lead to a higher, rather than a lower, age at maturity. Conversely, high resource levels can facilitate rapid decreases in age at maturity (Cuenca-Cambronero et al., 2018), likely because resources required for maturation are readily available, and both treatments with high resource levels had slightly lower age at maturity compared to treatments with low resource levels (Fig. 3D).

While speculative, these differences between maturation trait responses and predictions based on either age-selective predation (Reznick et al., 1990) or size-selective predation (Lyberger et al., 2021) may merely emphasize a key difference between these predation types. Specifically, size-selective predation has weaker impacts on adults with small body sizes (e.g., Galbraith, 1967), whereas age-selective predation could more broadly remove adults (e.g., with a variety of body sizes). Specifically, size-selective led to adults with small body sizes (i.e., size- vs. age-selective predation), and these size reductions corresponded with slow individual growth rates (i.e., long juvenile growth periods (Fig. 3B) that could lead to a more time until maturation, or a higher age at maturity (Fig. 3D; Charlesworth, 1980). Thus, observed increases in age at maturity under size-selective predation could be another potential downstream effect of reduced maximum body size, though contemplating adaptive pathways amongst traits should be relegated to future studies that map the genetic architecture of traits.

Similar lines of logic may also help explain the other counterintuitive trait change – low total fecundity under high resource levels and size-selective predation. Fecundity is often positively associated with resource levels (Tessier et al., 1992; Cuenca-Cambronero et al., 2018) and body size (Green, 1956), as larger individuals can have larger clutch sizes (Cuenca-

Cambronero et al., 2018) and potentially allocate excessive resource uptake toward reproduction. Thus, high resource levels and nonselective predation generating the highest average total fecundity aligns with a large body of work, although there was again a notable absence of an independent effect of resource level on traits related to maturation or fecundity. On one hand, treatments with low fecundity exhibited sharp declines in per capita growth rate (Fig. S2B) that is suggestive of critical resource limitation levels, which can reduce energetic allocation toward reproduction and lower fecundity (Noonburg et al., 1998). On the other hand, fecundity is often influenced by variety of related life history traits, and thus specific changes in related traits are often better understood as part of a combined response (Lynch et al., 1986; Tessier et al., 1992). For example, high resource levels and nonselective predation led to the largest average size at maturity (Fig. 3C) in addition to the highest fecundity (Fig. 3E), and increased size at maturity can lead to increased total fecundity by increasing clutch size (Lynch et al., 1986).

However, despite evidence for several life history tradeoffs, many life history trait correlations were weak and positive within treatments, and tended to vary strength and direction between treatments (Fig. 4). Positive trait correlations were particularly frequent between traits related to growth and the age or size of maturity, or traits related to fecundity and the age or size of maturity. This provided surprisingly limited evidence for the principle of allocation (Levins, 1968), which states that energy allocation towards several energetically costly processes, such as growth, maturation, and reproduction, hinders maximizing fitness (Levins, 1968). Thus, the frequent occurrence of positive correlations between these traits contradicted this notion, which may have been due to disproportionate resource allocation (van Noordwijk and de Jong, 1986) or genetically based functional constraints on trait responses (Charlesworth, 1990), though greater inference about mechanistic underpinnings requires additional studies.

There has been much interest in understanding whether rapid adaptive evolution is repeatable (Grainger et al., 2022) and when feedbacks exist between rapid evolutionary and ecological change (Post and Palovacs, 2009). This study demonstrates that selective predation can lead to partially divergent consumer life history trait evolution under contrasting resource levels, as well as lead to adaptive reductions in maximum body size that can thereby lower per capita growth rate under low resource levels. In nature, this ecological context may arise when environmental conditions are unfavorable for consumers, and thus could act in a manner that may imperil consumer persistence under intense predation. Given the strong impetus for better understanding consumer life history trait evolution in rapidly changing environments (e.g., Levins, 1968; Stearn, 1992), additional studies are warranted to determine how other biotic or abiotic drivers shape consumer trait evolution over short timescales. For example, high densities of toxic algal resources can lead to a different assortment of trait changes in consumers than observed here (Hairston et al., 2001). Additionally, there are often many predators in a single environment (Lima, 1992), and the presence of multiple predators can lead to yet another assortment of life history trait changes (Schwartz, 1984). Through time, this body of work may eventually resolve the major drivers of consumer life history trait evolution under important ecological contexts and thereby enhance the predictability of population responses to novel combinations of selective pressures.

Acknowledgements

We thank Dr. Matthew Walsh and his lab for providing *Daphnia*; the Culture Collection of Algae at the University of Texas (UTEX) for providing algae samples; Dr. Elizabeth Ruck, Dr. Kayla Downey, and Dr. Andrew Alverson for providing equipment and technical support; Samuel Dias for help with the autoclave; and Dr. Zachery Zbinden for providing tools and information that aided work with algae samples. SPT was supported in part by the NSF (GRFP 1842401). AMS was supported by NSF DEB 1748945.

Data and Code Availability

All data and code for analyses are available on a public GitHub repository at https://github.com/simontye/2022_MME_EcoEvo.

Population dynamics	Size-selective predation	High food resources	Combined effects	Source
Population density	−	+	+	Vanni, 1987
Per capita growth rate	+	+	+	Arendt and Reznick, 2005
Life history trait changes				
Maximum body size	−	+	−	Brooks and Dodson, 1965 Galbrath, 1967
Juvenile growth period	+/−	−	−	Arendt and Reznick, 2005
Size at maturity	+/−	+	+	NA
Age at maturity	−	+	+/−	Cuenca-Cambronero et al., 2018; Lyberger et al., 2021
Total fecundity	−	+	+/−	NA

Figure 1. Conceptual figure of expected effects of size-selective predation and high resource levels on consumer population dynamics and life history trait evolution. Specifically, this graphical table shows expected directional changes in two characteristics of population dynamics (top panel) and five life history traits (bottom panel) under size-selective predation (column dark grey header), high food resource levels (column with dark green header), and their combined effects (column with dark grey and green header). Expected directional changes are shown with positive (+) or negative (-) signs, and responses that may vary directionally or generate an antagonistic response are indicated by both positive and negative signs (+/-). Key observations and experiments that underly these predictions are shown in the rightmost column.

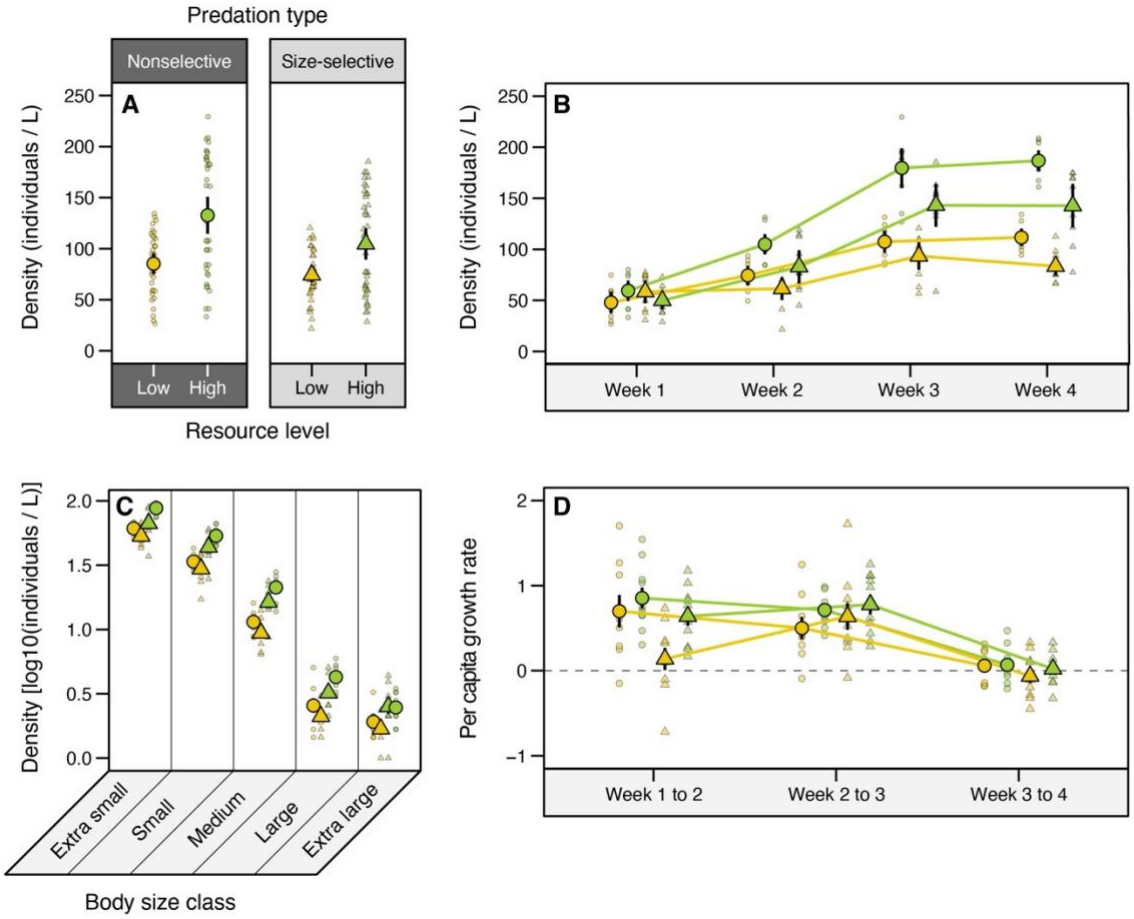

Figure 2. Resource level had a greater effect than predation type on population dynamics and size structure. Average population density of *Daphnia pulicaria* (individuals / L) across (A) and through time (B); average replicate density of each body size class (C); and average replicate per capita growth rate through time (D) under two different predation types (nonselective, circle; size-selective, triangle) and resource levels (low, yellow; high, green). For A-D, large points, small points, and black lines indicate treatment means, replicate values, and +/- 1 SE, respectively. For C, mean densities are shown for five different body size classes within replicate populations over time: extra small (90 µm to 500 µm), small (500 µm to 1 mm), medium (1 to 1.4 mm), large (1.4 to 2 mm), and extra large (>2 mm).

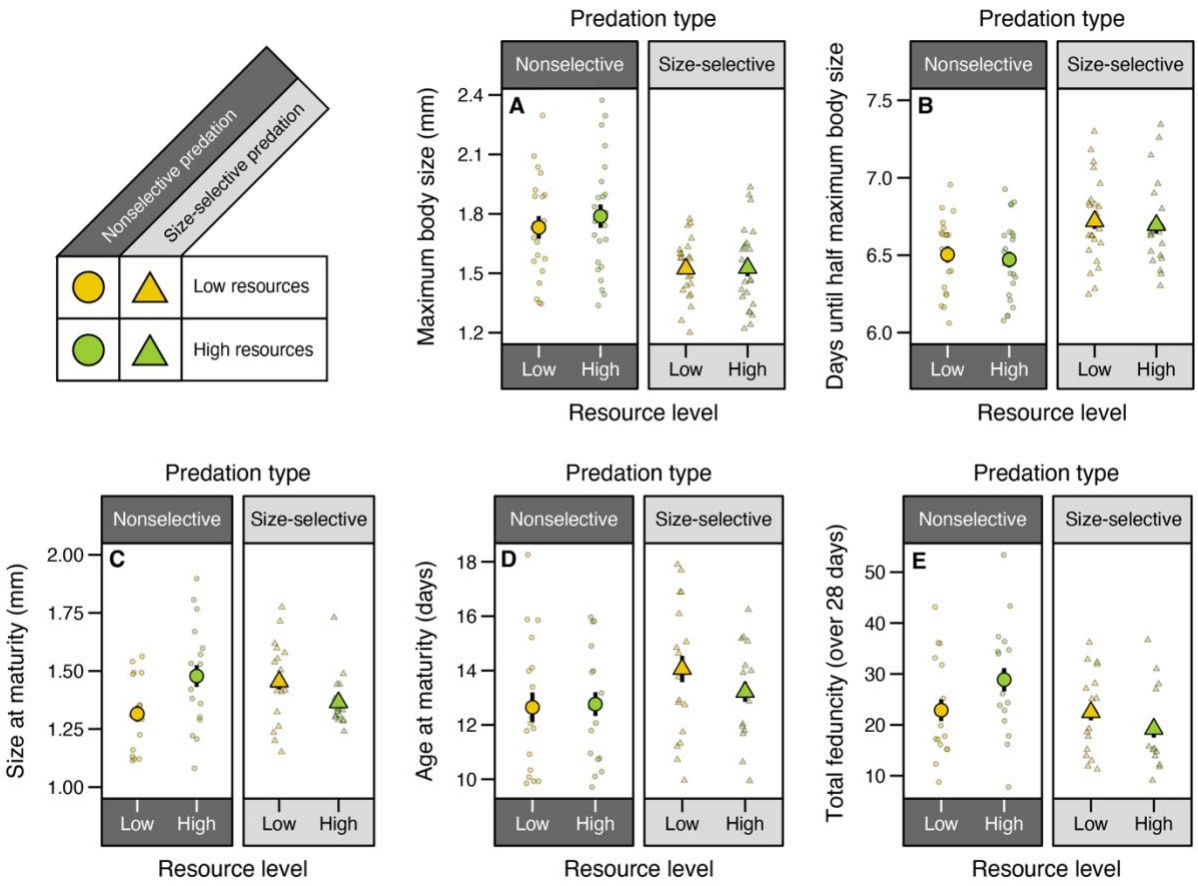

Figure 3. Predation type had a greater effect than resource level on most recorded life history traits. Average values of five life history traits of *Daphina puliciaria* individuals exposed to nonselective predation and low resources (yellow circle, n = 17), nonselective predation and high resources (green circle, n = 16), size-selective predation and low resources, (yellow triangle, n = 17), and size-selective predation and high resources (green triangle, n = 14). Life history traits included maximum body size (A, mm), days until half maximum body size (B, days), size at maturity (C, mm), age at maturity (D, days), and total fecundity (E, over 28 days). Large points, small points, and black lines indicate treatment means, replicate values, and +/- 1 SE, respectively.

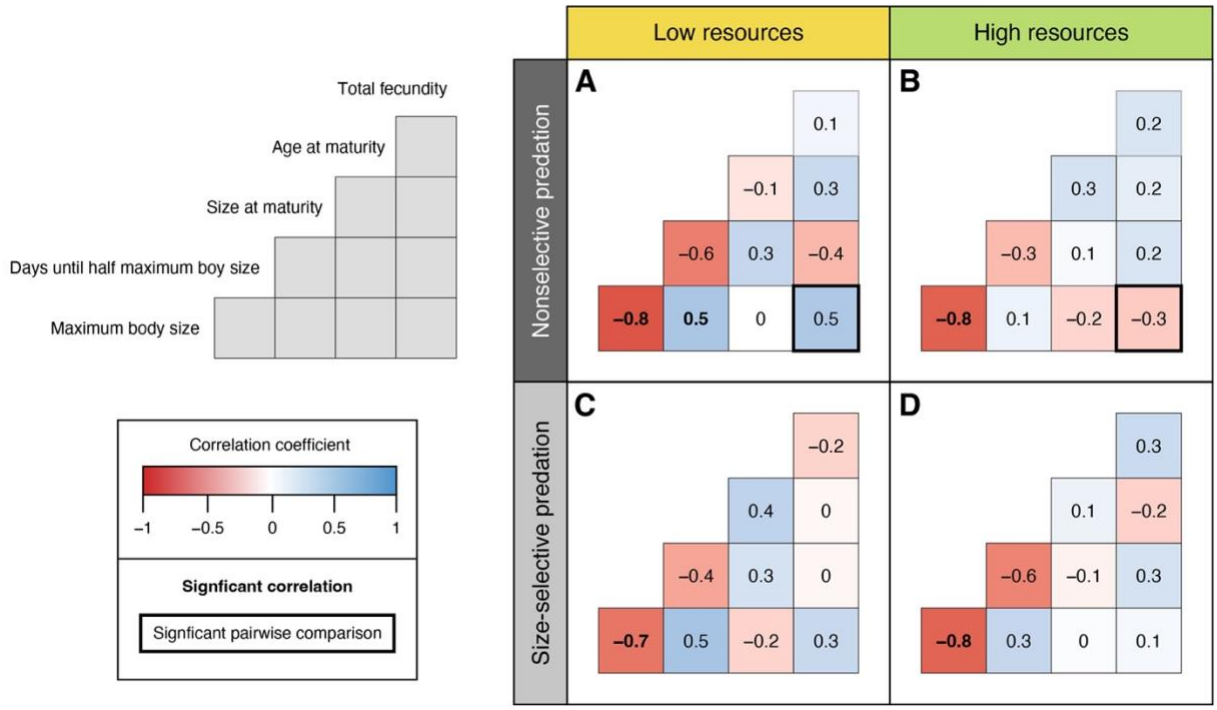

Figure 4. Maximum body size and juvenile growth period were strongly negatively correlated among individuals in each treatment. Correlation coefficients (Pearson's *r*) between *Daphnia pulicaria* life history traits separately for each treatment (A-D). Colors bordering main panels indicate different resource levels (yellow or green) and predation types (light or dark gray). Correlation matrices show whether trait correlations were negative (red), negligible (white), or positive (blue). Significant correlations are bolded, and significant pairwise comparisons between correlations of different treatments are bordered by a thick line (i.e., between maximum body size and total fecundity in treatments with nonselective predation and low resources (A) or high resources (B)).

References

Abrams, P. A., and L. Rowe. 1996. The effects of predation on the age and size of maturity of prey. *Evolution*, **50**(3):1052-1061. doi:10.1111/j.1558-5646.1996.tb02346.x.

Alekseev, V., and W. Lampert. 2004. Maternal effects of photoperiod and food level on life history characteristics of the cladoceran *Daphnia pulicaria* Forbes. *Hydrobiologia*, **526** (1):225-230. doi:10.1023/b:hydr.0000041600.16226.12.

Allee, W. C., and E. Bowen. 1932. Studies in animal aggregations: mass protection against colloidal silver among goldfishes. *Journal of Experimental Zoology*, **61**(2):185-207. Doi:10.1002/jez.1400610202

Anholt, B. R., and E. E. Werner. 1998. Predictable changes in predation mortality as a consequence of changes in food availability and predation risk." *Evolutionary Ecology*, **12**(6):729-738. doi:10.1086/285537

Arendt, J. D., and D. N. Reznick. 2005. Evolution of juvenile growth rates in female guppies (*Poecilia reticulata*): predator regime or resource level? *Proceedings of the Royal Society B*, **272**(1560):333-337. doi:10.1098/rspb.2004.2899

Brooks, J. L., and S. I. Dodson. 1965. Predation, Body Size, and Composition of Plankton. *Science*, **150**(3692):28-35. doi:10.1126/science.150.3692.28.

Burns, C. W. 1995. Effects of Crowding and Different Food Levels on Growth and Reproductive Investment of *Daphnia*. *Oecologia*, **101**(2):234-244. doi:10.1007/bf00317289

Carroll, S. P., A. P. Hendry, D. N. Reznick, and C. W. Fox. 2007. Evolution on Ecological Time-Scales. *Functional Ecology*, **21**(3):387-393. doi:10.1111/j.1365-2435.2007.01289.x.

Cerny, M., and J. Bytel. 1991. Density and Size Distribution of *Daphnia* Populations at Different Fish Predation Levels. *Hydrobiologia*, **225**:199-208. doi:10.1007/bf00028398

Charlesworth, B. 1994. *Evolution in age-structured populations*. Cambridge University Press.

Cuenca-Cambronero, M., H. Marshall, L. De Meester, T. A. Davidson, A. P. Beckerman, and L. Orsini. 2018. Predictability of the Impact of Multiple Stressors on the Keystone Species *Daphnia*. *Scientific Reports*, **8**(1):17572. doi:10.1038/s41598-018-35861-y.

Day, D., P. A. Abrams, and J. M. Chase. 2002. The role of size-specific predation in the evolution and diversification of prey life histories. *Evolution*, **56**(5):877-887. doi: 10.1111/j.0014-3820.2002.tb01401.x.

Diedenhofen, B., and J. Musch. 2015. cocor: a comprehensive solution for the statistical comparion of correlations. *PLoS ONE*, **10**(4):e0121945. doi:10.1371/journal.pone.0121945

Dodson, S. I., and J. E. Havel. 1988. Indirect Prey Effects: Some Morphological and Life History Responses of *Daphnia pulex* Exposed to *Notonecta undulata* 1: Prey Response in *Daphnia pulex*. *Limnology and Oceanography*, **33**(6):1274-1285. doi:10.4319/lo.1988.33.6.1274.

Ebert, D. 2022. *Daphnia* as a Versatile Model System in Ecology and Evolution. *EvoDevo*, **13**(1):16. doi:10.1186/s13227-022-00199-0.

Estes, J. A., J. Terborgh, J. S. Brashares, M. E. Power, J. Berger, W. J. Bond, S. R. Carpenter, et al. 2011. Trophic Downgrading of Planet Earth. *Science*, **333**(6040):301-306. doi:10.1126/science.1205106.

Galbraith, M. G. 1967. Size-Selective Predation on *Daphnia* by Rainbow Trout and Yellow Perch. *Transactions of the American Fisheries Society*, **96**(1):1–10. doi:10.1577/1548-8659(1967)96[1:spodbr]2.0.CO;2.

Gillis, M. K., and M. R. Walsh. 2017. Rapid Evolution Mitigates the Ecological Consequences of an Invasive Species (*Bythotrephes longimanus*) in Lakes in Wisconsin. *Proceedings of the Royal Society B*, **284**(1858):20170814. doi:10.1098/rspb.2017.0814.

Grainger, T. N., and J. M. Levine. 2022. Rapid Evolution of Life-history Traits in Response to Warming, Predation and Competition: A Meta-analysis. *Ecology Letters*, **25**(2):541–554. doi:10.1111/ele.13934.

Grant, P. R., and B. R. Grant. 2006. Evolution of Character Displacement in Darwin's Finches. *Science*, **313**(5784): 224–226. doi:10.1126/science.1128374

Green, J. 1956. Growth, size, and reproduction in *Daphnia* (Crustacea: Cladocera). *Proceedings of the Zoological Society of London*, **126**(2):173-204 doi:10.1111/j.1096-3642.1956.tb00432.x

Grether, G. F., D. F. Millie, M. J. Bryant, D. N. Reznick, and W. Mayea. 2001. Rain forest canopy cover, resource availability, and life history evolution in guppies. *Ecology*, **82**(6):1546-1559. doi:10.1890.0012-9658(2001)082[1546rfccra]2.0.co;2

Hairston, N. G., F. E. Smith, and L. B. Slobodkin. 1960. Community Structure, Population Control, and Competition. *The American Naturalist*, **94**(879):421–425. doi:10.1086/282146.

Hairston, N. G., C. L. Holtmeier, W. Lampert, L. J. Weider, D. M. Post, J. M. Fischer, C. E. Caceres, J. A. Fox, and U. Gaedke. 2001. Natural selection for grazer resistance to toxic cyanobacteria: evolution of phenotypic plasticity. *Evolution*, **55**(11):2202-2214. doi:10.1111/j.0014-3820.2001.tb00736.x

Hall, D. J., S. T. Threlkeld, C. W. Burns, and P. H. Crowley. 1976. The size-efficiency hypothesis and the size structure of zooplankton communities. *Annual Review of Ecology and Systematics*, **7**:177-208. doi:10.1146/annurev.es.07.110176.001141

Haloin, J. R., and S. Y. Strauss. 2008. Interplay between Ecological Communities and Evolution. *Annals of the New York Academy of Sciences*, **1133**(1):87-125. doi:10.1196/annals.1438.003

Harrell Jr., F. E. 2022. Hmisc: Harrell Miscellaneous. R package version 4.7-1, https://CRAN.R-project.org/package=Hmisc

Hendry, A. P., and M. T. Kinnison. 1999. The pace of modern life: measuring rates of contemporary microevolution. *Evolution*, **53**(6):1637-1653. doi:10.111/j.1558-5646.1999.tb04550.x

Hendry, A. P. 2019. A critique for eco-evolutionary dynamics. *Functional Ecology*, **33**(1):84-94. doi:10.1111/1365-2435.13244

Hutchinson, G. E. 1965. *The Ecological Theater and the Evolutionary Play*. Yale University Press.

Kilham, S. S, D. A Kreeger, S. G. Lynn, C. E. Goulden, and L. Herrera. 1998. COMBO: A Defined Freshwater Culture Medium for Algae and Zooplankton. *Hydrobiologia*, **377**:147-159. doi:10.1023/a:1003231628456

Kinnison, M. T., N. G. Hairston Jr., and A. P. Hendry. 2015. Cryptic eco-evolutionary dynamics. *Annals of the New York Academy of Sciences*, **1360**(1):120-144. doi:10.1111/nyas.12974

Levins, R. 1968. *Evolution in rapidly changing environments*. Princeton University Press.

Lima S. L., and L. M. Dill. 1990. Behavioral decisions made under the risk of predation: a review and prospectus. *Canadian Journal of Zoology*, **68**(4):619-640. doi:10.1139/z90-092.

Lima, S. L. 1992. Life in a multi-predator environment: some considerations for anti-predatory vigilance. *Annales Zoologici Fennici*, **29**(4): 217-226. doi:jstor.org/stable/23735623

Lyberger, K., T. W. Schoener, and S. J. Schreiber. 2021. Effects of Size Selection versus Density Dependence on Life Histories: A First Experimental Probe. *Ecology Letters*, **24** (7):1467–73. doi:10.1111/ele.13767.

Lynch, M. 1986. Measurement of the carbon balance in *Daphnia*. *Limnology and Oceanography* **31**(1):17-33. doi:10.4319/lo.1986.31.1.0017

Lynch, M. 1989. The Life History Consequences of Resource Depression in *Daphnia pulex*. *Ecology*, **70**(1):246–56. doi:10.2307/1938430.

McCauley, E., R. M. Nisbet, W. W. Murdoch, A. M. de Roos, and W. S. C. Gurney. 1999. Large-Amplitude Cycles of *Daphnia* and Its Algal Prey in Enriched Environments. *Nature*, **402**(6762):653–56. doi:10.1038/45223.

Noonburg, E. G., R. M. Nisbet, E. McCauley, W. S. C. Gurney, W. M. Murcdoch, and A. M. de Roos. Experimental testing of dynamic energy budget models. *Functional Ecology*, **12**(2):212-222. doi:10.1046/j.1365-2435.1998.00174.x

Paine, R. T. 1966. Food Web Complexity and Species Diversity. *The American Naturalist*, **100**(910):65–75. doi:10.1086/282400.

Paine, R. T. 1980. Food Webs: Linkage, Interaction Strength and Community Infrastructure. *The Journal of Animal Ecology*, **49**(3):666–85. doi:10.2307/4220.

Pinherio, J., D. Bates, and R Core Team. 2022. nlme: Linear and Nonlinear Mixed Effects Models. R Package.

Polis, G. A., W. B. Anderson, and R. D. Holt. 1997. Toward an Integration of Landscape and Food Web Ecology: The Dynamics of Spatially Subsidized Food Webs. *Annual Review of Ecology and Systematics*, **28**(1):289–316. doi:10.1146/annurev.ecolsys.28.1.289.

Post, D. M. and E. P. Palovacs. 2009. "Eco-evolutionary feedbacks in community and ecosystem ecology: interactions between the ecological theatre and the evolutionary play." *Philosophical Transactions of the Royal Society B*, **364**(1523):1629-1640. doi:10.1098/rstb.2009.0012

R Core Team, 2021. R: A language and environment for statistical computing. R Foundation for Statistical Computing, Vienna, Austria.

Reznick, D., and J. A. Endler. 1982. The impact of predation on life history evolution in Trinidadian guppies (*Poecilia reticulata*). *Evolution*, **36**(1):160-177. doi:10.2307/2407978

Reznick, D., M. J. Bryant, and F. Bashey. r- and K-selection revisited: the role of population regulation and in life-history evolution. *Ecology*, **83**(6):1509-1520. doi:10.1890/0012-9658(2002)083[1509:raksrt]2.0.co;2

Schwartz, S. S. 1984. Life history strategies in *Daphnia*: a review and predictions. *Oikos*, **42**(1):114-122. doi:10.2307/3544616

Schneider, C. A., W. S. Rasband, and K. W. Eliceiri. 2012. NIH Image to ImageJ: 25 years of Image Analysis *Nature Methods*, **9**(7):671-675. doi:10.1038/nmeth.2089

Siepielski, A. M., A. Z. Hasik, T. Ping, M. Serrano, K. Strayhorn, and S. P. Tye. 2020. Predators weaken prey intraspecific competition through phenotypic selection. *Ecology Letters*, **23**(6):951-961. doi:publons.com/publon/10.1111/ele.13491

Singmann, H., B.Bolker, J. Westfall, F. Aust, and M. S. Ben-Shachar. 2023. afex: analyses of factorial experiments. R package version 1.2-1, https://CRAN.R-project.org/package=afex

Slobodkin, L. B. 1961. Stochastic Population Models in Ecology. *Ecology*, **42**(4):852-852. doi:10.2307/19335333

Spitze, Ken. 1991. *Chaoborus* predation and life-history evolution in *Daphnia pulex*: temporal pattern of population diversity, fitness, and mean life history. *Evolution*, **45**(1):82-92. doi:10.1111/j.1558-5646.1991.tb05268.x.

Strauss, S. Y. 2014. Ecological and evolutionary responses in complex communities: implications for invasions and eco-evolutionary feedbacks. *Oikos*, **123**:257-266. doi:10.1111/j.1600-0706.2013.01093.x

Stearn, S. C. 1992. *The Evolution of Life Histories*. Oxford University Press, 249 pp.

Tessier, A. J., A. Young, and M. Leibold. 1992. Population Dynamics and Body-Size Selection in *Daphnia*. *Limnology and Oceanography*, **37**(1):1-13. doi:10.4319/lo.1992.37.1.0001

Vanni, M. J. 1987. Effects of food availability and fish predation on a zooplankton community. *Ecological Monographs*, **57**(1):61-88. doi:10.2307/1942639

Van Noordwijk, A. J., and G. De Jong. 1986. Acquisition and allocation of resources: their influence on variation in life history tactics. *The American Naturalist*, **128**(1):137-142. doi:10.1086/284547

Yoshida, T., L. E. Jones, S. P Ellner, G. F. Fussman, and N. G. Hairston Jr. 2003. Rapid evolution drives ecological dynamics in a predator-prey system. *Nature*, **424**:303-306. doi:10.1038/nature01767

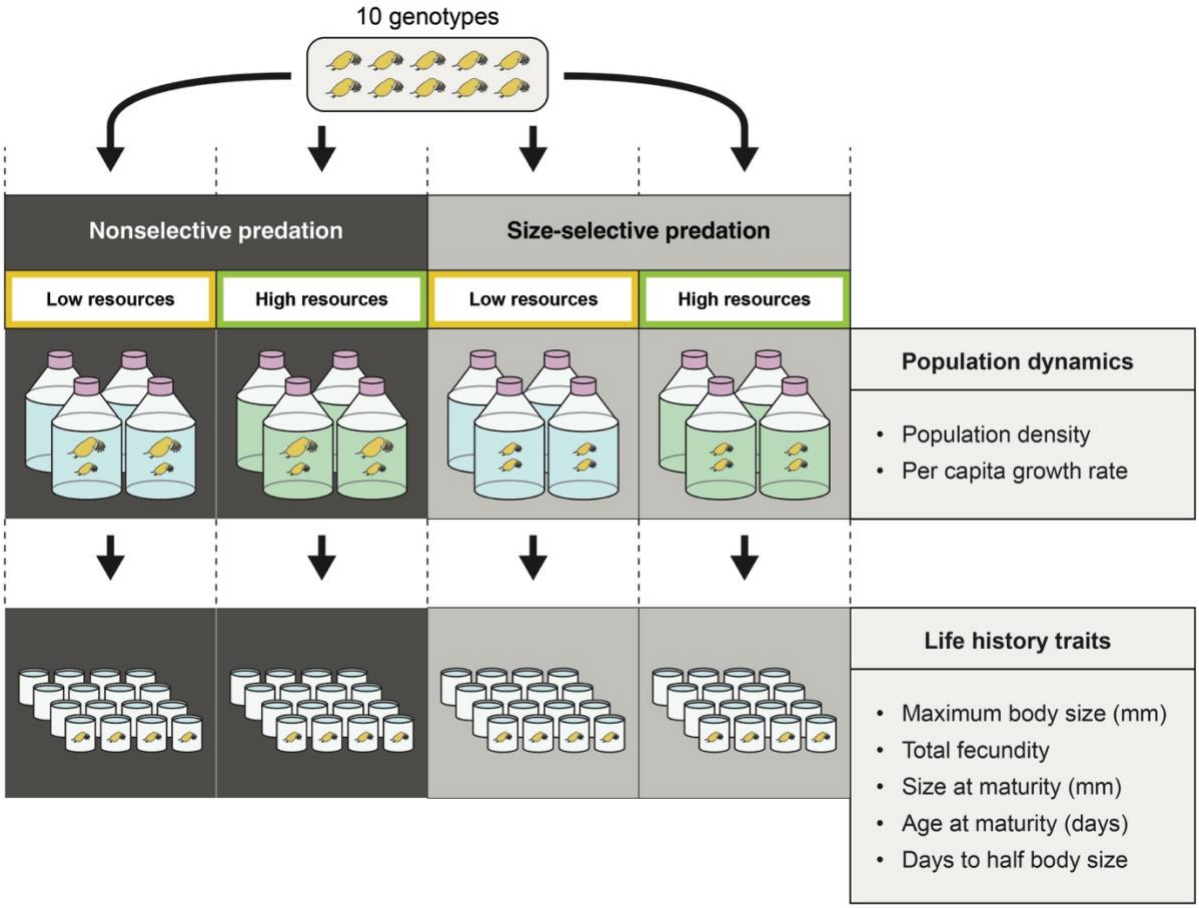

Figure S1. Experimental design and workflow for measuring population dynamics (top row with large containers) and life history traits (bottom row with small containers). We first exposed *Daphnia pulicaria* populations containing 10 genotypes to one of two types of predation (nonselective, dark gray; size-selective, medium gray), as well as either low (yellow) or high (green) resource levels. We measured characteristics of population dynamics (population density, density of each body size class, per capita growth rate) within these microcosms for 28 days (i.e., top row). Within these illustrated microcosms, *Daphnia* are shown at different body sizes to illustrate the different predation types and the growth medium is shown in different colors to illustrate different resource levels. We then sampled individuals, reared them in isolation for two generations, and measured five life history traits over 28 days (i.e., bottom row).

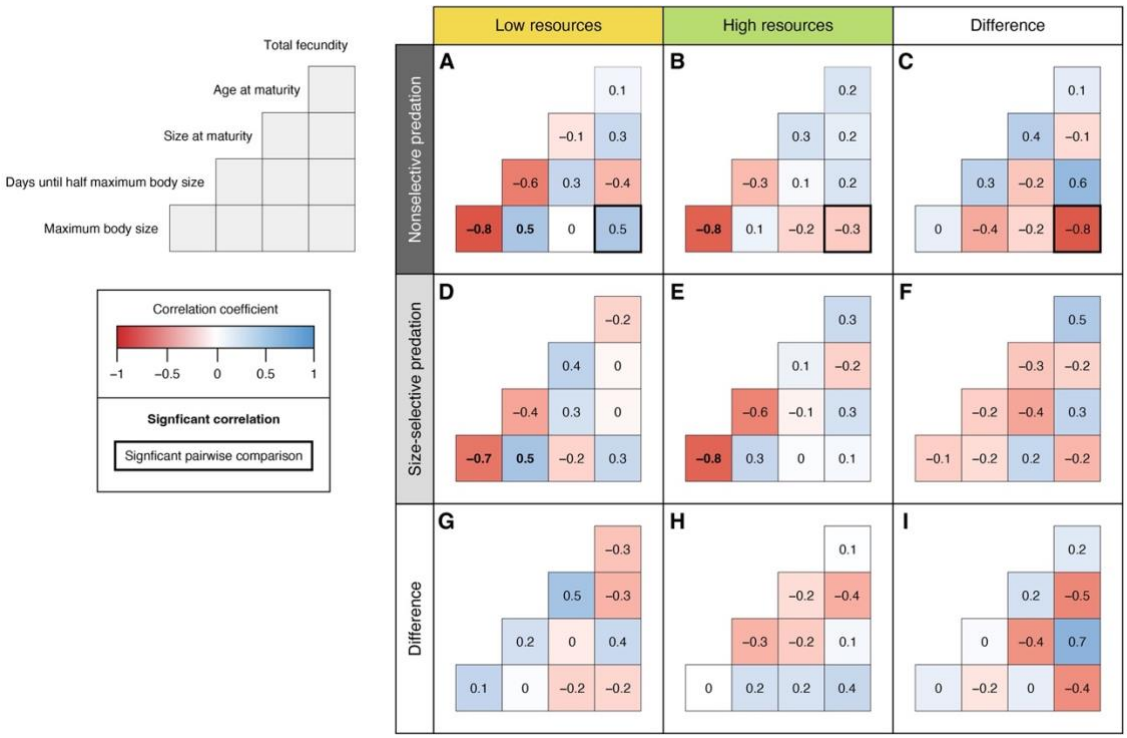

Figure S2. Correlation coefficients (Pearson's *r*) between recorded life history traits separately for each treatment (A-D) and differences between correlation coefficients of treatments (C, F-I). Colors bordering main panels indicate different resource levels (yellow or green), predation types (dark or light gray), and differences between correlation coefficients in different treatments (white). These differences are displayed such that treatments with low resource levels (A, D) or high resource levels (B, E) are shown in the same row (C, F); differences between treatments with nonselective predation (A, B) or size-selective predation (D, E) are shown in the same column (G, H); and differences between treatments with nonselective predation with low resources (A) and size-selective predation with high resources is shown on the diagonal (E). Correlation coefficients (A-B, D-E) and their differences (C, F-I) are filled based on their sign: negative (red), zero (white), or positive (blue). Significant correlation coefficients are bolded, and significant pairwise comparisons between correlations coefficients of different treatments are bordered by a thick line.

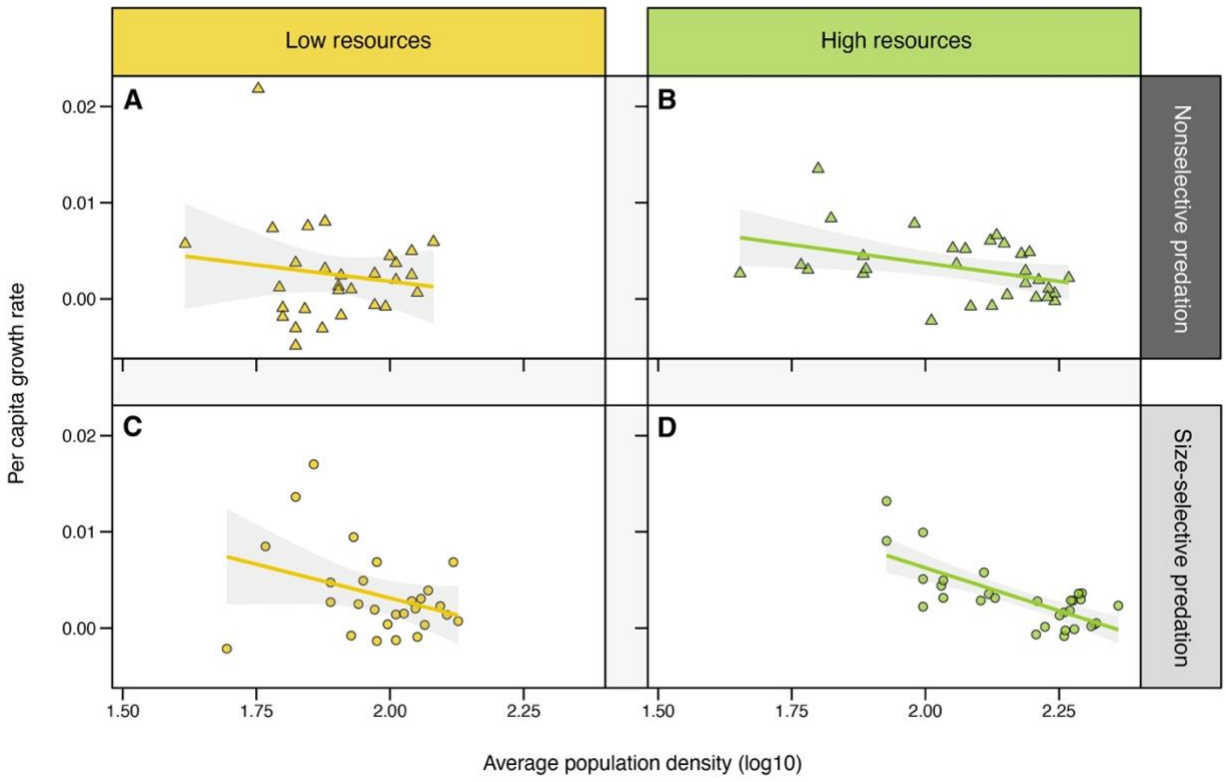

Figure S3. Linear regressions of replicate average population density (log10) and per capita growth rate for each treatment. Colors for different resource levels (yellow or green) and predation types (dark or light gray) are shown on the margin to differentiate treatments: nonselective predation and low resource levels (A; yellow circle), nonselective predation and high resource levels (B; green circle), size-selective predation and low resource levels (C; yellow triangle), and size-selective predation and high resource levels (D; green triangle). Points indicate specific microcosms and gray bands indicate 95% confidence intervals.

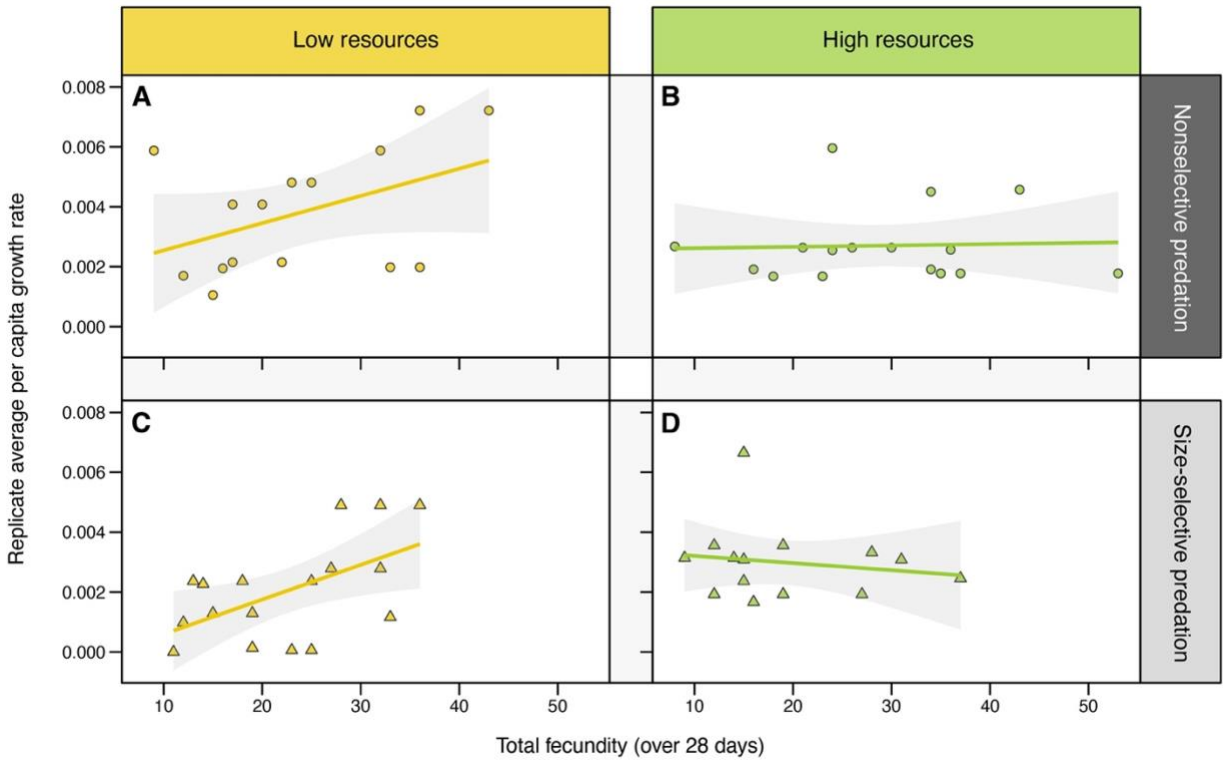

Figure S4. Linear regressions of total fecundity (over 28 days) of F3 individuals and the replicate average per capita growth rate (i.e., of their original microcosms). Colors for different resource levels (yellow or green) and predation types (dark or light gray) are shown on the margin to differentiate treatments: nonselective predation and low resource levels (A; yellow circle), nonselective predation and high resource levels (B; green circle), size-selective predation and low resource levels (C; yellow triangle), and size-selective predation and high resource levels (D; green triangle). Across all panels, points indicate individual *Daphnia* (i.e., individual trait value compared to a characteristic of population dynamics from their original microcosm), and gray bands indicate 95% confidence intervals.

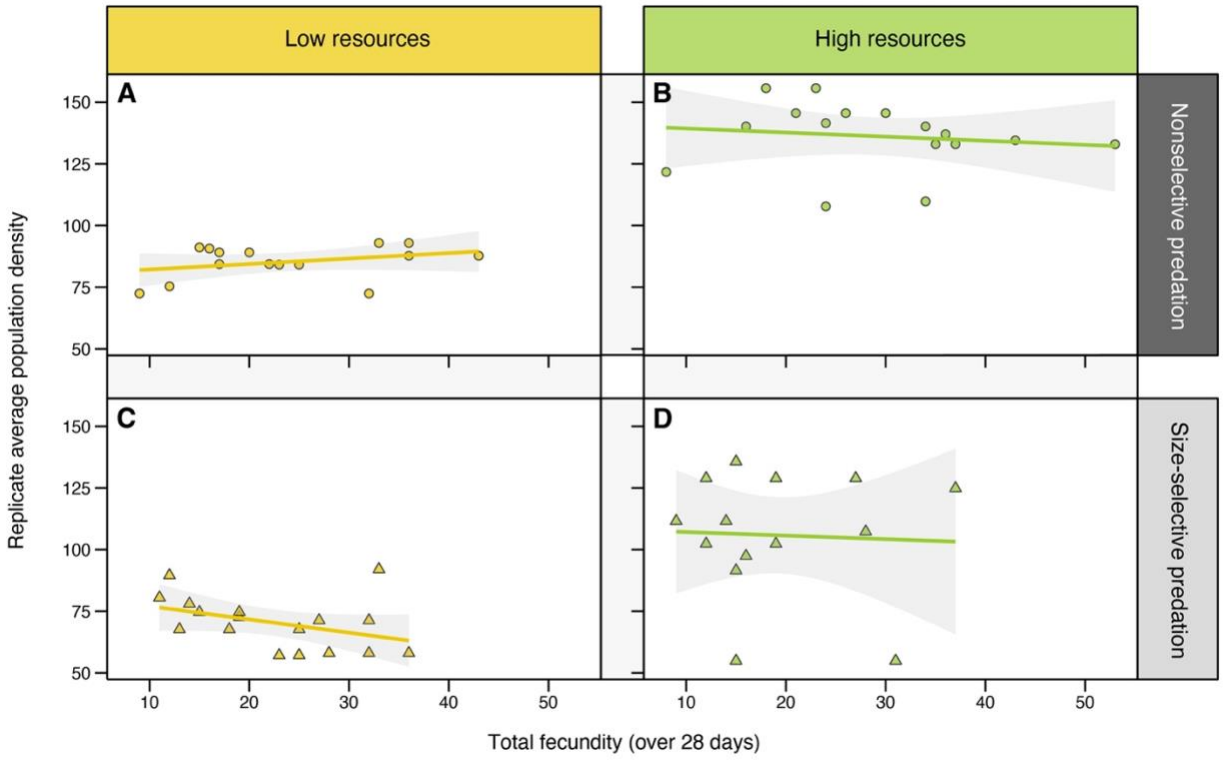

Figure S5. Linear regressions of total fecundity (over 28 days) of F3 individuals and the replicate average population density (i.e., of their original microcosms). Colors for different resource levels (yellow or green) and predation types (dark or light gray) are shown on the margin to differentiate treatments: nonselective predation and low resource levels (A; yellow circle), nonselective predation and high resource levels (B; green circle), size-selective predation and low resource levels (C; yellow triangle), and size-selective predation and high resource levels (D; green triangle). Across all panels, points indicate individual *Daphnia* (i.e., individual trait value compared to a characteristic of population dynamics from their original microcosm), and gray bands indicate 95% confidence intervals.

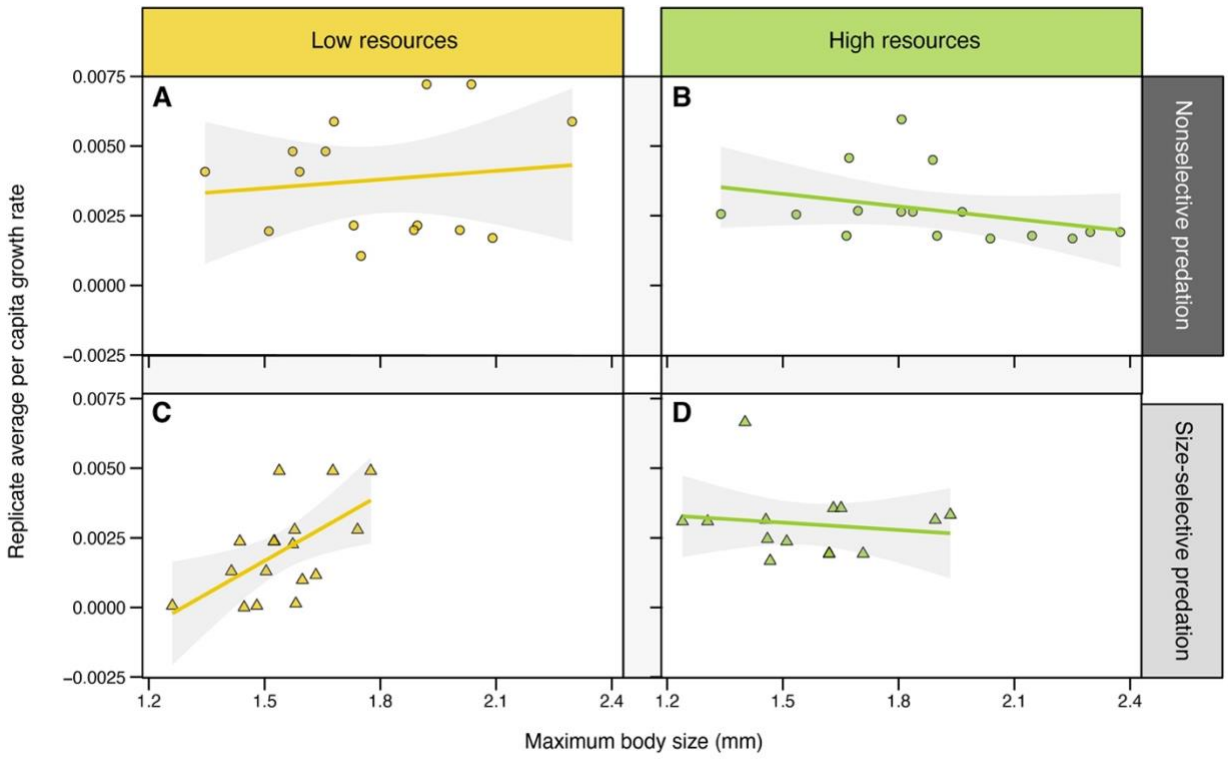

Figure S6. Linear regressions maximum body size of F3 individuals and the replicate average per capita growth rate (i.e., of their original microcosms). Colors for different resource levels (yellow or green) and predation types (dark or light gray) are shown on the margin to differentiate treatments: nonselective predation and low resource levels (A; yellow circle), nonselective predation and high resource levels (B; green circle), size-selective predation and low resource levels (C; yellow triangle), and size-selective predation and high resource levels (D; green triangle). Across all panels, points indicate individual *Daphnia* (i.e., individual trait value compared to a characteristic of population dynamics from their original microcosm), and gray bands indicate 95% confidence intervals.

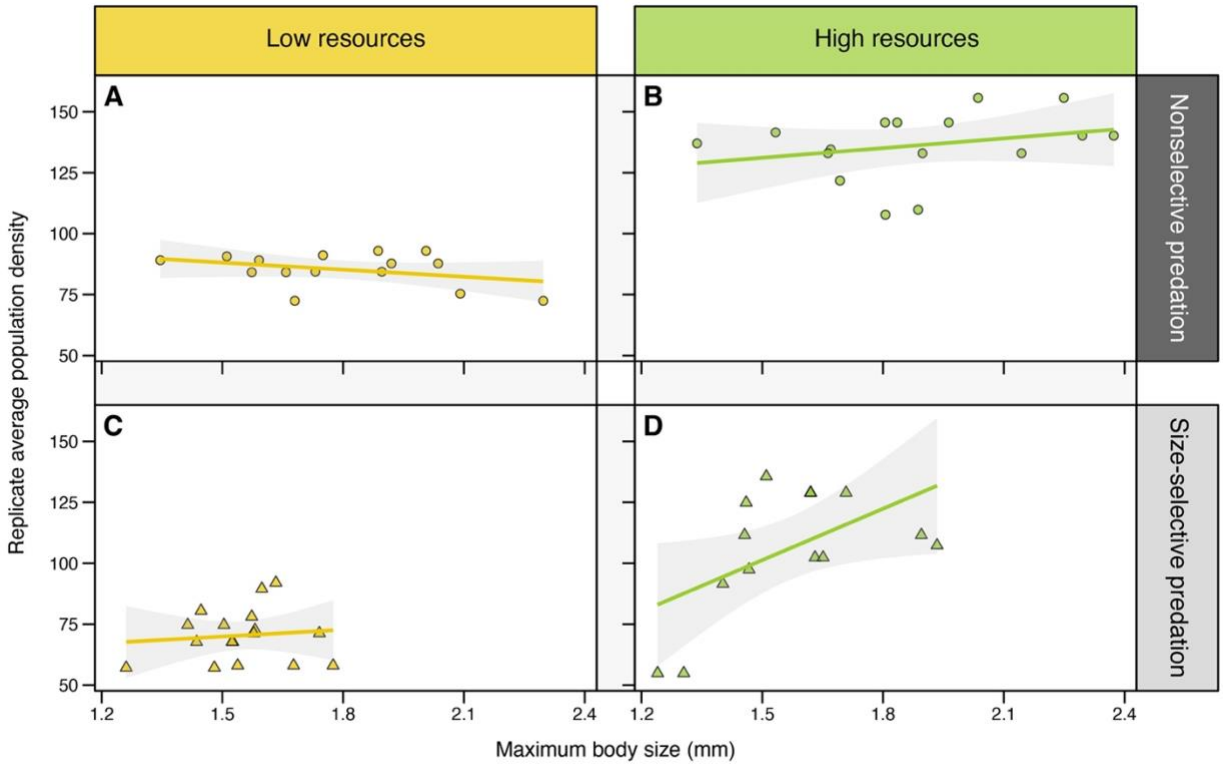

Figure S7. Linear regressions maximum body size of F3 individuals and the replicate average population density (i.e., of their original microcosms). Colors for different resource levels (yellow or green) and predation types (dark or light gray) are shown on the margin to differentiate treatments: nonselective predation and low resource levels (A; yellow circle), nonselective predation and high resource levels (B; green circle), size-selective predation and low resource levels (C; yellow triangle), and size-selective predation and high resource levels (D; green triangle). Across all panels, points indicate individual *Daphnia* (i.e., individual trait value compared to a characteristic of population dynamics from their original microcosm), and gray bands indicate 95% confidence intervals.

Table S1. Correlation coefficients (Pearson's *r*) between five recorded traits of *Daphnia pulicaria* under nonselective predation and low resource levels. *P*-values adjusted for multiple comparisons via Holm's method are shown in parentheses and asterisks indicate significant correlation coefficients.

	Maximum body size (mm)	**Size at maturity (mm)**	**Age at maturity (days)**	**Days until half maximum body size**
Size at maturity (mm)	0.52 (0.27)			
Age at maturity (days)	-0.01 (1.00)	-0.14 (1.00)		
Days until half maximum body size	0.83 (< 0.001)*	-0.64 (0.05)*	0.35 (0.98)	
Total fecundity (over 28 days)	0.50 (0.29)	0.33 (0.98)	0.09 (1.00)	-0.35 (0.98)

Table S2. Correlation coefficients (Pearson's *r*) between five recorded traits of *Daphnia pulicaria* under nonselective predation and high resource levels. *P*-values adjusted for multiple comparisons via Holm's method are shown in parentheses and asterisks indicate significant correlation coefficients.

	Maximum body size (mm)	**Size at maturity (mm)**	**Age at maturity (days)**	**Days until half maximum body size**
Size at maturity (mm)	0.15 (1.00)			
Age at maturity (days)	-0.20 (1.00)	-0.30 (1.00)		
Days until half maximum body size	-0.79 (0.001)*	-0.33 (1.00)	0.08 (1.00)	
Total fecundity (over 28 days)	-0.26 (1.00)	0.16 (1.00)	0.25 (1.00)	-0.26 (1.00)

Table S3. Correlation coefficients (Pearson's *r*) between five recorded traits of *Daphnia pulicaria* under size-selective predation and low resource levels. *P*-values adjusted for multiple comparisons via Holm's method are shown in parentheses and asterisks indicate significant correlation coefficients.

	Maximum body size (mm)	**Size at maturity (mm)**	**Age at maturity (days)**	**Days until half maximum body size**
Size at maturity (mm)	0.54 (0.22)			
Age at maturity (days)	-0.21 (1.00)	0.39 (0.83)		
Days until half maximum body size	-0.68 (0.03)*	-0.45 (0.56)	0.26 (1.00)	
Total fecundity (over 28 days)	0.34 (1.00)	-0.03 (1.00)	-0.21 (1.00)	-0.04 (1.00)

Table S4. Correlation coefficients (Pearson's *r*) between five recorded traits of *Daphnia pulicaria* under size-selective predation and high resources. *P*-values adjusted for multiple comparisons via Holm's method are shown in parentheses and asterisks indicate significant correlation coefficients.

	Maximum body size (mm)	**Size at maturity (mm)**	**Age at maturity (days)**	**Days until half maximum body size**
Size at maturity (mm)	0.41 (1.00)			
Age at maturity (days)	0.13 (1.00)	0.13 (1.00)		
Days until half maximum body size	-0.78 (0.008)*	-0.62 (0.16)	-0.17 (1.00)	
Total fecundity (over 28 days)	-0.01 (1.00)	-0.24 (1.00)	0.27 (1.00)	0.32 (1.00)

Chapter 3

Climate warming amplifies the frequency of fish mass mortality events across north temperate lakes

Simon P. Tye, Adam M. Siepielski, Andrew Bray, Andrew L. Rypel, Nicholas B. D. Phelps, and Samuel B. Fey

Abstract

Recent increases of animal mass mortality events have coincided with substantial changes in global climate. Yet tractable approaches that predict how climate change will accentuate occurrences these ecological catastrophes remain nascent. We compiled one of the most comprehensive datasets of lentic fish mortality events, thermal tolerances of affected families, and 1.2 million air and water temperature profiles across 8,891 north temperate lakes in North America. Temperature extremes within and across lakes were strongly associated with the three most frequent cause types (infectious agents, summerkills, winterkills). Thermal tolerances mediated the lethality of direct thermal stress, but mortalities of warm- and cold-water fishes occurred at similar temperature deviations. Water and air temperature-based models accurately predicted contemporary summerkills and suggested ~6 to 34-fold increases, respectively, in their frequency by 2100. These models forecast and contextualize impending ecosystem changes in an increasingly volatile world.

Introduction

Animal mass mortality events – sudden die-offs that affect many demographic classes within populations – have increased in frequency and magnitude since the mid-20th century (Fey et al., 2015) concomitant with ongoing global change (Garrabou et al., 2019). These extreme demographic events impact ecosystem function (McDowell et al., 2017), imperil population persistence (Mangel and Tier, 1994; Anderson et al., 2017), restructure ecological communities (Hansen et al., 2017; Fey et al., 2019), and reduce global food supply (Soon and Ransangan, 2019). Documented animal mortality events have disproportionately affected freshwater fishes (Fey et al., 2015), which are already experiencing global declines (He et al., 2010). Freshwater fish mortality events often coincide with environmental conditions related to warm temperature, such as thermal and oxygen stress (Barica, 1975; Till et al., 2019), infectious disease outbreaks (Marcos- López et al., 2010), and anthropogenic activities (Thronson and Quigg, 2008). Expanding and refining approaches to accurately predict extreme ecological events across broader scales (e.g., Denny et al., 2009; Sinervo et al., 2010; Bailey and van de Pol, 2016; Shen et al., 2018) remains imperative to understanding how recent and future climate warming will restructure ecosystems.

Most global freshwater lakes are in north temperate regions of North America (Verpoorter et al., 2014), and these lakes have recently experienced substantial increases in surface water temperature (Woolway et al., 2020), lake heatwaves (Woolway et al., 2021), widespread deoxygenation events (Jane et al., 2020), rapid thermal regime shifts (Kraemer et al., 2021), and intensified thermal stratification (Woolway et al., 2021). These conditions are major contributing factors to increased frequencies of fish mortality events (Thronson and Quigg, 2008; Fey et al., 2015), and strong positive relationships exist between the occurrence of fish mortality

events and either air (Phelps et al., 2019) or waterbody-specific water temperature (Till et al., 2019) in adjacent regions of North American north temperate lakes.

While regional air temperature variability is generally reduced by thermal inertia of the Laurentian Great Lakes (Notaro et al., 2013), the relationship between regional air and water temperature is dynamic across time (Kraemer et al., 2015) and space, partially due to lake geomorphology (e.g., lake surface area and depth; Kraemer et al., 2015) and dynamic environmental conditions such as productivity (O'Reilly et al., 2015). For example, regional lake geomorphology has strong effects on water temperature (Kraemer et al., 2015), and high productivity lakes frequently experience harmful algal blooms that rapidly reduce dissolved oxygen concentration (Barica, 1975). However, climate models that couple air and water temperature have predicted unanticipated temperature increases in terrestrial regions near large waterbodies (Gröger et al., 2021). Therefore, assessing the feasibility of using widely available air temperature estimates, versus less available depth-specific water temperature estimates, to predict future occurrences of fish mortality events is critical for understanding how future freshwater ecosystems may be restructured.

Here, we develop predictive air and water temperature-based models to examine how climate change has accelerated the frequency of fish mortality events across north temperate lakes. We assembled 526 lentic fish mortality events, thermal tolerances of affected fish taxa, and ~1.2 million air and water temperature profiles, productivity estimates (Secchi depth), and lake surface area across 8,891 north temperate lakes of North America (Winslow et al., 2017; PRISM Climate Group, Oregon State University). We compared air and water temperatures within and across lakes with the three most frequent cause types of regional fish mortality events: infectious agents, summerkills (mortalities associated with warm temperature; Barica,

1975), and winterkills (mortalities associated with cold temperature; Hurst, 2007). We then used air and water temperature-based models to predict frequencies of summerkills across ~3.9 million air and water temperature profiles of regional lakes during the mid- and late 21st century (2041-2059; 2081-2099; Maurer et al., 2007; Winslow et al., 2017) under Representative Concentration Pathway 8.5 (RCP 8.5), the only climate scenario with available regional water temperature estimates (Winslow et al., 2017). Our models predict substantial increases in the frequency of summerkills over coming decades and suggest complex air-water temperature dynamics strongly influence the maximum extent of anticipated mortality increases. This approach demonstrates the feasibility of tractable forecasting of thermally driven ecological catastrophes across broad spatiotemporal scales.

Materials and Methods

We compiled 526 documented lentic fish mortality events across Minnesota and Wisconsin lakes from 2003 to 2013, then used descriptions and diagnoses of observations to assign maximally general cause categories to each observation: anthropogenic, infectious disease, summerkill, winterkill, or unknown (Fig. 1; Table S1). Summerkills and winterkills are mortalities caused by seasonal environmental conditions associated with extreme temperatures (Greenbank, 1945; Barica, 1975) and, therefore, were differentiated by meteorological season. To compare thermal tolerances of affected taxa, we classified mortalities by taxonomic family, thermal category, and mean *CTmax* based on a regional assessment of freshwater fish thermal preferences (Lyons et al., 2009). We used waterbody identifier conversion tables provided by Minnesota IT Services and Wisconsin Department of Natural Resources to associate waterbodies with unique identifiers in the National Hydrological Dataset.

Because our focus was the relationship between summerkills and local temperature, we developed models to predict frequencies of summerkills in relation to concurrent local air (PRISM Climate Group, Oregon State University) and waterbody-specific water temperature profiles (Winslow et al., 2017) across north temperate lakes of North America. We compared 24 models that included different air or water temperature estimates and major environmental covariates (Table S2:S3). The best fit air and water temperature-based models included environmental covariates (latitude, longitude, lake surface area, mean annual Secchi depth, ice duration, precipitation, human population density) and either 1) maximum, mean, and minimum air temperature and z-scores (*logloss* = 2.44) or 2) mean surface water temperature and z-score (*logloss* = 2.48; Fig. S1).

We then used best fit air and water models to predict frequencies of summerkills based on modeled air and water temperature estimates for the mid- and late 21st century (2041-2059; 2081-2099) under Representative Concentration Pathway 8.5 – the worst-case climate scenario and only scenario with water temperature projections across our study region (Winslow et al., 2017). We acquired modeled air temperature estimates (monthly maximum, mean, and minimum) from the World Climate Research Programme's Coupled Model Intercomparison Project phase 3 multi-model dataset (CMIP3; Maurer et al., 2007), and associated waterbody centroids with the nearest temperature estimates (1/8-degree resolution). We used these slightly outdated air temperature projections because they were part of the model ensemble used to create regional water temperature estimates (Winslow et al., 2017) and therefore most directly comparable. We acquired modeled monthly water temperature variables from the same extensive assessment used in historical models (1/8-degree resolution; Winslow et al., 2017).

Several model adjustments were necessary for future predictions. First, we removed ice duration because future estimates are unavailable across most of the study region. Second, because we wanted to account for variation in productivity across lakes but are unable to predict future productivity, we considered annual mean Secchi depth by lake to be constant over time, as in the historical models. Third, because down-sampling and lambda regularization alter intercept terms, we performed future predictive models without down-sampling and lambda regularization. To visualize probabilities of best fit models over time, we performed thin plate spline regressions via the *fields* package (Nychka et al., 2017) and interpolated these data across the study region via the *raster* package (Hijmans, 2021). Additional details about data compilation, model selection, and statistical analyses are described in the Supplemental Materials.

Results and Discussion

Strong relationships exist between local air and water temperatures and the three most frequent drivers of mortality events across the study region: infectious disease (n = 281), summerkills (n = 103), and winterkills (n = 101; Fig. 1). Summerkills had the strongest, positive relationships with local temperatures and occurred when monthly mean air, surface water, and deep water temperature were ~15%, ~13%, and ~17% above median summertime temperatures, respectively (Fig. 2; *Dunnett test difference air* = 2.71, $p < 0.001$; *t-test*, $t = -8.08$, $df = 94.03$, $p < 0.001$; *Dunnett test difference surface water* = 2.47, $p < 0.001$; *t-test*, $t = -7.84$, $df = 94.04$, $p < 0.001$; *Dunnett test difference deep water* = 4.12, $p < 0.001$; *t-test*, $t = -5.79$, $df = 94.05$, $p < 0.001$). These air and surface water temperature patterns corroborate previous findings from geographically reduced datasets (Phelps et al., 2019; Till et al., 2019), while the previously

undocumented relationship with deep water temperature likely emerged due to the broadened spatial extent that incorporated numerous colder lakes (Notaro et al., 2013). Summerkills were also strongly affected by lake geomorphology and local environmental conditions (Fig. S1). In particular, small lakes are disproportionately susceptible to harmful algal blooms that can rapidly reduce dissolved oxygen concentration (Barica, 1975), and summerkills occurred in lakes with ~21% lower mean surface area (*t-test*, $t = 2.32$, $df = 95.44$, $p < 0.03$), yet ~31% higher annual mean Secchi depth (m), a common proxy for productivity (*Dunnett test difference* = -0.56, $p < 0.001$; *t-test*, $t = 27.38$, $df = 95.81$, $p < 0.001$).

Most summerkills affected warm-water fishes (Table S1), and there was a negative relationship between *CTmax* of fish families affected by summerkills and its difference with concurrent maximum surface water temperature (Fig. 3A; $r^2 = 0.40$, $F_{1,59} = 39.7$, $\beta = -0.41$, $SE = 0.07$, $t = -6.30$, $p < 0.001$). While cold-water fishes clearly experience high direct thermal stress from warming temperatures (Fig. 3A; Notaro et al., 2013), there was no statistically significant relationship between *CTmax* and the z-score of maximum surface water temperature (Fig. 3B; $r^2 = 0.03$, $F_{1,59} = 1.55$, $\beta = -0.64$, $SE = 0.52$, $t = -1.25$, $p = 0.22$). These findings imply similar deviations in surface water temperature have equally strong impacts on survival of both warm- and cold-water fishes; yet concerns about effects of climate change on freshwater fish have prioritized cold-water over warm-water fish (Myers et al., 2017), as well the effects of increased temperature over increased temperature variation on freshwater fish (Vasseur et al., 2014). Consequently, expectations for warm-water fish to increasingly contribute to global food supply (e.g., Ictaluridae; Dunham and Elaswad, 2017) and regional fisheries (e.g., Centrarchidae; Hansen et al., 2017) in light of continued overfishing of regional cold-water species (Embke et al., 2019) may be overly optimistic. On the other hand, temperate fish have high intraspecific

variation in thermal tolerance (Nati et al., 2021) and mechanisms underlying ecological shifts and thermal-related mortalities may differ, potentially providing opportunities for populations to evolve adaptations that enhance thermal tolerance (Chen et al., 2018)

Although summerkills were our main focus due their existing links with regional temperature increases (Phelps et al., 2019; Till et al., 2019), most mortality events were caused by infectious diseases (Fig. 1) – the dynamics, transmission, and virulence of which are often partially mediated by climate (Marcos-López et al., 2010). Importantly, mortality diagnoses were based on visual surveys, not pathological analyses, and speculations about temporal dynamics of infectious outbreaks in a warming climate are unwarranted with these data. Observationally, however, summertime infectious events occurred when monthly mean air and surface water temperature were ~7% and ~5% below median summertime temperatures (Fig. 2A), respectively (*Dunnett test difference air* = -0.88, $p < 0.001$; *t-test*, $t = 8.59$, $df = 234.78$, $p < 0.001$; *Dunnett test difference surface* = -1.14, $p < 0.001$; *t-test*, $t = 10.18$, $df = 234.7$, $p < 0.001$), and monthly mean deep water temperature was ~7% above median summertime deep water temperature (*Dunnett test difference* = 1.32, $p < 0.008$; *t-test*, $t = -3.85$, $df = 234.54$, $p < 0.001$). Additionally, there were no differences in temperature variation within lakes when summertime infectious events were and were not documented (Fig. 2B).

Most summertime infectious events were attributed to *Flavobacterium columnare* (81%, $n = 227$), an opportunistic pathogen that can cause increased mortality at higher temperature (Holt et al., 1975) but experiences trade-offs between increased thermal tolerance and lower virulence (Ashrafi et al., 2018). However, we cannot distinguish between infectious outbreaks due to natural community dynamics and temperature increases, and refrain from making broad inferences about how the frequency of infectious outbreaks may change over time. Better

understanding infectious disease dynamics in the wild is clearly an ongoing concern (Marcos-López et al., 2010), and broader considerations for other common infectious agents of regional fish, such as congener bacteria (*F. branchiophilum, F. psychropilum*) that cause gill and coldwater disease, respectively, and prefer slightly cooler temperatures (Starliper, 2011) are also warranted as seasonal temperature dynamics change across regional lakes (Woolway et al., 2020; Kraemer et al., 2021).

We anticipated winterkills to exhibit a negative relationship with temperature because sustained ice cover and weak thermal stratification can generate hypoxic conditions (Hurst, 2007). We found winterkills occurred when monthly mean surface water ($F_{1, 299907} = 3.95$ $p < 0.05$) and deep water temperatures ($F_{1, 299907} = 20.53$, $p < 0.001$) were ~32% and ~50% below median wintertime temperatures, respectively (Fig. 2C). Yet winterkills were negatively associated with ice duration (Fig. S2; $F_{1, 97799} = 24.58$, $p < 0.001$), but not snow accumulation ($F_{1, 272643} = 2.29$, $p < 0.13$), and occurred when mean air temperature was ~35% above median wintertime temperatures ($F_{1, 299907} = 9.74$, $p < 0.002$). While these results vaguely suggest low water temperatures (Greenbank, 1945; Hurst, 2007) or earlier thermal stratification (e.g., reduced ice duration and increased air temperature; Woolway et al., 2021) may have affected thermal-oxygen dynamics and led to hypoxic conditions, accurate dates of winterkills are difficult to obtain because of wintertime visibility constraints. Lastly, winterkills are strongly mediated by local processes of geomorphology, wind speed, and lake respiration (Greenbank, 1945), but are generally predicted to decrease in frequency across north temperate lakes because declines in snow and ice coverage are expected to increase wintertime dissolved oxygen concentrations (Woolway et al., 2020). While not explored here, due to paucities of future estimates of ice

duration and other key environmental variables, reductions in winterkills may partially offset mortality increases due to other causes.

Spatiotemporal trends of summerkill predictions

The best fit water and air temperature-based models for summerkills performed similarly well (Table S2) and included down-sampled ridge regressions with maximum, mean, and minimum air temperature and *z*-scores (Fig. S1; *logloss* = 2.44) and mean surface temperature and *z*-score (*logloss* = 2.48). Compared to the median of five documented summerkills per year across the historical time period and study region, both air and water temperature models generated slightly higher predictions of 8 summerkills per year (*n* = 19 years, *mean* = 9.36, *SE* = 1.90, *range* = 3-26; *n* = 19 years, *mean* = 9.36, *SE* = 1.38, *range* = 3-19), respectively (Fig. 4A, left). These models suggested air and water temperatures, as well as lake surface area, had similar positive effects (Fig. S1) and major environmental conditions including ice duration, lake size, and Secchi depth, had appreciable effects. In addition, there was a latitudinal effect that was evident in existing spatial variation of summerkills (Fig. 1) and contributed to significant spatial autocorrelation amongst summerkill probabilities from best fit air (*Moran I* > 0.23; $p < 0.001$) and water temperature-based models (*Moran I* > 0.06; $p < 0.001$; Table S4). Therefore, because recent regional air and water temperatures are more decoupled due to the proximity of the Laurentian Great Lakes (Notaro et al., 2013), recent air temperature estimates may be a reasonable predictor of fish mortality events for north temperature regions without depth-specific water temperature profiles, though not necessarily when predicting over future decades (Fig. 4C; Fig. S3).

During the mid-21st century, water and air temperature model predictions began to diverge and estimated 21 (*n* = 19 years, *mean* = 25.32, *SE* = 2.68, *range* = 14-63) and 41 summerkills per year (*n* = 19 years, *mean* = 72.25, *SE* = 14.87, *range* = 9-252), respectively (Fig. 4A, middle). Model predictions increasingly diverged over the late 21st century, with the water and air temperature model predicting 41 (*n* = 19 years, mean = 38.44, *SE* = 1.76, range = 25-56) and 182 summerkills per year (*n* = 19 years, *mean* = 223.03, *SE* = 27.23, range = 67-449), respectively by 2100 (Fig. 4A, right). These projections, based on the worst-case climate scenario, are ~6 to 34-fold increases compared to the median of historical summerkills frequencies across north temperate lakes. Importantly, though, these predictions do not consider the uncertainty in the underlying models that estimate future air or water temperatures.

Spatiotemporal differences between water and air model probabilities largely occurred across the mid- and late 21st century because 1) the water temperature-based model generated higher probabilities across lower latitudes, where most historical summerkills have been documented and few lakes occur, and 2) the air temperature-based model generated higher probabilities across eastern Wisconsin that borders the Laurentian Great Lakes, where fewer historical summerkills have been documented but many lakes occur (Fig. 4C). Spatial autocorrelation amongst summerkill predictions from the water temperature model, but not the air temperature model, deteriorated over the mid- and late-21st century, respectively (*Moran I* = 0.005, *p* = 0.16; *Moran I* = 0.003, *p* = 0.30; Table S3). This finding, in conjunction with divergent predicted future frequencies of summerkills, clearly demonstrates that the efficacy of our air temperature model depends upon the reliability of air temperature projections (Shen et al., 2018) and regional air-water temperature dynamics (Notaro et al., 2013; Winslow et al., 2017). While North American temperate lakes have recently undergone substantial water temperature

increases (Notaro et al., 2013; Woolway et al., 2020), the Great Laurentian Lakes generally mitigate increases in regional summertime air temperature and variation (Notaro et al., 2013), and lower rates of future water temperature increase are expected partially due to expectations for sustained declines in ice and snow coverage (Woolway et al., 2020).

Yet despite future predictions for buffered increases in water temperature, regional lakes are still expected to experience some of the largest air and surface water temperature increases across the United States under increased carbon dioxide concentrations (Fang and Stefan, 2009). In addition, warming temperatures have already decreased dissolved oxygen – the main underlying cause of documented summerkills (Thronson and Quigg, 2008; Fey et al., 2015) – across deep water habitats of north temperate lakes due to intensified thermal stratification and decreased water clarity (Jane et al., 2020). Moreover, regional eutrophication is expected to increase under a warming, more precipitous climate (Sinha et al., 2017), which will likely exacerbate increases in water temperature and decreases in dissolved oxygen concentrations (Williamson et al., 2016). Collectively, these circumstances suggest expanding approaches that use climate projections to predict frequencies of biological catastrophes in freshwater systems will largely depend upon better understanding multifaceted implications of global change on thermal-oxygen dynamics (Woolway et al., 2020; Kraemer et al., 2021).

The documented relationships between summerkills, winterkills, and infectious disease-induced mortality events suggest water temperature increases will alter the primary causes and frequencies of lentic fish mass mortality events. Indeed, similar approaches have been used to predict increases in extinction risk of lizard (Sinervo et al., 2010) and amphibian populations (Lowe, 2012). Because global temperatures will continue to increase over the coming century (Maurer et al., 2007), robust frameworks that provide baseline predictions regarding long-term

predictability of ecological catastrophes (Sinervo et al., 2010; Bailey and van del Pol, 2016), and highlight consequential uncertainties under future climate projections (Shen et al., 2018), are imperative for effective conservation management (McDowell et al., 2017; Soon and Ransangan, 2019). Development of future forecasting approaches should account for additional effects of warming temperatures such as declines in recruitment and production (Cohen et al., 2016; Hansen et al., 2017; Dahlke et al., 2020), as well as factors that could ameliorate the likelihood of future events such as adaptation and evolutionary rescue (Morgan et al., 2020) or management strategies for mitigating eutrophication (Williamson et al., 2016). Collectively, our results suggest sustained increases in local temperatures will greatly increase the likelihood of ecological catastrophes, especially as global efforts to mitigate climate warming remain nascent.

Acknowledgements

We thank three anonymous reviewers for helpful comments that improved the manuscript; all individuals that helped document mortality events; A Till for developing the original analytical framework; and E Edmonson, H Crisp, TJ Bartley, and U.S. Fish and Wildlife Service for contributing taxa silhouettes to PhyloPic. SPT was supported in part by the NSF (GRFP 1842401). AMS was supported by NSF DEB 1748945. ALR was supported by the Peter B. Moyle & California Trout Endowment for Coldwater Fish Conservation and by the California Agricultural Experimental Station of the University of California Davis, grant number CA-D-WFB-2467-H. SBF was supported by NSF DEB 1856415. NBDP was supported by the Minnesota Agricultural Experimental Station and the USDA-NIFA state project MIN-41-019.

Data and Code Availability

All data and code for analyses are available on a public GitHub repository at https://github.com/simontye/2020_MME_Temp.

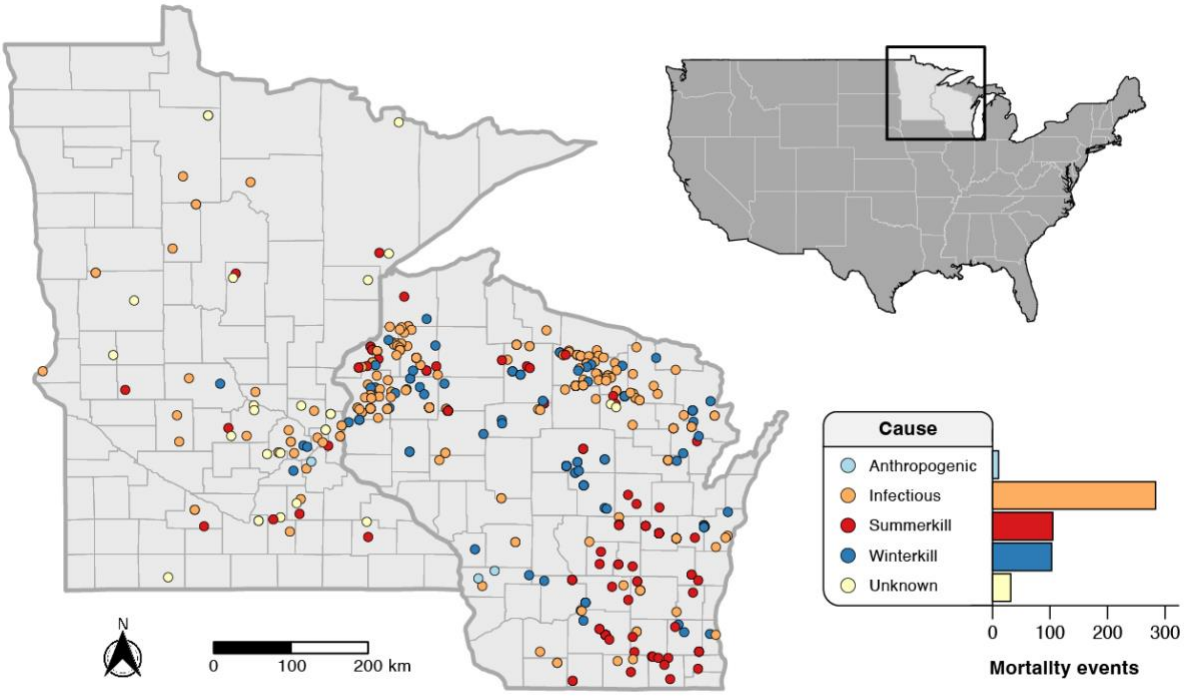

Figure 1. Locations and frequency of fish mortality events by cause across lakes of Minnesota and Wisconsin (*n* = 526; 2003-2013). Summerkills and winterkills describe elevated mortalities caused by seasonal, thermal-related environmental conditions, such as hypoxia and thermal stress. States and counties are separated by thick and thin dark gray lines, respectively.

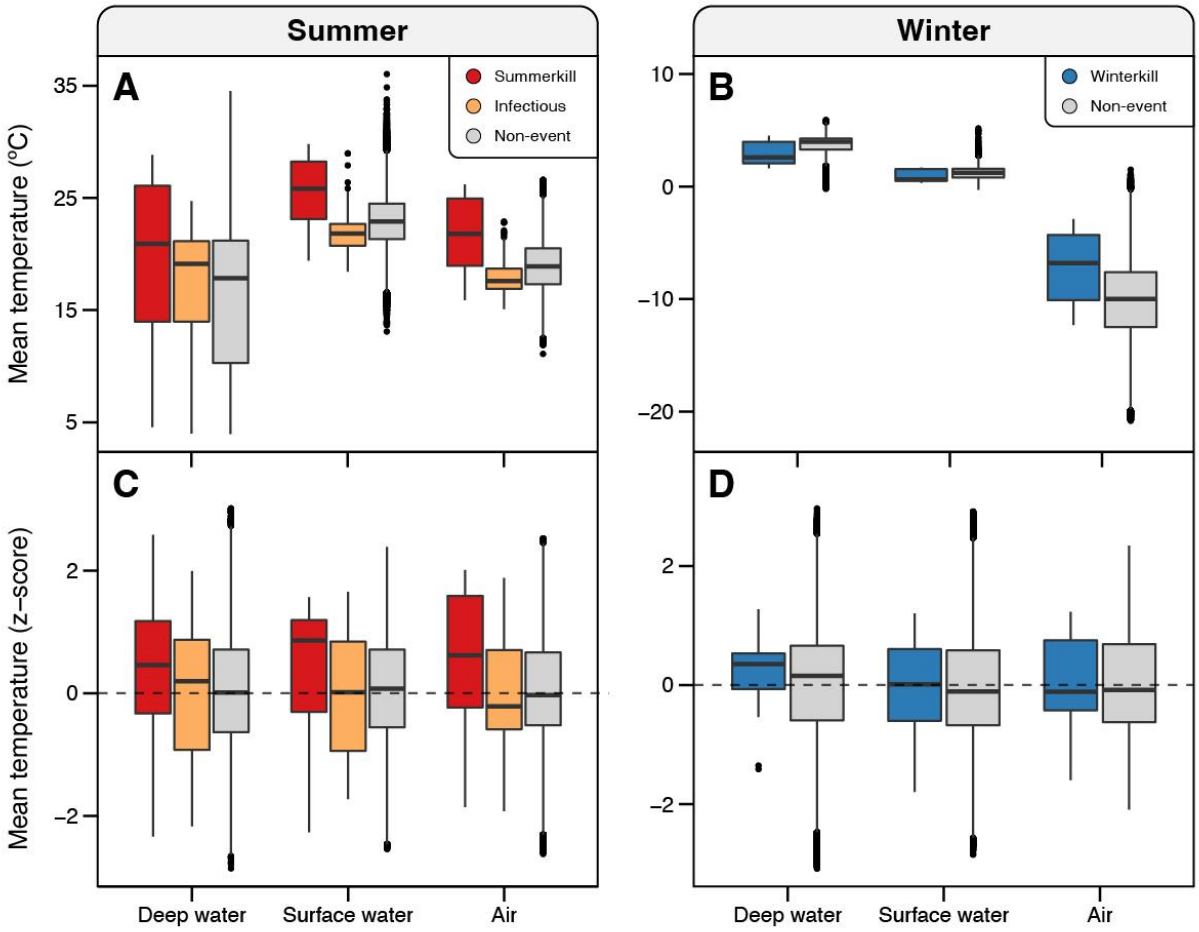

Figure 2. Monthly mean deep water, surface water, and air temperature estimates and *z*-scores when the most frequent causes of fish mortality events (infectious, summerkill, winterkill) were (colored boxes) and were not (gray boxes) documented across Wisconsin and Minnesota (2003-2013). Left column shows temperature estimates (A) and *z*-scores (B) when summerkills (red) and infectious events (orange) were documented compared to summer non-events (gray); right column shows temperature estimates (C) and *z*-scores (D) when winterkills (dark blue) were documented compared to winter non-events (gray). *Z*-scores represent standardized deviations from mean temperatures within lakes over the study period. Boxplots show medians (thick line) bounded by upper and lower quartiles (thin lines) with outliers (black circles).

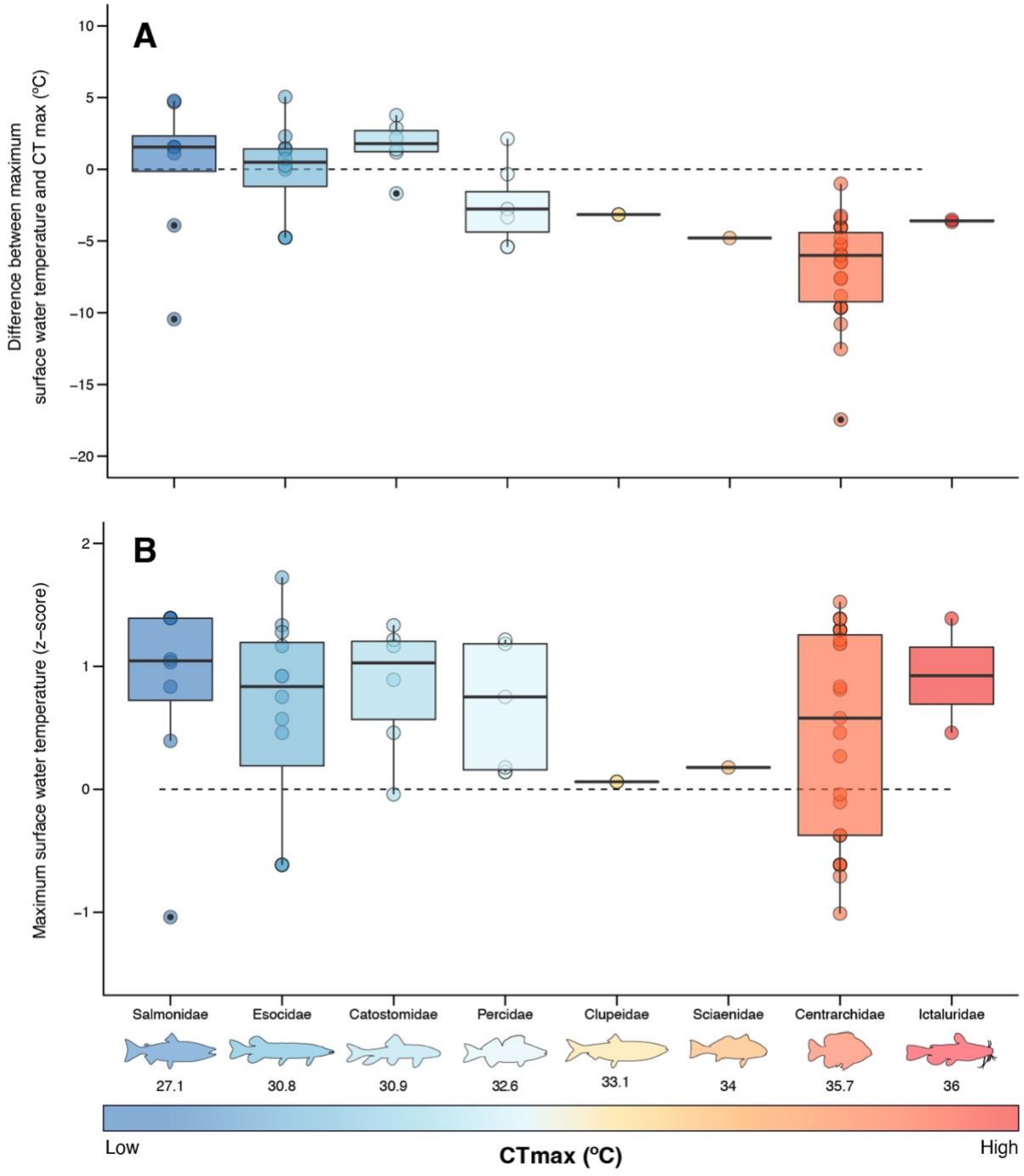

Figure 3. Critical thermal maximum (*CTmax*) of fish families (Table S2) that were affected by summerkills across Minnesota and Wisconsin (2003-2013) compared to concurrent raw (A) and *z*-scores of (B) monthly maximum surface water temperature estimates. *Z*-scores represent

deviations from standardized maximum surface water temperature within lakes over the study period. Colors represent relatively low (blue) and high (red) *CTmax* of each affected family. Black circles indicate outliers and dashed lines indicate whether temperatures were above or below *CTmax* (A) and standardized maximum surface water temperature (B), respectively.

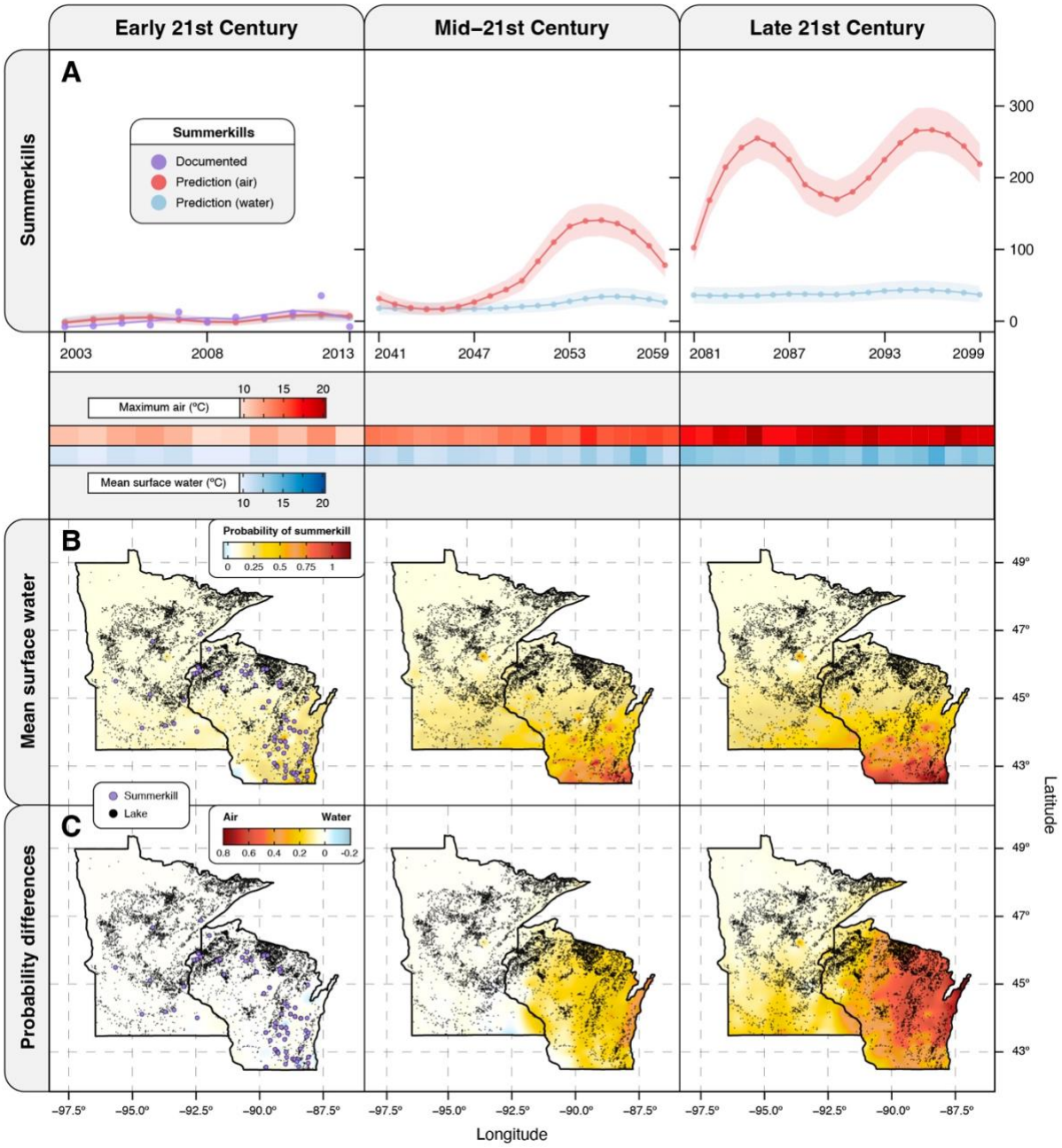

Figure 4. Documented and estimated future frequencies of summerkills over time (A), probabilities of summerkills based on the water temperature model (B), and differences between probabilities of summerkills from air and water temperature models (C). For (A), documented (purple circles) and predicted annual frequencies of summerkills based on maximum air or water temperature models (red or blue circles, respectively) with 95% confidence intervals (shaded

areas) across each time period; the temperature panel (bottom) shows annual mean air and surface water temperature across the study region. For (B & C), locations of documented summerkills (early 21st century) and regional lakes are shown via purple and black circles, respectively.

References

Anderson, S. C., T. A. Branch, A. B. Cooper, and N. K. Dulvy. 2017. Black-swan evens in animal populations. *Proceedings of the National Academy of Sciences*, **144**:3252-3257.

Ashrafi, R., M. Bruneaux, L. R. Sundberg, K. Pulkkinen, J. Valkonen, and T. Ketola. 2018. Broad thermal tolerance is negatively correlated with virulence in an opportunistic bacterial pathogen. *Evolutionary Applications*, **11**(9):1700-1714.

Bailey, L. D., and M. van de Pol. 2016. Tackling extremes: challenges for ecological and evolutionary research on extreme climatic events. *Journal of Animal Ecology*, **85**:85-96.

Barica, J. 1975. Summerkill risk in prairie ponds and the possibilities of its prediction. *Journal of the Fisheries Board of Canada*, **32**:1283-1288.

Chen, Z., A. P. Farrell, A. Matala, and S. R. Narum. 2018. Mechanisms of thermal adaptation and evolutionary potential of conspecific populations to changing environments. *Molecular Ecology*, **27**:659-674.

Cohen, A. S., E. L. Gergurich, B. M. Kraemer, M. M. McGlue, P. B. McIntyre, J. M. Russell, J. D. Simmons, and P. W. Swarzenski. 2016. Climate warming reduces fish production and benthic habitat in Lake Tanganyika, one of the most biodiverse freshwater ecosystems. *Proceedings of the National Academy of Sciences*, **34**:9563-9568.

Dahlke, F. T., S. Wohlrab, M. Butzin, and H. O. Pörtner. 2020. Thermal bottlenecks in the life cycle define climate vulnerability of fish. *Science*, **369**:65-70.

Denny, M. W., L. H. H. Hunt, L. P. Miller, and C. D. G. Harley. 2009. On the prediction of extreme ecological events. *Ecological Monographs*, **79**:397-421.

Dunham, R. A., and A. Elaswad. 2017. Catfish biology and farming. *Annual Review of Biosciences*, **6**:305-325.

Embke, H. S., A. L. Rypel, S. R. Carpenter, G. G. Sass, D. Ogle, T. Cichosz, J. Hennessy, T. E. Essington, and M. J. Vander Zanden. 2019. Production dynamics reveal hidden overharvest of inland recreational fishes. *Proceedings of the National Academy of Sciences*, **116**:24676-24681.

Fang, X, and H. G. Stefan. 2009. Simulations of climate effects on water temperature, dissolved oxygen, and ice and show covers in lakes of the contiguous United States under past and future climate scenarios. *Limnology and Oceanography*, **54**(6):2359-2370.

Fey, S. B., A. M. Siepielski, S. Nusslé, K. Cervantes-Yoshida, J. L. Hwan, E. R. Huber, M. J. Fey, A. Catenazzi, and S. M. Carlson. 2015. Recent shifts in the occurrence, cause, and magnitude of animal mass mortality events. *Proceedings of the National Academy of Sciences*, **112**(4):1083-1088.

Fey, S. B., J. P. Gibert, and A. M. Siepielski. 2019. The consequences of mass mortality events for the structure and dynamics of biological communities. *Oikos*, **128**(12):1679-1690.

Garrabou, J., D. Gómez-Gras, J. B. Ledoux, C. Linares, N. Bensoussan, P. López-Sendino, H. Bazairi F. Epinosa, M. Ramdani, S. Grimes, M. Benabdi, et al. 2019. Collaborative database to track mass mortality events in the Mediterranean Sea. *Frontiers in Marine Science*, **6**:707.

Greenbank, J. 1945. Limnological conditions in ice-covered lakes, especially as related to winter-kill of fish. *Ecological Monographs*, **15**:343-392.

Gröger, M., C. Dieterich, and H. E. M. Meier. 2021. Is interactive air sea coupling relevant for simulating the future climate of Europe? *Climate Dynamics*, **56**:419-514.

Hansen, G. J. A., J. S. Read, J. F. Hansen, and L. A. Winslow. 2017. Projected shifts in species dominance in Wisconsin lakes under climate change. *Global Change Biology*, **23**:1463-1476.

He, F., C. Zarfl, V. Bremerich, J. N. W. David, Z. Hogan, G. Kalinkat, K. Tockner, and S. C. Jähnig. 2010. The global decline of freshwater megafauna. *Global Change Biology*, **25**:3883-3892.

Hijmans, R. J. 2021. raster: geographic data analysis and modeling. R package version 3.4-1. https://CRAN.R-project.org/package=raster

Holt, R. A., J. E. Sanders, J. L. Zinn, J. L. Fryer, and K. S. Pilcher. 1975. Relation of water temperature to *Flexibacter columnaris* infection in steelhead trout (*Salmo gairdneri*), coho (*Oncorhynchus kisutch*) and chinook (*O. tshawyscha*) salmon. *Journal of the Fisheries Research Board of Canada*, **32**:1553-1559.

Hurst, T. P. 2007. Causes and consequences of winter mortality in fishes. *Journal of Fish Biology*, **71**(2):315-345.

Jane, S. F., G. J. A. Hansen, B. M. Kraemer, P. R. Leavitt, J. L. Mincer, R. L. North, R. M. Pilia, J. T. Stetler, C. E. Williamson, R. I. Woolway, et al., 2021. Widespread deoxygenation of temperate lakes. *Nature*, **594**:66-70.

Kraemer, B. M., O. Anneville, S. Chandra, M. Dix, E. Kuusisto, D. M. Livingstone, A. Rimmer, S. G. Schladow, E. Silow, L. M. Sitoka, et al. 2015. Morphometry and average temperate affect lake stratification responses to climate change. *Geophysical Research Letters*, **42**(12):4981-4988.

Kraemer, B. M., R. M. Pilla, R. I. Woolway, O. Anneville, S. Ban, W. Colom-Montero, S. P. Delvin, M. T. Dokulil, E. E. Gaiser, K. D. Hambright, et al., 2021. Climate change drives widespread shifts in lake thermal habitat. *Nature Climate Change*, 11**:**521-529.

Lowe, W. H. 2012. Climate change is linked to long-term decline in a stream salamander. *Biological Conservation*, **145**:48-53.

Lyons, J., T. Zorn, J. Stewart, P. Seelbach, K. Wehrly, and L. Wang. 2009. Defining and characterizing coolwater streams and their fish assemblages in Michigan and Wisconsin, USA. *North American Journal of Fisheries Management*, **29**:1130-1151.

Mangel, M., and C. Tier. 1994. Four facts every conservation biologist should know about persistence. *Ecology*, **75**(3):607-614.

Marcos-López, M., P. Gale, B. C. Oidtmann, and E. J. Peeler. 2010. Assessing the impact of climate change on disease emergence in freshwater fish in the United Kingdom. *Transboundary and Emerging Diseases*, **57**:293-304.

Maurer, E. P., L. Brekke, T. Pruitt, and P. B. Duffy. 2007. Fine-resolution climate projections enhance regional climate change impact studies. *Eos, Transactions, American Geophysical Union*, **88**:504.

McDowell, W. G., W. H. McDowell, and J. E. Byers. 2017. Mass mortality of a dominant invasive species in response to an extreme climatic event: implications for ecosystem function. *Limnology and Oceanography*, **62**:177-188.

Morgan, R., M. H. Finnøen, H. Jensen, C. Pélabon, and F. Jutflet. 2020. Low potential for evolutionary rescue from climate change in a tropical fish. *Proceedings of the National Academy of Sciences*, **117**(52):33365-33372.

Myers, B. J., A. J. Lynch, D. B. Bunnell, C. Chu, J. A. Falke, R. P. Kovach, T. J. Krabbenhoft, T. J. Kwak, and C. P. Paukert. 2017. Global synthesis of the documented and projected effects of climate change on inland fishes. *Reviews in Fish Biology and Fisheries*, **27**:339-361.

Nati, J. J. H., M. B. S. Svendsen, S. Marras, S. S. Killen, J. F. Steffensen, D. J. McKenzie, and P. Domenici. 2021. Intraspecific variation in thermal tolerance differs tropical and temperate fishes. *Scientific Reports*, **11**:21272.

Notaro, M., K. Holman, A. Zarrin, E. Fluck, S. Vavrus, and V. Bennington. 2013. Influence of the Laurentian Great Lakes on regional climate. *Journal of Climate*, **26**:789-804.

Nychka, D., R. Furrer, J. Paige, and S. Sain. 2017. fields: tools for spatial data. doi: 10.5065/D6W957CT, R package version 12.5, https://github.com/NCAR/Fields

O'Reilly, C. M., S. Sharma, D. K. Gray, S. E. Hampton, J. S. Read, R. J. Rowley, P. Schneider, J. D. Lenters, P. B. McIntyre, B. M. Kraemer, et al. 2015. Rapid and highly variable warming of lake surface waters around the globe. *Geophysical Research Letters*, **42**(24):10773-10781.

Phelps, N. D. B., I. Bueno, D. A. Poo-Muñoz, S. J. Knowles, S. Massarani, R. Rettkowski, L. Shen, H. Ranatala, P. L. F. Phelps, and L. E. Escobar. 2019. Retrospective and predictive investigation of fish kill events. *Journal of Aquatic Animal Health*, **31**(1):61-70.

PRISM Climate Group, Oregon State University, https://prism.oregonstate.edu, data created 4 Feb 2014, data accessed 6 Nov 2020.

Shen, M., J. Chen, M. Zhuan, H. Chen, C. Y. Xu, and L. Ziong. 2018. Estimating uncertainty and its temporal variation related to global climate models in quantifying climate change impacts on hydrology. *Journal of Hydrology*, **556**:10-24.

Sinervo, B., F. Méndez de la Cruz, D. B. Miles, B. Heulin, E. Bastiaans, M. Villagrán-Santa Cruz, R. Lara-Resendiz, B. Martínez-Méndez, M. Lucía Calderón-Espinosa, R. Nelsi Meza-Lázaro, et al., 2010. Erosion of lizard diversity by climate change and altered thermal niches. *Science*, **328**(5980):894-899.

Sinha, E., A. M. Michalak, and V. Balaji. 2017. Eutrophication will increase during the 21st century as a result of precipitation changes. *Science*, **357**(6349):405-408.

Soon, T. K., and J. Ransangan. 2019. Extrinsic factors and marine bivalve mass mortalities: an overview. *Journal of Shellfish Research*, **38**(2):223-232.

Starliper, C. E. 2011. Bacterial coldwater disease of fishes caused by *Flavobacterium psychrophilum*. *Journal of Advanced Research*, **2**:97-108.

Thronson, A., and A. Quigg. 2008. Fifty-five years of fish kills in coastal Texas. *Estuaries and Coasts*, **31**:802-813.

Till, A., A. L. Rypel, A. Bray, and S. B. Fey. 2019. Fish die-offs are concurrent with thermal extremes in north temperature lakes. *Nature Climate Change*, **9**:637-641.

Vasseur, D. A., J. P. DeLong, B. Gilbert, H. S. Greig, C. D. G. Harley, K. S. McCann, V. Savage, T. D. Tunney, and M. I. O'Connor. 2014. Increased temperature variation poses a greater risk to species than climate warming. *Proceedings of the Royal Society B*, **281**:20132612.

Verpoorter, C., T. Kutser, A. Seekell, and L. J. Tranvik. 2014. A global inventory of lakes based on high-resolution satellite imagery. *Geophysical Research Letters*, **41**(18):6396-6402.

Williamson, C. E., E. P. Overholt, R. M. Pilla, T. H. Leach, J. A. Brentrup, L. B. Knoll, E. M. Mette, and R. E. Moeller. 2016. Ecological consequences of long-term browning in lakes. *Scientific Reports*, **5**:18666.

Winslow, L. A., G. J. A. Hansen, J. S. Read, and M. Notaro. 2017. Large-scale modeled contemporary and future water temperature estimates for 107444 midwestern US lakes. *Scientific Data*, **4**:170053.

Woolway, R. I., B. M. Kraemer, J. D. Lenters, C. J. Merchant, C. M. O'Reilly, and S. Sharma. 2020. Global lake responses to climate change. *Nature Reviews Earth and Environment*, **1**:388-403.

Woolway, R. I., S. Sharma, G. A. Weyhenmeyer, A. Debolskiy, M. Golub, D. Mercado-Bettin, M. Perroud, V. Stepanenko, Z. Tan, L. Grant, et al. 2021. Phenological shifts in lake stratification under climate change. *Nature Communications*, 12**:**2318.

Young, H. S., D. J. McCauley, M. Galetti, and R. Dirzo. 2016. Patterns, causes, and consequences of Anthropocene defaunation. *Annual Review of Ecology, Evolution, and Systematics*, **47**:333-358**.**

Supplemental Materials

Fish mortality events

Fish mortality events accrue deaths over time (Mhlanga et al., 2006) and when entire lentic fish communities are experimentally culled, most fish carcasses are not recovered or observed (Schneider, 1998). This broad criterion aimed to address the cause and frequency, but not magnitude, of events because accurate temporal comparisons of magnitudes (i.e., number of mortalities) is improbable given logistical limitations of monitoring agencies, as well as the likelihood of not observing fish carcasses after known fish mortalities (Schneider, 1998). Therefore, rather than use an established threshold for minimum number of fish mortalities to constitute a mortality event (La and Cooke, 2011), which are often referred to as "fish kills", we included all mortality observations in our analyses. To account for multiple observations of the same mortality event and match the temporal resolution of modeled thermal data, we consolidated observations that occurred in the same waterbody and month into single events. For events with consolidated observations, we used the most frequent cause type across observations, and all deceased fish taxa were considered to be affected by the single event. We then used conversion tables provided by Minnesota IT Services and Wisconsin Department of Natural Resources (WDIR) to translate state-specific waterbody identifiers into unique waterbody identifiers from the National Hydrological Database.

Based on these criteria, we compiled 526 fish mortality events across Minnesota and Wisconsin lakes from 2003 to 2013 (Fig. 1), a timespan when local air (PRISM Climate Group, Oregon State University) and waterbody-specific water temperature estimates (Winslow et al., 2017) and mortality data were available. Records of fish mortality events from Minnesota were originally obtained from the Minnesota Department of Natural Resources (MNDNR) Pathology

Laboratory and staff reports (see Phelps et al., 2019), and records of mortality events from Wisconsin were obtained from WDNR (see Till et al., 2019). Some documented winterkills in Minnesota were stored by separate agencies and were not available for analysis. We excluded all observations that were described as occurring in rivers and creeks, then used conversion tables provided by Minnesota IT Services and Wisconsin Department of Natural Resources (DNR) to translate state-specific waterbody identifiers into unique waterbody identifiers from the National Hydrological Database. Waterbodies represented by multiple sets of coordinates were described by the mean coordinates.

We used descriptions and diagnoses of observations to assign maximally general cause categories to each observation: anthropogenic, infectious disease, summerkill, winterkill, or unknown (Fig. 1). Summerkills and winterkills refer to mortalities caused by seasonal environmental conditions associated with extreme temperatures such as low dissolved oxygen concentrations, direct thermal stress, and/or rapid temperature changes (Greenbank, 1945; Barica, 1975) and, therefore, were differentiated by meteorological season. No summerkills or winterkills were documented in May and October; therefore, summerkills were restricted to between June and September, and winterkills to between November and April.

To understand whether temperatures during documented summerkills were related to the thermal categories (cool-, cold-, warm-water) and tolerances of affected fish families (Lyons et al., 2009), we classified fish taxa by taxonomic family, when possible, and associated each family with the most frequent thermal category based on a regional assessment of freshwater fish thermal preferences (Lyons et al., 2009). In addition, because critical thermal maximum (*CTmax*) across fishes has a strong phylogenetic signal (Comte and Olden, 2017), we calculated a mean

CTmax of each affected family using the mean, or lower bound if a range was given, *CTmax* of regional freshwater fish species (Lyons et al., 2009).

Historical fish mortality events and extreme temperatures (2003-2013)

To examine relationships between different causes of mortality events and concurrent temperatures, we assembled waterbody-specific water temperature variables from an extensive assessment of thermal dynamics across north temperate waterbodies of North America (Winslow et al., 2017) with local air temperature estimates (monthly minimum, mean, and maximum; PRISM Climate Group, Oregon State University, https://prism.oregonstate.edu, data created 4 Feb 2014, data accessed 6 Nov 2020). Deep water temperature estimates were based on the deepest simulated lake layer (Winslow et al., 2017). We then used the *rgeos* package (Bivand and Rundell, 2020) to associate each lake with the nearest air temperature estimates (1/8-degree resolution). To compare standardized thermal conditions within lakes, we calculated *z*-scores by comparing air (monthly minimum, mean, and maximum), surface water (monthly mean and maximum), and deep-water temperatures (monthly mean and maximum) when mortality causes were and were not observed in summer (i.e., summer non-event) or winter (i.e., winter non-event).

To help account for a potential effect of more observations of mortality events in regions with high human population abundances, we obtained 2010 US census block data (U.S. Census Bureau, https://www.census.gov/geographies/reference-maps/2010/geo/2010-census-block-maps.html), rounded the coordinates of each waterbody centroid to the nearest 0.1º, and associated waterbody coordinates with the nearest census estimates. Lastly, because lake geomorphology and productivity can strongly affect temperature-oxygen dynamics (Barcia,

1975), we acquired lake surface area (km^2) and satellite-derived Secchi depth for regional lakes (m; Olmanson et al., 2008; Rypel et al., 2019) for regional lakes. Because future projections of Secchi depth are unavailable and to obtain a static, waterbody-specific proxy for productivity, we calculated annual mean Secchi depth (m) for each lake from estimates obtained available over the historical study period (2003-2013; Olmanson et al., 2008; Rypel et al., 2019), then associated lake surface area and annual mean Secchi depth with waterbodies via unique waterbody identifiers.

Because preceding work suggested strong relationships between fish mortality events and air (Phelps et al., 2019) or surface water temperature (Till et al., 2019), we created two sets of models based on either air or water temperature to predict frequencies of summerkills. We created four different models that included major geographic and environmental variables (latitude, longitude, season, precipitation, ice duration, lake surface area, Secchi depth, 2010 census block estimates) as well as different subsets of thermal-related variables that included either 1) maximum air temperature and *z*-score or mean surface water temperature and *z*-score, or 2) all available air or water temperature variables that were not strongly correlated ($r < 0.7$; Table S2:S3).

We partitioned data into training (75%) and testing sets (25%), then conducted both penalized and non-penalized logistic regressions (lasso and ridge) of each model. For non-penalized regressions, we used stepwise procedures to reduce model complexity. For penalized regressions, we performed 5-fold cross-validations to determine the appropriate lambda values via the *caret* package (Kuhn, 2021). To account for rarity of events, and abundance of regional lakes, we conducted down-sampled and non-down-sampled penalized regressions via the *glmnet* package (Friedman et al., 2010). We used logloss to compare all model fits ($n = 24$; Fig. S1;

Table S2) and consider the potential effect of each variable without overfitting models, removing variables with appreciable effects, or including variables with negligible effects.

Statistical analyses

We first examined homogeneity of variance for air, surface water, and deep water temperature (minimum, mean, and maximum with respective z-scores) when mortality causes were and were not documented during summer or winter (i.e., summer or winter non-events). If variance was heterogenous, we used Welch's t-test and Dunnett's test, and, if variance was homogenous, we used ANOVA and Tukey HSD. To examine relationships between winterkills and ice duration (days) or snow accumulation (cm), we performed ANOVA and Tukey HSD. For analyses of possible relationships between local temperature and documented fish mortality events, we consider *p*-values as being useful in drawing loose inferences about the parameters of a population of lake-months that is broader than our sample both geographically and temporally. The physiological mechanisms underlying these events likely hold for a broader set of north temperate freshwater lakes and for time periods both preceding and following our study period.

To examine whether fish families with relatively low and high thermal tolerances may have been affected by direct or indirect effects of warm temperatures, respectively, we used linear regression with *CTmax* (Lyons et al., 2009) and differences with estimated monthly maximum surface water temperature when documented summerkills occurred (Winslow et al., 2017). To evaluate spatial autocorrelation of historical and future summerkill probabilities, we performed Moran's tests (Table S4). Data visualizations were created via the *ggplot2* (Wickham, 2016) and *maddog* (Tye, 2021) packages. All analyses were performed in R (version 4.0, R

Development Core Team) and considered an alpha value of 0.05 to be significant unless Bonferroni corrections were implemented.

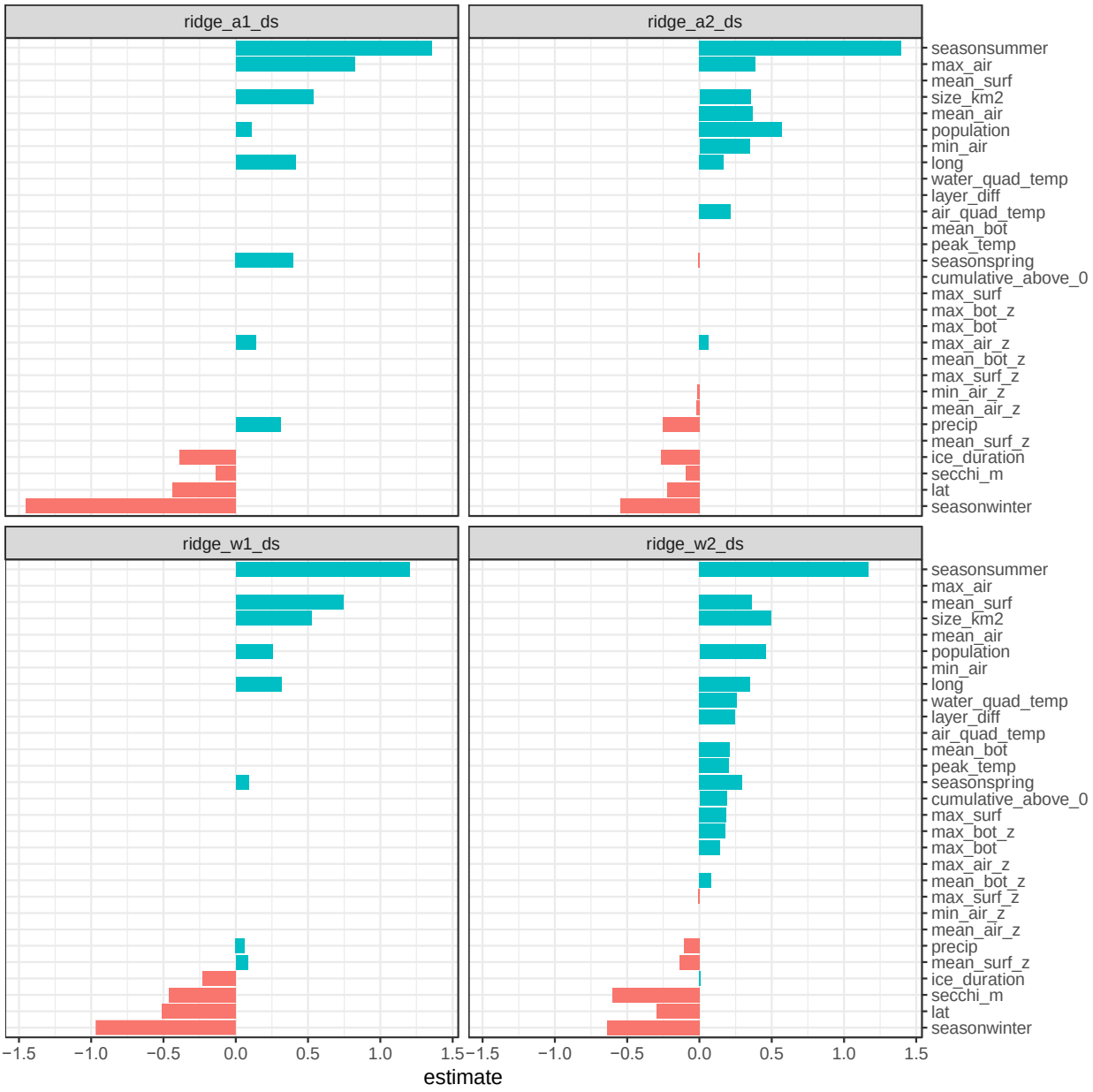

Figure S1. Coefficient estimates of best fit models (downsampled, ridge regressions) based on all available air temperature estimates (top right; ridge_a2_ds; logloss = 2.44) or mean surface water temperature (bottom left; logloss = 2.48). These models slightly outperformed models with fewer air variables (top left; ridge_13_ds; logloss = 2.64) and additional water (bottom right; ridge_w2_ds; logloss = 2.74), respectively. Positive (blue) and negative (red) coefficient estimates of each model are primarily in descending order. Variables for the best fit air (ridge_a1_ds) and water (ridge_w1_ds) models included season (e.g., seasonsummer = summer,

seasonspring = spring, seasonwinter = winter), latitude (lat), longitude (long), ice duration (ice_duration; days), precipitation (precip; cm), population, Secchi depth (m) and lake surface area (km2; lake_size) and either the raw and z-score of maximum, mean, and minimum air temperature (max_air, max_air_z, mean_air, mean_air_z, min_air, min_air_z) or the raw and z-score of mean surface water temperature (mean_surf_z, mean_surf), respectively. The only temperature variables for the second-best fit air temperature model (ridge_a1_ds) included raw and z-scores of maximum air (max_air_z, max_air) temperature, and the second-best fit water temperature model (ridge_w2_ds) included all available water temperature variables that were not strongly correlated (*rho* < 0.7). All model logloss values and variables are listed in Tables S2 and S3, respectively.

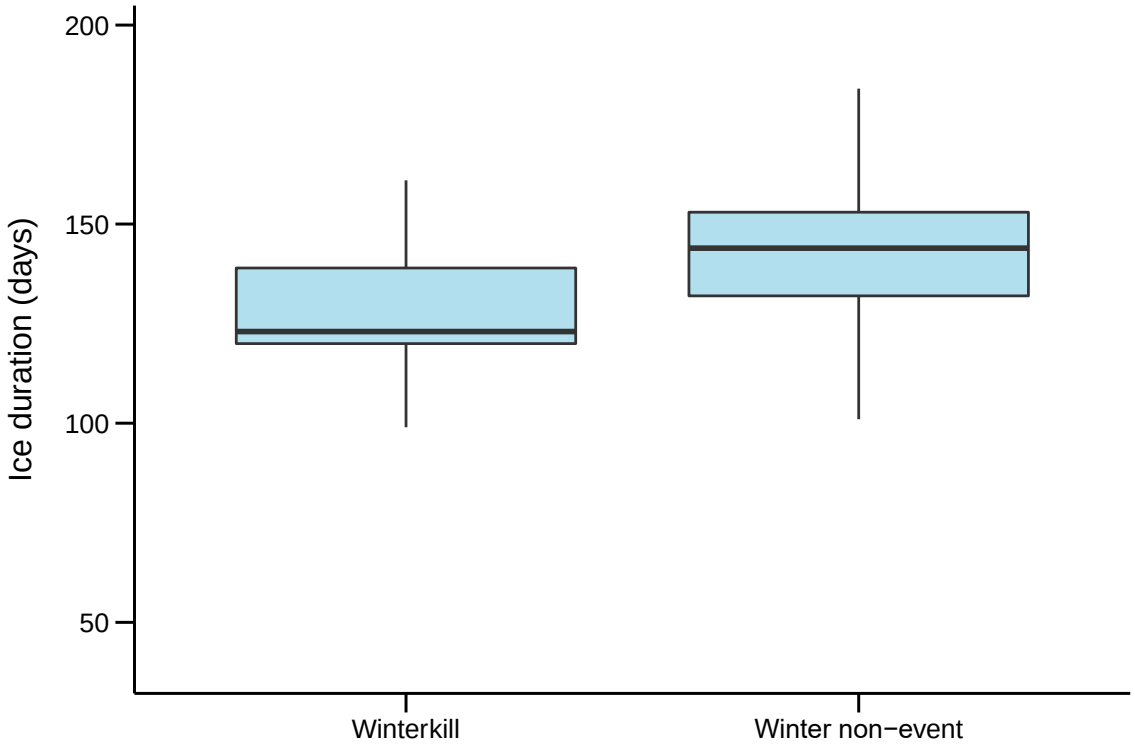

Figure S2. Ice duration for Minnesota and Wisconsin lakes with (winterkill) and without (winter non-event) documented, thermal-related, wintertime fish mortalities (i.e., winterkill) from 2003-2013.

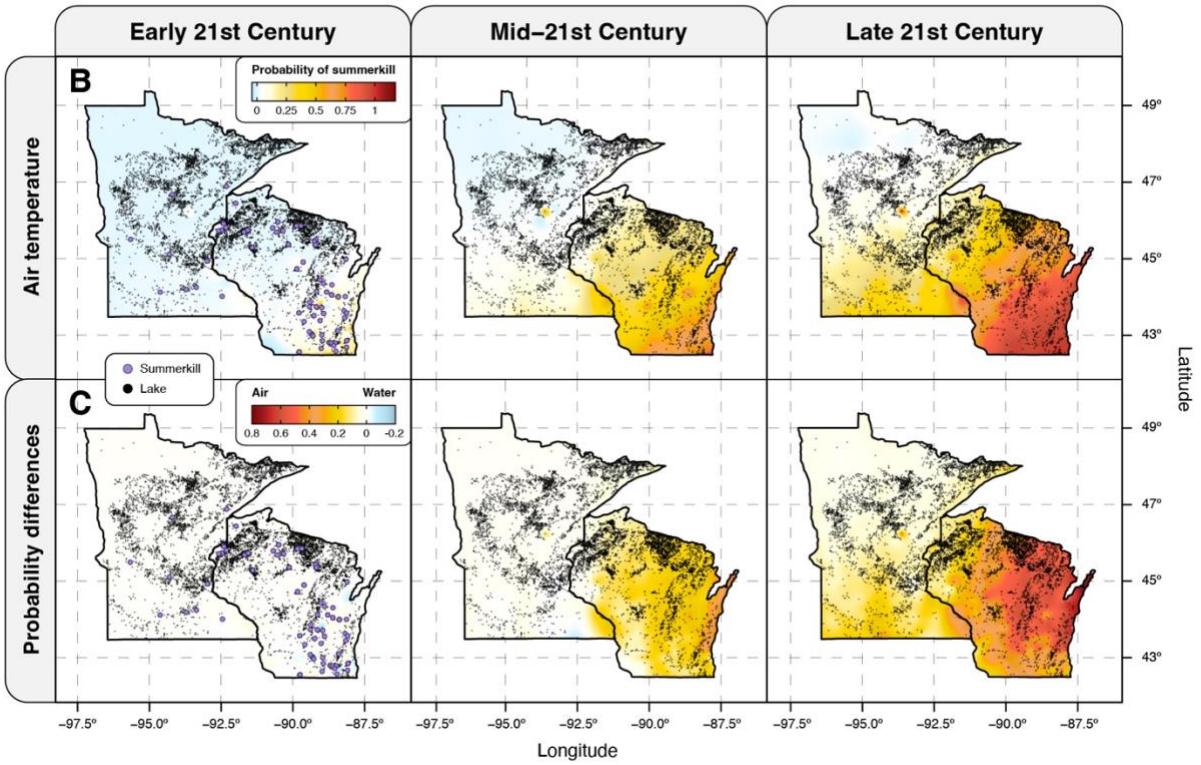

Figure S3. Probabilities of summerkills based on the air temperature model (A), and differences between probabilities of summerkills from air and water temperature models (B) as shown in Figure 4 of the main text. For A and B, locations of documented summerkills (early 21st century) and regional lakes are shown via purple and black circles, respectively.

Table S1. Mortality events of freshwater fish families across lakes of Minnesota and Wisconsin from 2003 to 2013. Major causes of events were classified as anthropogenic (A), infectious (I), summerkill (S), winterkill (W), and unknown (U). Thermal categories were assigned to fish families based on the most frequent thermal category for each family in an extensive review of thermal dynamics of regional freshwater fish (Lyons et al., 2009). Mean critical thermal maximum (*CTmax*, ºC) of each family was calculated via means and lower bounds of *CTmax* of regional family members (Lyons et al., 2009). Number of mortality events and total number of events with designated cause types vary due to missing information for some events.

Family	**Mortality events**	**Major cause(s)**	**Proportion of summerkills**	**Thermal category**	**CTmax (ºC)**
Centrarchidae	222	I	23/222	Warm	35.7
Ictaluridae	44	I	2/44	Warm	36
Percidae	32	I	7/32	Warm	32.6
Esocidae	37	S	12/23	Warm	30.8
Cyprinidae	23	S	11/23	Warm	NA
Salmonidae	11	S	8/11	Cold	27.1
Catostomidae	10	S	6/10	Warm	30.9
Clupeidae	10	W	2/10	Cool	33.1
Acipenseridae	6	A, S	3/6	Unknown	NA
Sciaenidae	3	NA	1/3	Warm	34
Osmeridae	1	NA	0/1	NA	NA

Table S2. Logloss values for air or water temperature-based logistic models for summerkills across lakes of Minnesota and Wisconsin (2003-2013; Phelps et al., 2019; Till et al., 2019). Models included non-penalized, with or without stepwise reduction, and penalized logistic regressions: both lasso and ridge regressions with or without downsampling. All models included major geographic and anthropogenic variables [latitude, longitude, season, population (2010 census block estimates), Secchi depth (m), lake surface area (km^2), precipitation (cm), ice duration (days)]. In addition to these variables, the first group of models (e.g., Air_1, Water_1) included either maximum air temperature and z-score or maximum surface water temperature and z-score, while the second group of models (e.g., Air_2, Water_2) included all air or water temperature variables that were not strongly correlated (*rho* < 0.7; Table S4).

Variables	Model	Stepwise	Downsampled	Logloss
Air_1	Logistic	N	N	15.9
Air_2	Logistic	N	N	14.8
Water_1	Logistic	N	N	15.3
Water_2	Logistic	N	N	15.7
Air_1	Logistic	Y	N	13.8
Air_2	Logistic	Y	N	11.9
Water_1	Logistic	Y	N	12.5
Water_2	Logistic	Y	N	15.6
Air_1	Lasso	N	N	12.6
Air_2	Lasso	N	N	11.4
Water_1	Lasso	N	N	11.9
Water_2	Lasso	N	N	11.5
Air_1	Lasso	N	Y	3.70
Air_2	Lasso	N	Y	8.10
Water_1	Lasso	N	Y	3.80
Water_2	Lasso	N	Y	6.30
Air_1	Ridge	N	N	11.5
Air_2	Ridge	N	N	11.6
Water_1	Ridge	N	N	11.4
Water_2	Ridge	N	N	11.5
Air_1	Ridge	N	Y	2.64

Table 3-S2 (Cont.)

Variables	Model	Stepwise	Downsampled	Logloss
Air_2	Ridge	N	Y	2.44
Water_1	Ridge	N	Y	2.48
Water_2	Ridge	N	Y	2.74

Table S3. Variables used in air and water temperature-based models for summerkills (Table S2).

Variable	**Unit**	**Source**
Max. air temperature	ºC	PRISM, Oregon State University
Mean air temperature	ºC	PRISM, Oregon State University
Min. air temperature	ºC	PRISM, Oregon State University
Max. surface water temperature	ºC	Winslow et al., 2017
Max. deep water temperature	ºC	Winslow et al., 2017
Mean surface water temperature	ºC	Winslow et al., 2017
Mean deep water temperature	ºC	Winslow et al., 2017
Peak temperature (water)	ºC	Winslow et al., 2017
Layer difference (water)	ºC	Winslow et al., 2017
Quadratic temperature (water)	ºC	Winslow et al., 2017
Ice duration	Days	Winslow et al., 2017
Cumulative above 0ºC	Days	Winslow et al., 2017
Max. air temperature (*z*-score)	NA	See Materials and Methods
Mean air temperature (*z*-score)	NA	See Materials and Methods
Min. air temperature (*z*-score)	NA	See Materials and Methods
Max. surface water temperature (*z*-score)	NA	See Materials and Methods
Max deep water temperature (*z*-score)	NA	See Materials and Methods
Mean surface water temperature (*z*-score)	NA	See Materials and Methods
Mean deep water temperature (*z*-score)	NA	See Materials and Methods
Latitude	Degrees	Phelps et al., 2019; Till et al., 2019
Longitude	Degrees	Phelps et al., 2019; Till et al., 2019
Season	NA	Phelps et al., 2019; Till et al., 2019
Precipitation	cm	PRISM, Oregon State University
Human population	individuals	U.S. Census Bureau, 2010
Secchi depth	m	Olmanson et al., 2008; Rypel et al., 2019
Lake surface area	km^2	Olmanson et al., 2008; Rypel et al., 2019

Table S4. Moran I statistics for spatial autocorrelation of summerkill probabilities, based on air or water temperature-based models, over the early (2003-2013), mid- (2041-2059), and late 21st century (2081-2099) under Representative Concentration Pathway 8.5.

Model	Time	I	p	k	Expectation
Air	2003-2013	0.2339	< 0.0001	2	-0.0001
Air	2041-2059	0.1865	< 0.0001	2	-0.0001
Air	2081-2099	0.1450	< 0.0001	2	-0.0001
Water	2003-2013	0.0612	< 0.0001	2	-0.0001
Water	2041-2059	0.0054	0.1556	2	-0.0001
Water	2081-2099	0.0023	0.2939	2	-0.0001

References

Barica, J. 1975. Summerkill risk in prairie ponds and the possibilities of its prediction. *Journal of the Fisheries Board of Canada*, 32**:**1283-1288.

Bivand, R., and C. Rundell. 2020. rgeos: interface to geometry engine - open source (`GEOS`). R package version 0.5-5. https://CRAN.R-project.org/package=rgeos

Comte, L., and J. D. Olden. 2017. Evolutionary and environmental determinants of freshwater fish thermal tolerance and plasticity. *Global Change Biology*, **23**:728-736.

Friedman, J., T. Hastie, and R. Tibshirani. 2010. Regularization paths for generalized linear models via coordinate descent. *Journal of Statistical Software*, **33**(1):1-22.

Greenbank, J. 1945. Limnological conditions in ice-covered lakes, especially as related to winter-kill of fish. *Ecological Monographs*, **15**:343-392.

Kuhn, M. 2021. caret: classification and regression training. R package version 6.0-88. https://CRAN.R-project.org/package=caret

La, V. T., and S. J. Cooke. 2011. Advancing the science and practice of fish kill investigations. *Reviews in Fisheries Science*, **19**:21-33.

Lyons, J., T. Zorn, J. Stewart, P. Seelbach, K. Wehrly, and L. Wang. 2009. Defining and characterizing coolwater streams and their fish assemblages in Michigan and Wisconsin, USA. *North American Journal of Fisheries Management*, **29**:1130-1151.

Mhlanga, L., J. Day, M. Chimbari, N. Siziba, and G. Cronberg. 2006. Observations on limnological conditions associated with a fish kill of *Oreochromis niloticus* in Lake Chivero following collapse of an algal bloom. *African Journal of Ecology*, **44**:199-208.

Olmanson, L. G., M. E. Bauer, and P. L. Brezonik. 2008. A 20-year Landsat water clarity census of Minnesota's 10,000 lakes. *Remote Sensing of Environment*, **112**(11):4086-4097.

Phelps, N. D. B., I. Bueno, D. A. Poo-Muñoz, S. J. Knowles, S. Massarani, R. Rettkowski, L. Shen, H. Ranatala, P. L. F. Phelps, and L. E. Escobar. 2019. Retrospective and predictive investigation of fish kill events. *Journal of Aquatic Animal Health*, **31**(1):61-70.

PRISM Climate Group, Oregon State University, https://prism.oregonstate.edu, data created 4 Feb 2014, data accessed 6 Nov 2020.

Rypel, A. L., T. D. Simonson, D. L. Oele, J. D. T. Griffin, T. P. Parks, D. Seibel, C. Roberts, S. Toshner, L. Tate, and J. Lyons. 2019. Flexible classification of Wisconsin lakes for improved fisheries conservation and management. *Fisheries*, **144**:225-238.

Schneider, J. C. 1998. Fate of dead fish in a small lake. *The American Midland Naturalist*, **140**(1):192-196.

Till, A., A. L. Rypel, A. Bray, and S. B. Fey. 2019. Fish die-offs are concurrent with thermal extremes in north temperature lakes. *Nature Climate Change*, **9**:637-641.

Tye, S. P. 2021, maddog: https://github.com/simontye/maddog

Wickham, H. 2016. ggplot2: Elegant Graphics for Data Analysis. Springer-Verlag, New York.

Winslow, L. A., G. J. A. Hansen, J. S. Read, and M. Notaro. 2017. Large-scale modeled contemporary and future water temperature estimates for 107444 midwestern US lakes. *Scientific Data*, **4**:170053.

Conclusion

Recent human history has been marked by rapid declines in animal abundances (Estes et al., 2011; Myers and Worm, 2003; Dirzo et al., 2014; Rosenberg et al., 2019; Genin et al., 2020; Fricke et al., 2022). These abundance declines have occurred alongside extreme climate conditions (e.g., Garrabou et al., 2019; Genin et al., 2020), rampant environmental degradation (e.g., eutrophication; Schindler, 1974), and other human-driven changes on the environment that are expected to worsen in coming years (e.g., Egan and Mullin, 2016; Sinha et al., 2017). Indeed, better understanding the biological implications of animal declines is imperative for predicting and comprehending future extents of ecosystem change. The experiments and data synthesis that encompass this dissertation increases our knowledge about one important aspect of recent animal declines – mass mortality events of predator populations – as well as provides more general information about the mechanistic underpinnings of rapid ecological and evolutionary changes that may occur in their aftermath.

In Chapter 1, an outdoor mesocosm experiment demonstrated that predator MMEs generate predictable trophic biomass responses, as well as surprisingly stable ecological dynamics compared to similar perturbations. In Chapter 2, a microcosm experiment indicated that size-selective predation generates partially divergent consumer life history trait responses under contrasting resource levels, and appreciable evidence for eco-evolutionary dynamics only arise under low resource levels. In Chapter 3, the largest existing data synthesis of freshwater fish mortality events and concurrent temperatures indicated that the annual frequency of fish mortality events because of warm temperature will likely substantially increase over coming decades. Collectively, this body of work increases our basic knowledge about animal declines

and refines an approach to predict the future frequency of these events in an effort to raise awareness about and mitigate their occurrences.

In Chapter 1, we experimentally induced predator MMEs in freshwater food webs to understand whether these events generated ecological dynamics that could be predicted by considering the combined effect of predator removals (Paine, 1966; Paine, 1980) and resource pulses (Polis et al., 1997), as surmised by theory (Fey et al., 2019). MMEs generated predictable trophic biomass responses that involved the co-proliferation of diverse consumer and producer communities due to weakened top-down predator control (Hairston et al., 1960; Paine, 1966; Paine, 1980) and stronger bottom-up effects via decomposition of predator carrion (Fey et al., 2019). In addition, MMEs led to the most stable functional trait and food web dynamics, which suggested that these extreme demographic events may be rather cryptic disturbances in nature. These ensuing community dynamics may be best described as a "trophic reshuffling", in which indirect effects of predators on primary producers were initially lost but then appeared as stronger direct bottom-up effects. More generally, there was a brief temporal lag between the observed increase in algal biomass and increase in consumer biomass following predator MMEs. Collectively, these results highlight potential ecological signatures of MMEs and demonstrate the feasibility of forecasting novel ecological dynamics arising amidst intensifying global change by synthesizing enduring theories of community ecology (Paine, 1966; Paine, 1980; Polis et al., 1997).

In Chapter 2, we examined how selective predation and resource level – two major biotic drivers of ecological and evolutionary change (Hairston et al., 1960; Paine, 1966; Paine, 1980; Reznick and Endler, 1982; Stearn, 1992; Reznick et al., 2002) – shaped consumer population dynamics, life history trait evolution, and eco-evolutionary dynamics. We chose these two

selective pressures because both may be affected to a degree following predator MMEs. To partition the effects of selective predation and resource level, we conducted an artificial selection that exposed *Daphnia pulicaria* populations to different combinations of selective predation and resource level. Size-selective predation slightly increased population density, reduced maximum body size, and extended juvenile growth period. By comparison, high resource levels increased population density and mediated changes in size at maturity and total fecundity. In addition, there was weak evidence for eco-evolutionary dynamics via a positive relationship between maximum body size and per capita growth rate under size-selective predation and low resource levels. Collectively, these findings indicated that size-selective predation generated life history trait responses that partially diverge from predictions under contrasting resource levels (Cuenca-Cambronero et al., 2018; Lyberger et al., 2021), and eco-evolutionary dynamics may only from these major biotic drivers of ecological and evolutionary change under certain contexts.

In Chapter 3, we aimed to extend applied knowledge about animal mass mortality events, which have increased in frequency and intensity (Fey et al., 2015) alongside substantial changes in global climate (e.g., Garrabou et al., 2019; Genin et al., 2020). Few tractable approaches exist to predict how climate change will accentuate occurrences these ecological catastrophes (e.g., Till et al., 2019). We thus compiled one of the most comprehensive datasets of lentic fish mortality events, thermal tolerances of affected families, and local temperature profiles across north temperate lakes of North America. Temperature extremes both within and across lakes were strongly associated with the three most frequent cause types of fish mortality events: infectious agents, summerkills, winterkills. Thermal tolerances mediated the lethality of direct thermal stress and mortalities of warm- and cold-water fish families occurred at similar temperature deviations, which indicated local heatwaves may be a driving contributor to these

events (e.g., Garrabou et al., 2019; Genin et al., 2020). Water and air temperature-based models accurately predicted contemporary summerkills and suggested ~6 to 34-fold increases, respectively, in their frequency by 2100 under the worst-case climate scenario. These models provide reasonable forecasts for impending ecosystem changes across lakes in north temperate regions, where most lakes occur (Verpoorter et al., 2014). Indeed, most mass mortality events of animals have affected freshwater fish (Fey et al., 2015), and often because of the direct or indirect effects of high temperature or temperature change (Till et al., 2019)

In total, this body of work enhances our basic and applied knowledge about animal mortality events and addresses general ecological and evolutionary changes that may occur in their aftermath. In complex experimental systems, predator MMEs generate surprisingly predictable but eerily stable ecological dynamics – hinting that these events could potentially be difficult to detect if carrion is not readily observable. Even so, however, major biotic drivers of ecological and evolutionary change that may be altered in the aftermath of predator MMEs can lead to several counterintuitive consumer life history adaptations. These intellectual contributions suggest that additional research is urgently needed to better understand the ecological and evolutionary implications of predator MMEs. Indeed, animal abundances have globally declined (Dirzo et al., 2014), and the most robust approach available for predicting the future frequency of animal mortality events indicates substantial increases in a warmer world. I hope this information encourages deep contemplation about the future that lies ahead without more cooperation, empathy, and constructive dialogue.

References

Cuenca-Cambronero, M., H. Marshall, L. De Meester, T. A. Davidson, A. P. Beckerman, and L. Orsini. 2018. Predictability of the impact of multiple stressors on the keystone species *Daphnia*. *Scientific Reports*, **8**(1):17572. doi:10.1038/s41598-018-35861-y.

Dirzo, R., H. S. Young, M. Galetti, G. Ceballos, N. J. B. Issac, and B. Collen. 2014. Defaunation in the Anthropocene. *Science*, **345**:401-406. doi:10.1126/science.1251817

Egan, P. J., and M. Mullin. 2016. Recent improvement and projected worsening of weather in the United States. *Nature*, **537**: 357-360. doi:10.1038/nature17441

Fey, S. B., A. M. Siepielski, S. Nusslé, K. Cervantes-Yoshida, J. L. Hwan, E. R. Huber, M. J. Fey, A. Catenazzi, and S. M. Carlson. 2015. Recent shifts in the occurrence, cause, and magnitude of animal mass mortality events. *Proceedings of the National Academy of Sciences*, **112**:1083-1088. doi:10.1073/pnas.1414894112

Fey, S. B., J. P. Gibert, and A. M. Siepielski. 2019. The consequences of mass mortality events for the structure and dynamics of biological communities. *Oikos*, **128**:1679-1690. doi:10.1111/oik.06515

Fricke, E. C., C. Hsieh, O. Middleton, D. Gorczynski, C. D. Cappello, O. Sanisidro, J. Rowan, J. C. Svenning, and L. Beaudrot. 2022. Collapse of terrestrial mammal food webs since the Late Pleistocene. *Science*, **377**:1008-1011. doi:10.1126/science.abn4012

Estes, J. A., J. Terborgh, J. S. Brashares, M. E. Power, J. Berger, W. J. Bond, S. R. Carpenter, T. E. Essington, R. D. Holt, J. B. C. Jackson, R. J. Marquis, L. Oskanen, T. Oksanen, R. T. Payne, E. K. Pikitch, W. J. Ripple, S. A. Sandin, M. Scheffer, T. W. Schoener, J. B. Shurin, A. R. E. Sinclair, M. E. Soulé, R. Virtanen, and D. A. Wardle. 2011. Trophic downgrading of planet Earth. *Science*, **333**:301-306. doi:10.1126/science.120510

Garrabou, J., D. Gómez-Gras, J. B. Ledoux, C. Linares, N. Bensoussan, P. López-Sendino, H. Bazairi F. Epinosa, M. Ramdani, S. Grimes, M. Benabdi, et al. 2019. Collaborative database to track mass mortality events in the Mediterranean Sea. *Frontiers in Marine Science*, **6**:707.

Genin, A., L. Levy, G. Sharon, and A. Diamant. 2020. Rapid onsets of warming events trigger mass mortality of coral reef fish, *Proceedings of the National Academy of Sciences*, **117**:25378-25385. doi:10.1073/pnas.2009748117

Hairston, N. G., F. E. Smith, and L. B. Slobodkin. 1960. Community structure, population control, and competition. *The American Naturalist* **94**:421-425. doi:10.1086/282146

Lyberger, K., T. W. Schoener, and S. J. Schreiber. 2021. Effects of size selection versus density dependence on life histories: a first experimental probe. *Ecology Letters*, **24**(7):1467–73. doi:10.1111/ele.13767.

Myers, R. A., and B. Worm. 2003. Rapid worldwide depletion of predatory fish communities. *Nature*, **423**:280-283. Doi.10.1038/nature01610

Paine, R. T. 1966. Food web complexity and species diversity. *The American Naturalist*, **100**:65-75. doi:10.1086/282400

Paine, R. T. 1980. Food webs: linkage, interaction strength, and community infrastructure. *Journal of Animal Ecology*, **49**:666-685. doi:10.2307/4220

Polis, G. A., W. B. Anderson, and R. D. Holt. 1997. Toward an integration of landscape and food web ecology: the dynamics of spatially subsidized food webs. *Annual Review of Ecology and Systematics*, **28**:289-316. doi:10.1146/annurev.ecolsys.28.1.289

Phelps, N. B. D., I. Bueno, D. A. Poo-Muñoz, S.J. Knowles, S. Massarani, R. Rettkowski, L. Shen, H. Rantala, P. L. F. Phelps, and L. E. Esobar. 2019. Retrospective and predictive investigation of fish kill events. *Journal of Aquatic Animal Health*, **31**:61-70. doi:10.1002/aah.10054

Reznick, D., and J. A. Endler. 1982. The impact of predation on life history evolution in Trinidadian guppies (*Poecilia reticulata*). *Evolution*, **36**(1):160-177. doi:10.2307/2407978

Reznick, D., M. J. Bryant, and F. Bashey. 2002. r- and K-selection revisited: the role of population regulation and in life-history evolution. *Ecology*, **83**(6):1509-1520. doi:10.1890/0012-9658(2002)083[1509:raksrt]2.0.co;2

Rosenberg, K. V., A. M. Dokster, P. J. Blancher, A. C. Smith, P. A. Smith, J. C. Stanton, A. Panjabi, L. Helft, M. Parr, and P. P. Marra. 2019. Decline of the North American avifauna. *Science*, **366**(5461):120-124. doi.101126/science.aaw1313

Stearn, S. C. 1992. *The Evolution of Life Histories*. Oxford University Press, 249 pp.

Schindler, D. W. 1974. Eutrophication and recovery in experimental lakes: implications for lake management. *Science*, **184**:897-899. doi:10.1126/science.184.4139.897

Sinha, E., A. M. Michalak, and V. Balaji. 2017. Eutrophication will increase during the 21st century as a result of precipitation changes. *Science*, **357**(6349):405-408. doi:10.1126/science.aan2409

Till, A., A. L. Rypel, A. Bray, and S. B. Fey. 2019. Fish die-offs are concurrent with thermal extremes in north temperate lakes. *Nature Climate Change*, **9**:637-641. doi:10.1038/s41558-019-0520-y

Verpoorter, C., T. Kutser, A. Seekell, and L. J. Tranvik. 2014. A global inventory of lakes based on high-resolution satellite imagery. *Geophysical Research Letters*, **41**:6396-6402. doi:10.1002/2014GL060641